CHEMICAL REVIEWS

Review

pubs.acs.org/CR

Chemical Components for the Design of Temperature-Responsive Vesicles as Cancer Therapeutics

Zahraa Al-Ahmady[†,‡,§] and Kostas Kostarelos*[,†,‡]

[†]Nanomedicine Lab, Faculty of Medical & Human Sciences, University of Manchester, AV Hill Building, Manchester M13 9PT, United Kingdom

[‡]UCL School of Pharmacy, Faculty of Life Science, University College London, Brunswick Square, London WC1N 1AX, United Kingdom

[§]Manchester Pharmacy School, University of Manchester, Stopford Building, Manchester M13 9PT, United Kingdom

ABSTRACT: In this Review, we attempt to offer a thorough description of all of the chemical components and the rationale behind the design of temperature-sensitive vesicle systems, as well as the critical pharmacological parameters that need to be combined to achieve their successful clinical translation. The focus of this Review will be predominantly on the design principles around the construction of temperature-sensitive liposomes (TSL) and their use in combination with external local hyperthermia to achieve heat-triggered drug release. The emphasis lies on the chemical components synthesized and incorporated in the design and engineering of TSL. We conclude that the development of TSL with ultrafast drug release capabilities needs to progress in parallel with vesicle pharmacokinetic profiling, imaging, and monitoring capacity and technologies for accurate temperature elevation and control. The development of heat-triggered liposome systems offer the greatest opportunity for clinical translation of the next generation, nanoscale "smart" vesicle systems of enhanced functionality, following from the successful legacy and rich clinical history from multiple earlier liposome technologies.

CONTENTS

1. INTRODUCTION

Liposomes are spherical phospholipid vesicles consisting of one or more concentric lipid bilayers enclosing an aqueous core.[1,2] Although liposomes form spontaneously by self-assembly of amphiphilic lipids after dispersion in water, they can effectively entrap both hydrophilic[3] and hydrophobic compounds[4,5] in the aqueous core or in the lipid bilayer, respectively. Gregory Gregoriadis was the first to demonstrate liposomes for the entrapment of drugs,[6,7] and since then their use in drug delivery has been extensively explored. One of the most important advantages was that encapsulation of drugs inside liposomes reduced the drug-associated toxicity. However, such traditional liposomes were found to be rapidly cleared by the reticuloendothelial system, specifically opsonized, and taken up by Kupffer cells of the liver.[8,9]

Received: September 30, 2015
Published: March 2, 2016

DOI: 10.1021/acs.chemrev.5b00578
Chem. Rev. 2016, 116, 3883−3918

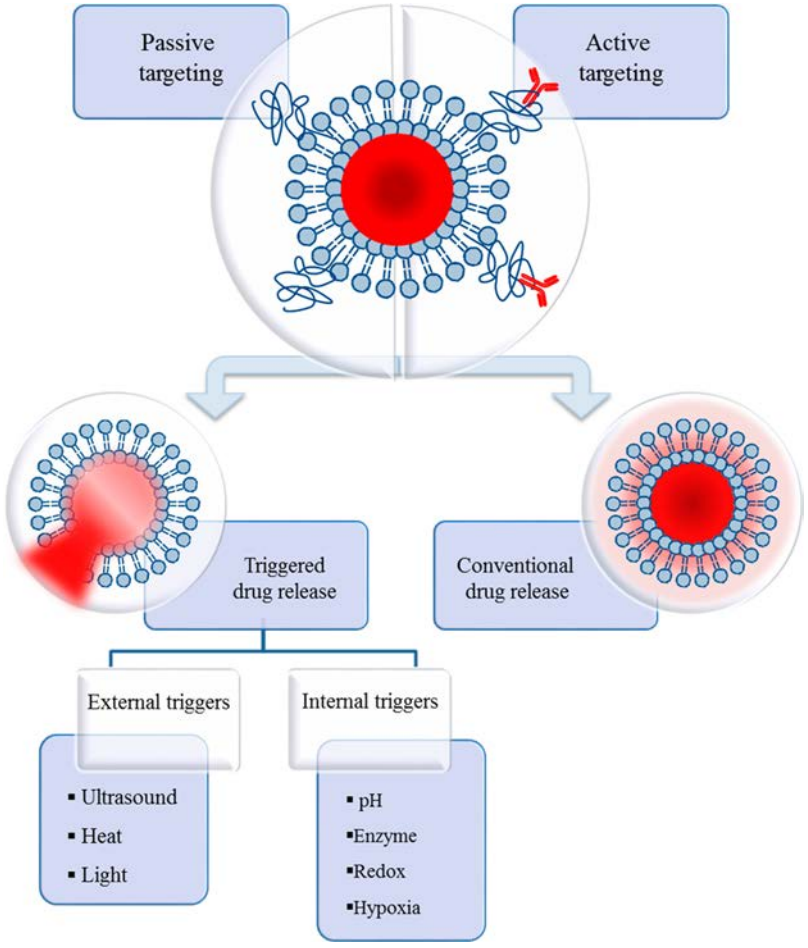

Figure 1. Schematic presentation of the different types of liposomes with triggered-release capabilities.

With the emergence of longer circulating liposomes, there was improved biodistribution of chemotherapeutic agents to the anatomical sites of leaky vasculature.[10,11] Moreover, prolonged circulation time of stealth liposomes led to the appearance of new toxicological side-effects, such as chemotherapy-induced palmer planter erythrodysesthesia, expressed as a swelling and inflammation of hands and feet as a result of changing the biodistribution and pharmacokinetics of the drug.[12] At this point in therapeutic liposome development, especially against cancer, it was becoming clear that there was a delicate balance between the degree of systemic toxicity and therapeutic efficacy. The encapsulation of drug (reduced toxicity), PEGylation of the membrane (increased circulation time but new toxicity), the potential for extravasation into tumor tissue (see below – EPR), and the retention of drug (meaning slow release, but less-than-required efficacy) were all becoming essential, but sometimes compromising, components in the design of the evolving liposomal therapeutic system.

Dvorak[13] first described that tumor vasculature can be hyperpermeable, especially to circulating macromolecules. A lot of implanted tumors in animal models have been shown to be "leaky", characterized by enlarged endothelial pores. It was then shown that, especially in subcutaneously implanted tumors, there was perivascular extravasation of 100 nm diameter liposome particles.[14] The proposed mechanism behind the preferential accumulation of liposomes into the tumor tissue rather than other healthy organs was the hyperpermeability of the tumor vasculature.[13] This phenomenon was termed as the enhanced permeability and retention effect (EPR)[15,16] and depends on the differences in vascular architecture between healthy tissues and some pathological sites (e.g., tumors, arthritic lesions).[16−18]

PEGylated liposomal doxorubicin (DOX) known as Doxil was clinically approved in 1995 as the first nanoscale drug delivery system.[19] Doxil showed a unique safety profile, with a lower risk of cardiac toxicity as compared to conventional doxorubicin at cumulative doses of 500 mg/m^2 and more.[12,20,21] However, the significant decrease in cardiac toxicity of DOX after encapsulation into liposomes did not necessarily translate into improved therapeutic efficacy. Extravasation of liposomes into the tumor is a heterogeneous process that is primarily dependent on the size of nanoparticles, and the interstitial fluid pressure that might hamper their movement into the extracellular matrix especially in large-size tumors.[22,23] The clinical role of EPR effect in the passive accumulation of nanoparticles in patients is also not yet conclusive.[24] In addition, despite the increase in the tumor accumulation of liposomal DOX as compared to free DOX, not all of the drug was bioavailable for tumor cells.[25] Laginha et al. studied the bioavailable DOX levels from Doxil into 4T1 (mammary carcinoma) orthotopically implanted in mice.[25] Administration of Doxil showed 87-fold higher total tumor DOX accumulation 7 days after injection as compared to free DOX. From the total amount of Doxil encapsulated, only 49% of DOX was freely bioavailable at the tumor site to bind with nuclear DNA as a result of the slow release process.[25] Similar findings have been observed for the long circulating liposomal cisplatin; however, a significantly less fraction of the drug

DOI: 10.1021/acs.chemrev.5b00578
Chem. Rev. 2016, 116, 3883−3918

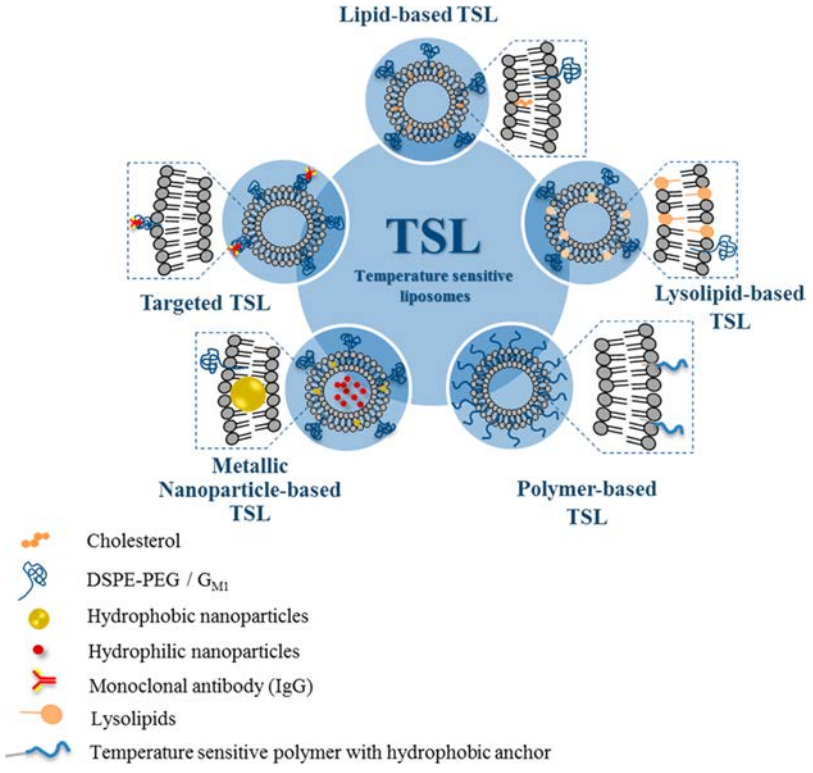

Figure 2. Schematic presentation of different types of TSL and different chemical components included in their design.

molecules becomes bioavailable (only 0.14% of the total administered drug dose). That was reflected in the poor therapeutic outcomes in clinical evaluation, but dramatically improved the safety profile.[26,27]

It is now recognized that following accumulation within the tumor tissue, drug release from both conventional and stealth liposomes is a slow process; however, the exact mechanism of drug release and internalization by the tumor cells is not fully understood.[19,28] Two mechanisms have been suggested to explain the uptake of liposomal drugs by cancer cells: (a) the uptake of the whole vesicle encapsulated drug within the tumor cells followed by drug release intracellularly; and (b) the nonspecific degradation of the liposomal lipid membrane and drug release into the tumor interstitium followed by the uptake of free drug by the cancer cells. It is now generally accepted that internalization of intact liposomes by cancer cells is less frequent; therefore, tumor cell uptake of free drug released in the tumor interstitial fluid remains the most common working hypothesis.[19,28] In the case of Doxil therapy, the process by which DOX is released from liposomes and becomes bioavailable to tumor cells may include the collapse of the ammonium sulfate gradient[19] and the destabilization of the vesicle lipid bilayer via macrophage-mediated liposome degradation and subsequent drug release (often after killing the macrophages).[29−31] In addition to that, the fate of liposomes after extravasation can be heterogeneous due to the variation in tumor vascular permeability between different types of tumors and even within the same tumor that will greatly affect overall therapeutic outcomes.[17]

The ensuing challenge from the liposomal engineering point of view has been whether these limitations could be overcome by triggering drug release from the vesicles to increase therapeutic agent bioavailability to the tumor cells. The ideal liposomal formulation of chemotherapy should retain the drug while circulating in the bloodstream and be able to release the drug locally within the tumor tissues or vasculature.[32,33] A wide range of research has been conducted over the last three decades to investigate the possibilities of triggering drug release from liposomes. Two main classes of "triggers" have been developed: (a) external, such as heat, light, and ultrasound; and (b) internal, those present at the disease site such as changes in pH, enzymes, alterations in the level of glutathione (redox responsiveness), and hypoxia.[34−36] Examples of the different types of liposomes that respond to external and internal triggering mechanisms are summarized in Figure 1.

Whereas most of these systems are still under development at various preclinical stages, temperature-sensitive liposomes (TSLs) have progressed to an advanced stage of clinical development (Phase III clinical trials).[37] The focus of this Review will be predominantly on the design principles around the construction of TSL and their use in combination with external local hyperthermia to achieve heat-triggered drug release. The chemical components synthesized and incorporated in the design and engineering of TSL will be thoroughly explained. The potential of other nonvesicular temperature sensitive systems will not be covered here. The reader can refer to a number of comprehensive reviews on this topic for additional information.[38−43]

2. RATIONAL DESIGN OF TEMPERATURE-RESPONSIVE VESICLES

Since the concept of TSL was first introduced by Yatvin in the late 1970s,[44] a lot of effort has been invested to explore the potential of such vesicle systems. Indeed, over the past 30 years the development of TSL has been widely expanded starting from the molecular design of TSL all of the way to clinical testing and determining their therapeutic aptitude. Here, TSLs have been classified into five subgroups on the basis of the chemical

DOI: 10.1021/acs.chemrev.5b00578
Chem. Rev. 2016, 116, 3883−3918

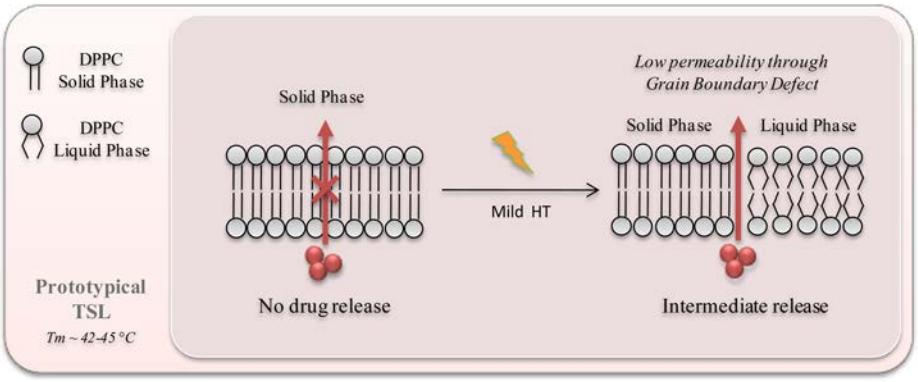

Figure 3. Schematic presentation of the phase transition behavior of TSL. When the lipid membrane passes through the transition temperature,[35] the bilayer permeability increases, while below that temperature, lipid membranes exist in solid phase only and therefore no drug release is expected. At the T_m, the existence of both the solid and the liquid phases leads to the formation of grain boundary defects in the bilayer through which drug release occurs. Adapted with permission from ref 45. Copyright 2013 Royal Society of Chemistry.

components included in their design. Figure 2 illustrates the different types of TSL systems described in the literature. The chemical design of TSL, mechanism of thermal responsiveness, drug release kinetics, heating protocols, and clinical values of TSL are all discussed.

2.1. Lipid-Based TSL – Exploiting Phase Transition Temperatures of Lipids

The pioneering TSL system described by Yatvin et al. in 1978 was composed of DPPC:DSPC lipids mixed at certain molar ratios. This formulation showed an increase in the release of encapsulated neomycin in vitro after heating to their phase transition temperature,[35] which was associated with inhibition of bacterial growth.[44] This formulation represents the prototypical type of TSL in a class of systems produced by mixing DPPC bilayers, which have a phase transition temperature (T_m) of 42 °C with DSPC lipids of T_m = 55 °C at 7:3 molar ratios. This ratio allowed a T_m range between 41 and 43 °C. The temperature sensitivity of prototypical TSL is based on the tendency of the lipid components to undergo phase transition as a response to heat. When TSLs were heated through their T_m, areas of the phospholipid molecules start to change from the solid (ordered) gel phase to the liquid (disordered) crystalline phase, creating boundaries between the two phases through which the drug permeability is enhanced (Figure 3).[44] In the gel phase, lipid molecules are highly ordered and condensed. The hydrocarbon chains are fully extended, and the head groups are immobile at the interface with water.

When the temperature is elevated, the headgroup mobility begins to increase, and with further increases in temperature toward the T_m of lipids, a transition of hydrocarbon chains from the gel to the liquid crystalline phase occurs. At T_m the orientation of the C−C single bonds in the hydrophobic chains is changed from trans to gauche state.[46] The existence of both solid and liquid lipid domains at the T_m leads to the formation of leaky regions at the interface between these domains. As a result, lipid membrane permeability increases at the interfaces, which has been signified previously by a dramatic increase in Na^+ ions' diffusion. Although ion permeability is highest at the T_m, it reduces as the temperature is elevated beyond, due to the reduction in the existence of those boundary regions. When the lipid membrane fully melts with further temperature increase, the membrane permeability is increased again as the lipid bilayer is predominantly in the fluid phase.[47] Grain boundaries result from defects in the crystalline arrangement of lipid molecules in that region. The crystalline structure is produced during the liposome preparation process that involves cooling of the lipid bilayer from its liquid phase into solid phase. When the lipid bilayer is cooled toward T_m of the lipids, solidification of the lipid membrane appears as nucleation of the solid domain within the melted lipid membrane. These individual solid domains continue to grow by orienting lipid molecules into crystal-lattice-like structures. The growth of these domains then stops when they approach each other in the final gel phase membrane, and this leads to the formation of grain boundaries.[48]

Similar to the prototypical TSL, most of the early examples of TSL systems were composed mainly of DPPC or DPPG lipids mixed with other types of lipids like DSPC and HSPC lipids to tune the T_m and the rate of drug release.[49−53] The selection of lipid combinations can also contribute to improved lipid membrane permeability by increasing the defects in lipid packing. Prototypical TSLs were further developed by inclusion of cholesterol to optimize their serum stability. However, this can also has a negative effect on the rate and extent of drug release in response to temperature that can be linked to the increase and broadening of T_m after inclusion of cholesterol.[53] The blood circulation time of prototypical TSL was also increased by adopting the same approaches used with other stealth liposomes. The inclusion of G_{M1} or DSPE-PEG_{2000} lipids into TSL led to a reduction in the interaction with MPS cells and enhancement of their blood profile, which resulted in better control over tumor growth rate.[49,54] Recently Li et al. showed that incorporating 5 mol % of DSPE-PEG_{2000} is the optimal concentration to provide a balance between the stability of TSL at 37 °C without jeopardizing the temperature sensitivity at mild HT.[55]

In addition to the typical benefits provided by DSPE-PEG_{2000} as mentioned above, the inclusion of this lipid adds to the thermal sensitivity of prototypical TSL. DSPE-PEG_{2000} inclusion at 4−5 mol % drives the switch from mushroom or brush configuration. The heterogeneous structure of DSPE-PEG_{2000} causes destabilization of lipid membrane when close to T_m and increases content release without significantly affecting the T_m.[55] An interesting example of that is the DPPC:HSPC:CHOL:DSPE-PEG_{2000} TSL system that contains 3.2 mol % of DSPE-PEG_{2000} lipids. The addition of DSPE-PEG_{2000} revealed the thermal sensitivity of the liposomes even with the presence of cholesterol as observed from differential scanning calorimetry (DSC) thermograms, releasing 60% of DOX in vitro in 50% plasma.[53] Alternatively, Lindner et al.

DOI: 10.1021/acs.chemrev.5b00578
Chem. Rev. 2016, 116, 3883−3918

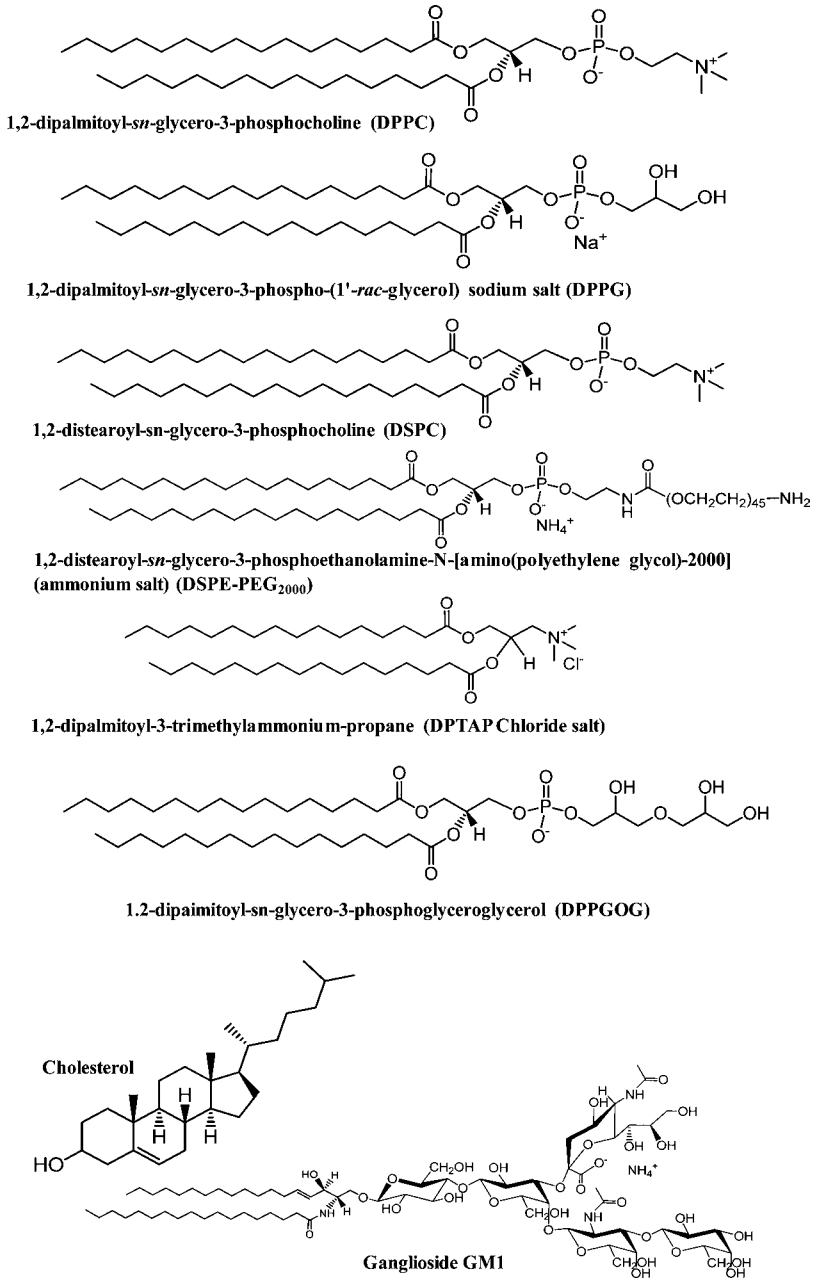

Figure 4. Chemical structures of the lipids used in the design of prototypical TSL.

showed that the inclusion of DPPGOG lipid (Figure 4) into DPPC:DSPC liposomes can prolong their circulation time in vivo together with significant enhancement in their content release upon heating.[56,57] In addition, Dicheva et al. described recently that targeting TSL to the tumor tissue can be improved by the preparation of a cationic TSL (CTSL) by including 7.5% or 10 mol % of DPTAP cationic lipid (Figure 4) into DPPC:DSPC:DSPE-PEG_{2000} liposomes. The outcome of that was a moderate positive surface charge (zeta potential) as compared to the slightly negative charge of most other TSLs and, consequently, better targeting ability to endothelial and tumor cells with content release upon temperature triggering.[58,59] The inclusion of positively charged lipids in this formulation increased its capacity to deliver DOX to tumors by 3-fold as compared to noncationic TSL. This was confirmed by the high DOX uptake by both tumor cells and angiogenic endothelial cells and resulted in dramatic ablation of the tumor vasculature.[58]

For a long time, prototypical TSLs have been mistaken for having slow and incomplete release profiles under mild HT. Likewise, the relatively high T_m of this class of TSL (42−45 °C) suggested that high thermal dose is required to achieve effective drug release (1 h heating at temperature >42 °C).[60] However, most of the release profile data were generated in a buffer, and this does not reflect real physiological conditions.[53,54,61] It is also important to note the differences in the mechanism of DOX release as compared to that of other commonly used fluorescent dyes, such carboxyfluorescein (CF), due to the variation in their vesicle encapsulation. Higher rates of release are usually reported for DOX as compared to CF under the same conditions, due to the collapse of the pH gradient mechanism used for DOX loading as a result of the increase in proton diffusion across the lipid membrane at T_m. Approximately 95% DOX release was reported from DPPC:DSPC:DSPE-PEG_{2000} (90:10:5 molar

DOI: 10.1021/acs.chemrev.5b00578
Chem. Rev. 2016, 116, 3883−3918

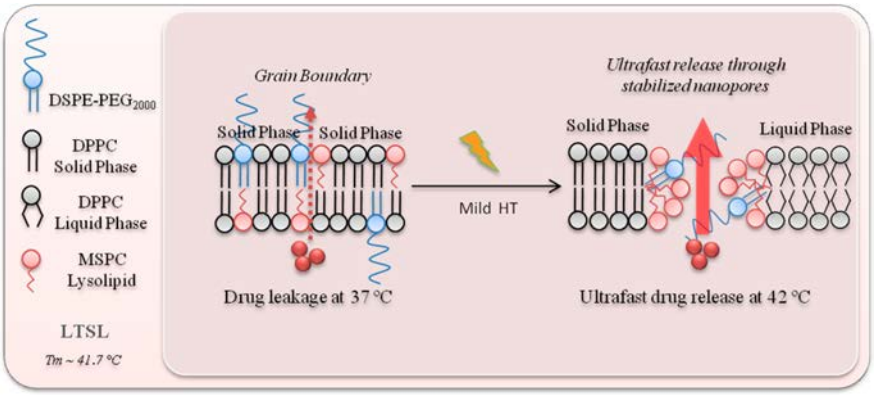

Figure 5. Schematic presentation of nanopore formation facilitating drug leakage in LTSL. Below the phase transition (37 °C) drug leakage from the DPPC:MSPC:DSPE-PEG$_{2000}$ (LTSL) bilayer can occur through grain boundary in the bilayer due to the presence of lysolipids. Ultrafast drug release at the phase transition region through MSPC nanopores that were stabilized by DSPE-PEG$_{2000}$. Adapted with permission from ref 45. Copyright 2013 Royal Society of Chemistry.

ratio) liposomes after 1 min of heating at 42 °C, as compared to <50% of CF under similar conditions.[55,62]

Interestingly, the presence of serum proteins can have a favorable effect on temperature sensitivity of this type of TSL and results in an increase in the rate of drug release, presumably by gaining access into the grain boundary of the lipid membrane at T_m.[53,57,61,63−65] Moreover, the presence of cholesterol in the serum can also contribute to better permeability. The ability of cholesterol to exchange between vesicles leads to disturbance in the lipid packing and leads to improved permeability.[65] The effect of serum on the release profile can vary with the origin of the serum used, its concentration, and the duration of exposure. This can explain the discrepancy in the release data reported from prototypical TSL systems.[53,66] The effect of serum components on the thermal sensitivity of prototypical TSL can also justify the increase in therapeutic activity observed in a number of preclinical studies over a wide range of tumor models using mild heating conditions (42 °C).[63] This was also confirmed recently by a real-time imaging study Li et al. that showed efficient intravascular DOX release after heating at 42 °C followed by rapid uptake of DOX by endothelial cells and tumor cells. This resulted in high and homogeneous DOX penetration into tumor cells and improved tumor growth control.[62]

2.2. Lysolipid-Based Temperature-Sensitive Liposomes (LTSLs)

The concept of lysolipid-containing thermosensitive liposomes was first described by Anyarambhatla and Needham in 1999[67] and led to a new concept in the field of drug delivery by demonstrating triggered drug release in the tumor blood vessels, or what is now termed "intravascular drug release".[45,48,68,69] They first proposed that the incorporation of ∼10 mol % of MPPC lysolipids into DPPC:DSPE-PEG (90:4) liposomes lowered the T_m of DPPC:DSPE-PEG liposomes from 41.9 to 41 °C and led to rapid drug release in a concentration-dependent manner.[67] As compared to the traditional thermosensitive liposomes by Yatvin et al.,[44] lowering the T_m to 41 °C is a critical parameter for temperature-triggered drug release. For clinical applications, mild HT < 43 °C is recommended because higher temperature can result in hemorrhage[70] and also cause necrotic damage to the neighboring healthy tissues.[48,71]

The design of LTSL required the presence of these essential components: (a) a solid-phase lipid able to offer grain boundary deformation (DPPC lipids) that could act as the "host" lipid and formed the main vesicle bilayer component; and (b) monoalkyl lysolipids and PEGylated lipids at several mol % that act as permeabilizing ingredients and steric stabilizing components.[45] The combination of these lipid components allows drug release in only few seconds when heated to their phase transition temperature.[72] MSPC lysolipid was then used instead of MPPC to increase the liposome stability during processing and offer drug retention capability. The longer acyl chain (C18) of MSPC lysolipid increased the T_m to 41.3 °C, while preserving ultrafast release capabilities.[72]

To understand the release mechanism of LTSL liposomes, Mills and Needham studied the permeability of the liposome membrane using a dithionite ($S_2O_4^{2-}$) permeability assay.[73] The membrane permeability was studied by preparing NBD (1%) labeled DPPC:DSPE-PEG$_{2000}$ (4%) liposomes with and without MSPC (10%). The addition of dithionite at 30 °C quenched the signal of NBD lipids in the outer membrane only due to the impermeability of the lipid membranes to dithionite ions. Repeating the experiment at the T_m quenched the absorbance of the NBD lipids at the inner membrane as the lipid membranes become permeable to dithionite ions. This decrease in absorbance is faster for DPPC:DSPE-PEG (4%) liposomes having 10% MSPC and dramatically increased at 42 °C, demonstrating the role of lysolipid (MSPC) in increasing the permeability of LTSL liposomes at T_m.[72]

The permeability coefficient of the liposomal membranes with and without MSPC lysolipid was also measured using the following formula: $C(t) = C_0(\exp(-m^2t)$, where m^2 is the permeability rate constant, $C(t)$ is the concentration of unreacted NBD molecules at time t, and C_0 is the concentration of unreacted NBD molecules on the inner monolayer at zero time point. The permeability coefficient of DPPC:DSPE-PEG (4%) having 10% MSPC was measured as 1.09×10^{-8} cm/s, 10-fold higher than liposomes without MSPC (1.9×10^{-9} cm/s). A similar 10-fold increase in a DOX permeability coefficient at 42 °C was evidenced by adding MSPC (10%) as compared to liposomes without MSPC measured at 3.3×10^{-9} and 3.4×10^{-10} cm/s, respectively.[72] Mills and Needham compared the permeabilities of the liposomes to dithionite ion (radius 3 Å) and DOX (radius 500 Å) with and without lysolipid at the T_m. For pure DPPC membranes, dithionite permeability was 6 times higher as compared to DOX, indicating higher permeability to smaller ions. Liposomes having 10% MSPC showed 3 times higher permeability for dithionite ions as compared to DOX,

DOI: 10.1021/acs.chemrev.5b00578
Chem. Rev. 2016, 116, 3883−3918

which was believed to be through a water-filled pore rather than the hydrocarbon chain.[72] Therefore, the ultrafast release of LTSL contents appeared to be due to the enhancement of the grain boundary caused by the inclusion of the lysolipid component (Figure 5) through which both ions and small molecular weight drugs can permeate.[72] The size of these nanopores appeared to be ∼10 nm as estimated from dextran permeation measurements.[45]

Lysolipids have a relatively large headgroup as compared to their single acyl chain, which gives them a positive intrinsic curvature and a tendency for micelle formation in aqueous solution above their CMC (∼0.4 μM).[45] Upon approaching the phase transition, the increase in lateral lipid movement encourages lysolipid accumulation at the melted grain boundaries and the formation of stabilized defects (nanopores) in the lipid membrane. Similar to what was observed before with prototypical TSL, the presence of DSPE-PEG_{2000} can add to the thermosensitivity of the system but through a different mechanism. Despite having two hydrocarbon chains, DSPE-PEG_{2000} also has the capability for micelle formation in aqueous solution. The shape factor of DSPE-PEG_{2000} is close to lysolipids as it has much larger head groups in relation to the tail groups because of the PEG_{2000} polymer. Therefore, in principle, the presence of DSPE-PEG_{2000} lipids can help to some extent in the formation and stabilization of the nanopore structure by bringing a second property, a repulsive force within the nanopore.[45]

Different concentrations of lysolipids and DSPE-PEG_{2000} lipids were matched against the release profiles of DOX and CF. Despite not being optimum regarding DSPE-PEG_{2000} coverage (the boundary concentration of DSPE-PEG_{2000} between mushroom and brush conformation is 5 mol %), the exact lipid vesicle system that progressed into preclinical and clinical studies consisted of DPPC:MSPC:DSPE-PEG_{2000} (86.5:9.7:3.8 mol/mol). More than 80% release of encapsulated DOX can be achieved after 20 s in mild HT.[48] Mill and Needham demonstrated that the mechanism of drug release at T_m is through lysolipid-stabilized nanopores, rather than enhancement of drug solubility in the lipid membrane.[72] Employing mass spectrometry and dialysis experiments, they also confirmed that the lysolipid was sufficiently retained in the lipid membrane above T_m after extensive dilution. These studies were performed in buffer to demonstrate the effect of micromolar solubility on the desorption of lysolipids from the liposomal membrane. As such, these experiments were performed in the absence of serum proteins and lipids that could act as a sink for lysolipids and, by design, did not simulate physiological conditions.[72]

In the presence of biological components (serum protein, whole blood), lysolipids could be extracted from the liposome membrane to these components. Banno et al. showed the dissociation of almost 70% of lysolipids from LTSL liposomes within 1 h after in vivo administration and postulated that this might be through exchange with plasma proteins or cellular membranes.[74] They and others showed that DOX retention by LTSL liposomes in blood circulation is ∼1 h, showing significant DOX leakage from LTSL liposomes at 37 °C after in vivo administration.[74,75] However, Needham speculated that the loss of DOX from LTSL is more likely due to the H^+ ion transport that can result in DOX cation deprotonation and increase its solubility followed by leakage through even a solid-phase membrane.[45]

The inclusion of DSPE-PEG lipids in LTSL liposomes was expected to prevent the lipid bilayer from interaction with serum proteins. Despite that, incubation of LTSL liposomes in serum at 37 °C resulted in ∼20−30% leakage of DOX contents in 30 min, as compared to other TSL formulations[65,66] having higher serum stability. Chiu et al. also observed 50% loss of encapsulated DOX within 1 h after in vivo administration;[76] however, in this system DOX encapsulation was performed using a transition metal, manganese, which may have an impact. On the contrary, Anyarambhatla et al. showed that LTSL formulation exhibited good retention of encapsulated CF (in FBS and 50% bovine serum) and DOX (in plasma) at 37 °C.[67]

The loss of the lysolipid from the LTSL formulation can have a negative effect on the thermal sensitivity of the vesicle. A time-dependent decrease in the percentage of DOX release was observed from LTSL liposomes recovered after in vivo administration that was consistent with the increase in the percentage of lysolipid loss overtime.[74] DOX leakage from LTSL might be related to the adsorption of serum proteins that could destabilize the lipid bilayer. Previous data and models of protein adsorption through a PEG mushroom coverage[77] suggested that only monomer surfactants can penetrate the PEG stabilizing layer. Further studies on serum adsorption or association with LTSL are needed to reveal the exact mechanism of serum-induced DOX leakage from LTSL. Needham[45] has attempted to offer an explanation, attributing it as a consequence of the relative instability of LTSL upon dilution in biological media. This characteristic of LTSL makes the exact timing between LTSL administration and application of HT as perhaps the most critical parameter to determine its clinical success.

The LTSL vesicle system showed tumor growth retardation in multiple tumor models (colon HCT116, squamous cell FaDu, prostate PC-3, ovarian SKOV-3, and mammary 4T07) as compared to traditional TSL and NTSL.[78] In a FaDu tumor model, LTSL treatment in combination with HT (1 h at 42 °C immediately after injection) showed complete tumor regression up to 60 days as compared to only some tumor growth control (31−35 days) from TTSL and Doxil-like NTSL combined with 1 h HT at 42 °C.[79] Similar results were observed from another study showing complete tumor growth regression 60 days after treatment.[79] The increase in therapeutic efficacy was consistent with the amount of DOX tumor accumulation. Quantification of DOX concentration in the tumor showed that LTSL + HT resulted in the highest tumor drug level (25.6 ng/mg), a 30-fold increase as compared to free DOX and 3−5 times higher than other liposomal treatments at the same temperature.

In addition, the bioavailability of DOX was also improved. LTSL has shown significant DNA-bound fraction of DOX (quantified by sliver nitrate extraction), with almost one-half of the DOX delivered to the tumor tissue becoming bioavailable to tumor cells just 1 h after HT.[79] In contrast, the bioavailable fraction of DOX from free DOX, TTSL, and NTSL was not detectable. These findings indicated that the increased drug release rate of LTSL was crucial to enhance DOX bioavailability, whereas the relatively slow leakage from other liposomal formulations was responsible for their poor bioavailability.[79] A caveat may be that DOX quantification data were restricted to only 1 h after injection, while longer time points (during which increased liposome extravasation is anticipated) were not studied. The conclusion from these studies was that both drug release rate and the drug levels available to tumor cells were crucial to achieve higher therapeutic efficacy.

LTSL offered a novel concept for the delivery of anticancer drugs by promoting ultrafast drug release at the tumor vasculature resulting both in antivascular antineoplastic effects.[79] To allow for intravascular drug release, the loaded drug release

DOI: 10.1021/acs.chemrev.5b00578
Chem. Rev. 2016, 116, 3883−3918

needs to be faster than the transient time of the liposomes in the vasculature of the heated tumor. This is estimated to be around 50 s for a 2-cm tumor.[80] This new paradigm of drug release offered by LTSL overcomes the problems of heterogeneous vascularity and limited penetration as it does not depend on liposomal extravasation.[48] Indeed, a recent preclinical study by Manzoor et al. confirmed that a LTSL injection into preheated tumor not only resulted in DOX release in the bloodstream, but was associated with deeper tumor penetration as observed using intravital fluorescence imaging using the FaDu tumor model.[69] Intravascular release of DOX from LTSL significantly increased the penetration distance within the interstitial space and the time during which tumor cells remained exposed to maximum drug concentration as compared to free DOX and the Doxil-like NTSL.[69] LTSL injection into warm tumor delivered 3.5 times higher DOX levels as compared to the free drug infusion and up to 78 μm from both sides from blood vessels (double the penetration distance of Doxil).

The LTSL thermosensitive system established by Needham has been further developed by Celsion under the trademark ThermoDox and is currently in clinical trials.[81] A Phase I trial was initiated in canine tumors to determine the maximum tolerated dose (MTD) and various pharmacokinetic (PK) parameters.[82] LTSL MTD was 0.93 mg/kg slightly less than that reported for free drug and Doxil. PK parameters of LTSL were closer to free DOX as compared to Doxil. Some differences in drug delivery were observed in this study due to variability in tumor heating, especially for bigger sized tumors, and the possibility of increased core body temperature. Despite that, overall DOX tumor levels for LTSL were 10 times higher than those for free DOX infusion, and an improved therapeutic outcome was observed. Overall, the tumor response observed was considered encouraging for further evaluation in human patients.[82]

Some examples of the human clinical trials undertaken include that of combination therapy with radiofrequency ablation (RFA) in patients with hepatocellular carcinoma (HCC) (Phase III).[37] ThermoDox is also currently clinically tested with other external heating techniques such high intensity focused ultrasound (HIFU) for HCC[83] or with external microwave hyperthermia for recurrent chest wall breast cancer.[84]

Inspired by the developments of LTSL, other TSLs that share similar design principles have been recently described in the literature. The HaT vesicle system, developed by Tagami, is one example. This is based on DPPC lipids with Brij 78 surfactant at 96:4 molar ratios. The Brij surfactant, compromised of a single acyl chain attached to a PEG moiety, has the properties of both lysolipid and DSPE-PEG; therefore, it can theoretically offer both the steric stabilization and the pore-formation capabilities of LTSL.[85] The HaT liposomes released small molecules in a time scale similar to that of LTSL and had very similar drug retention properties at 37 °C (~20% release in 30 min) in vitro, which was consistent with the blood profile data (only 40% remained in the blood in 1 h after injection). Preclinical studies of the HaT vesicles showed slightly higher DOX levels delivered in mouse mammary carcinoma (EMT-6) heated tumors at 43 °C as compared to LTSL. Single treatment with HaT at 3 mg/kg DOX concentration into tumor-bearing mice in combination with HT resulted in enhanced tumor growth retardation as compared to LTSL.[86] HaT-II is an optimized system that was obtained by using Cu^{2+} gradient instead of pH gradient for DOX loading. Slight improvement in the pharmacokinetics (2.5-fold reduction in blood clearance as compared to HaT and LTSL) and tumor accumulation (2-fold relative to LTSL and 1.4 fold vs HaT) was observed from HaT-II that resulted in improved therapeutic efficacy.[87]

Liposomes composed of HePC:DPPC:DSPC:DPPGOG designed by Lindner et al. are another example of this class of TSL. HePC is structurally similar to MPPC lysolipids but chemically and metabolically more stable and can act as an anticancer drug themselves (Figure 6). DPPGOG lipid was used

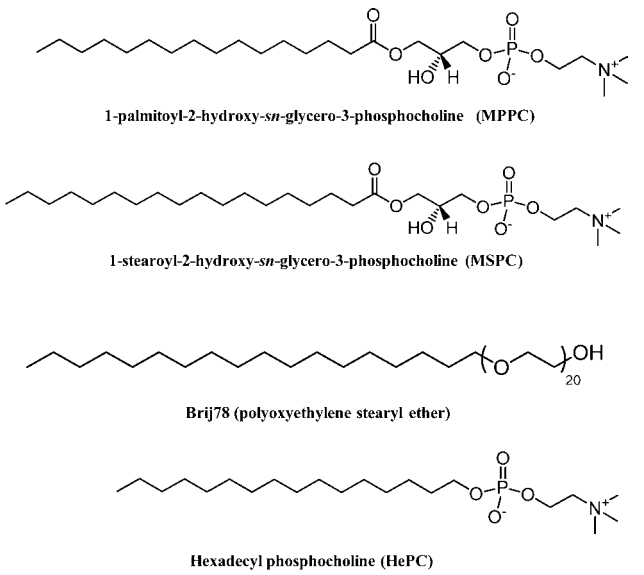

Figure 6. Chemical structures of the lipids used for the design of lysolipids-containing TSL.

to replace DSPE-PEG_{2000} as it was shown previously by the same group to prolong the circulation half-life of liposomes and enhance temperature sensitivity.[88] This liposome system performed in a very similar way to lysolipid-containing vesicles, resulting in 90% CF release at 42 °C after 5 min incubation in the presence of 90% fetal calf serum.

2.3. Polymer-Based TSL

2.3.1. TSL Based on Synthetic Temperature-Responsive Polymers. Another strategy for designing temperature-responsive liposomal systems is to attach thermosensitive amphiphilic molecules (particularly temperature-responsive polymers) to the liposomal membrane. These polymers have a temperature-disruptive effect on the lipid membrane because they change in conformation in response to changes in environmental temperature. Temperature-sensitive polymers can either attain a thermoresponsive property to nontemperature-sensitive liposomes or improve thermal responsiveness of thermosensitive liposomes. At the molecular level, thermosensitive polymer chains undergo a coil to globule transition as the temperature passes through their low critical solution temperature (LCST) (Figure 7). Below LCST, the polymer is hydrated and sterically stabilizes the liposomes surface. As the temperature increases (T > LCST), condensation of the polymer results in exposing the liposome surface, which leads to destabilization and content release.[89]

Some polymer molecules change from hydrophilic to hydrophobic with temperature; therefore, stabilization and destabilization of polymer-modified TSL can be controlled by temperature, in this way also controlling drug release and interaction with cells and serum proteins.[89] Table 1 summarizes the different examples of polymer-modified TSL described in the

DOI: 10.1021/acs.chemrev.5b00578
Chem. Rev. 2016, 116, 3883−3918

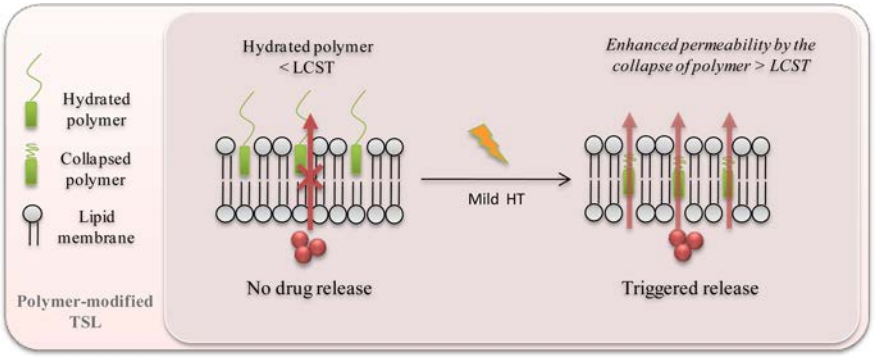

Figure 7. Mechanism of drug release from polymer-modified TSL. Below the LCST, polymer chains are hydrated, which gives a stabilizing effect to the liposomes. When the ambient temperature exceeds LCST, the polymer becomes dehydrated and changes into globule status. This destabilizes the lipid membrane and releases liposomal content.

Table 1. Examples of Polymer-Modified Temperature-Sensitive Liposomes

liposomal composition	temperature-sensitive polymer	LCST (°C)	dye/drug	experimental design	refs
EPC and DPPC	p-(NIPAM-ODA)	27	CF calcein	in vitro release study	92
DOPE	p-(NIPAM-ODA)	32	calcein	in vitro release study	95
EPC, DMPC:DPPC	p-(NIPAM-AA-ODA)	30−43	calcein	in vitro release study	94
DPPC and DSPC					
DLPC	p-(NIPAM-ODA)	32	calcein	in vitro release study	96
DPPC					
DSPC					
EPC and EPC:DOPE	p-(NIPAM-NDDAM)	28	calcein	in vitro release study	91
EPC	p-(APr-NIPAM)-$2C_{12}$	40	MTX	in vitro release study and cellular cytotoxicity	97
DOPE	p-(APr-NIPAM)-$2C_{12}$ p-(APr-NIPAM-NDDAM)	33−34	calcein	in vitro release study	98
DOPE:EPC	p-(NIPAM-NDDAM-AAM) p-(NIPAM-AAM)	39−46	calcein	in vitro release study (increasing LCST)	99
DOPE	p-(APr-NIPAM)-$2C_{12}$ PEG_{550}-$2C_{12}$	38	calcein	in vitro release study and serum stability (effect of PEG)	100
EPC	p-(APr-NIPAM)-$2C_{12}$ p-(DMAM-NIPAM)-$2C_{12}$ p-(NIPAMAM-NIPAM)-$2C_{12}$	40	calcein	in vitro release study (effect of ΔH)	101
DOPE:EPC	p-(EOEOVE-ODVE)	36	calcein	in vitro release study	102
DPPC:HSPC:CHOL:DSPE-PEG-2000	p(NIPAM-AAM)	40 and 47	DOX	in vitro release and stability study	93
DPPC:HSPC:CHOL:DSPE-PEG_{2000}[a]	p(NIPAM-AAM)	40	DOX	in vitro and in vivo study	103
DPPC:CHOL and DOPE-EPC	p(HPMA mono/dilactate)-CHOL	42	calcein DOX	in vitro release study/HIFU	104,105
DPPC:HSPC:CHOL:DSPE-PEG_{2000}	p(NIPAM-PAA)-DMP	42 °C at pH 6.5	DOX	in vitro pH and temperature sensitivity	106
EPC:CHOL-DSPE-PEG_{2000}[a]	p(EOEOVE-ODVE)	40	DOX	in vitro and in vivo study	107,108
EPC:CHOL-DSPE-PEG_{2000}-Gd[a]					
EPC:DSPE-PEG_{5000}-Fe 3O4	p(EOEOVE-ODVE)	40	pyrene	magnetic imaging and heat triggered release	109

[a]These studies represent polymer-modified liposomes that progressed to preclinical investigation.

literature. The "host" lipid vesicle bilayers, the types of thermosensitive polymers used, and their LCSTs are explained. For chemical structures of temperature-sensitive polymers used, please refer to Figure 8. Most of the early examples of polymer-modified TSL were designed with *N*-isopropylacrylamide (p-NIPAM), the most extensively studied thermosensitive polymer. It has an LCST around 32 °C; however, it can be adjusted by copolymerization with other monomers with different hydrophilic or hydrophobic moieties.[90] LCST decreases by copolymerization with hydrophobic monomers such as ODA and NDDAM,[91,92] and it can be increased by copolymerization with hydrophilic polymers, for example, AA or AAM.[93,94]

Polymer-modified TSL was first proposed by Kono et al. with the engraftment of p-(NIPAM-ODA) polymer into the lipid bilayer through the hydrophobic group of ODA. The long alkyl chain of ODA serves as an anchor to fix the hydrated part of the polymer into the liposome surface.[92] In this early study, Kono and co-workers studied the effect of surface modification of both nontemperature sensitive liposomes (EPC) and thermosensitive liposomes (DPPC) with p-(NIPAM-ODA) and found an

DOI: 10.1021/acs.chemrev.5b00578
Chem. Rev. 2016, 116, 3883−3918

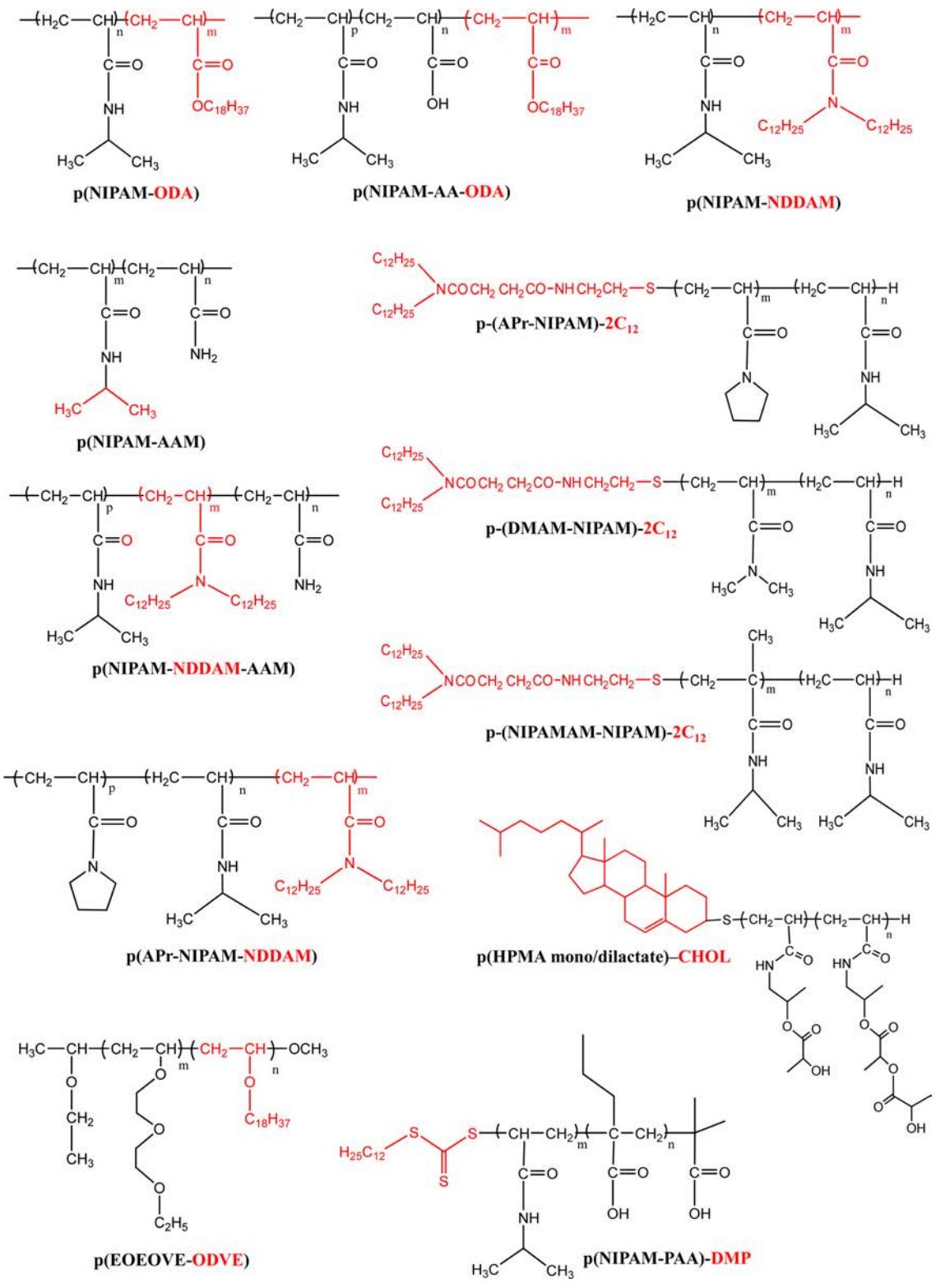

Figure 8. Chemical structures of temperature-sensitive polymers used for the design of TSL. Chemical groups represented in red color stand for the hydrophobic anchor groups used to fix the polymers into the lipid bilayer.

increased release of encapsulated fluorescent dye molecules at temperatures greater than the LCST of the polymer (~70% calcein release from DPPC liposomes and ~45% CF release from EPC liposomes at 41 °C), with minimum release below the LCST (<10% at 20 °C). The higher release observed from polymer-modified DPPC liposomes as compared to EPC indicated a synergistic effect between the thermal responsiveness of DPPC liposomes and the membrane destabilization induced by the polymer.

The hydrophobic anchors used for polymer fixation can be either randomly distributed along the polymer backbone or attached at the end of the polymer. Kono et al. studied the effect

DOI: 10.1021/acs.chemrev.5b00578
Chem. Rev. 2016, 116, 3883−3918

of the anchor position on the content release properties of calcein-loaded DOPE liposomes. Dramatic release over a narrow temperature range was seen from DOPE liposomes modified with polymer having the terminal anchor (p-(APr-NIPAM)-C_{12}) (70−90% release over temperature range from 41 to 42 °C) as compared to those modified with the middle anchor p-(APr-NIPAM-NDDAM) (only 60% release at 45 °C).[98] Polymers attached to one end can change easily from a hydrophilic to a hydrophobic status as compared to polymers fixed through multiple points because of the higher conformational freedom of the former.[89,98] Stronger attachment of the polymer-anchor chain to liposomes in the gel phase was observed as compared to fluid lipid bilayer vesicles.[92] The interaction between the polymer and the lipid bilayer was not dependent on the T_m of the lipid bilayer, but rather took place above the LCST.[92] This phenomenon was explored systematically by Kono et al. and Kim et al. by studying the effect of pNIPAM-AA-ODA and pNIPAM-ODA polymers on the release of a fluorescent dye from fluid and gel-phase bilayers. The release from liposomes having fluid nature is covered by the LCST of the polymer itself. In contrast, liposomes in the gel phase showed maximum release at the T_m of the liposomes. In both cases, maximum content release was achieved from polymer-modified liposomes as compared to plain liposomes.[92,94]

The interaction of the polymer with the lipid bilayer can be improved by changing the lipid composition of liposomes, especially for those of fluid phase bilayers. Inclusion of DOPE in EPC liposomes-surface coated with p(NIPAM-NDDAM) increased the content release above the LCST. An almost 20% increase in calcein release was measured from DOPE:EPC liposomes (64:36 mol/mol) as compared to pure EPC liposomes. This was probably because of H-bond formation between DOPE lipids and the polymer and the thermodynamic tendency of DOPE lipid to self-assemble in nonbilayer structures.[91]

Early examples of polymer-modified TSL were designed with polymers having LCST below the body temperature, therefore not clinically suitable. New copolymers of NIPAM were later synthesized to have LCST around physiological temperatures. Hayashi et al. showed that the LCST of NIPAM can be adjusted around body temperature by free radical copolymerization with AAM monomers. An increase in NIPAM LCST was obtained by increasing the percentage of AAM monomers in a concentration-dependent manner.[99] Therefore, the release of encapsulated calcein can be adjusted at the desired temperature by controlling LCST of the polymer. Similar findings were observed by Han et al. using DOX-loaded DPPC:HSPC:CHOL:DSPE-PEG_{2000} modified with p(NIPAM-AAM).[93]

The effect of comonomer type on content release was also investigated by studying three copolymers of NIPAM having the same LCST (40 °C) but with different transition endotherms (ΔH): p-(APr-NIPAM)-$2C_{12}$, p-(DMAM-NIPAM)-$2C_{12}$, and p-(NIPAMAM-NIPAM)-$2C_{12}$. To test if the structural difference between the polymers affects their interaction with lipid membranes and the percentage of content release, all three polymers were fixed to EPC liposomes by two dodecyl anchors at the termini of the polymer. Although all three polymers tested have the same LCST (40 °C), when interacted with EPC lipid membranes different percentages of calcein were released. Although LCSTs of these three polymers measured by cloud point and DSC were almost similar, the enthalpy of their transition (ΔH) was different because it correlated with the loss of water around the hydrophobic groups. The percentage release of entrapped calcein from polymer-modified EPC liposomes increased with higher ΔH of the polymers in the following order: p-(APr-NIPAM)-$2C_{12}$ < p-(DMAM-NIPAM)-$2C_{12}$ < p-(NIPAMAM-NIPAM)-$2C_{12}$. The high ΔH of p-(NIPAMAM-NIPAM)-$2C_{12}$ indicated that this polymer formed the most hydrophobic domains above LCST and therefore resulted in the highest membrane disruptive effect. Although these liposomes showed rapid drug release at 42 °C, this was associated with poor content retention capacity (~40% released within 15 min) at 37 °C.[101]

Modification of liposomes with thermosensitive polymers also has the advantage of increasing the blood circulation time of liposomes and minimizing the uptake by MPS cells in a way similar to surface modification of liposomes with PEG polymer.[103] Han et al. have studied the interaction of DPPC:HSPC:CHOL liposomes modified with p(NIPAM-AAM) (LCST at 40 °C) with serum proteins by quantifying the amount of adsorbed protein over time at 37 °C up to 48 h. Below the LCST, the polymer existed in the hydrated state that reduced the amount of adsorbed proteins as compared to plain liposomes. In the same study, protein adsorption was significantly reduced by introducing DSPE-PEG_{2000} lipid into p(NIPAM-AAM) modified liposomes.[103]

Along with other types of TSL, the inclusion of PEGylated lipid into polymer-modified liposomes was shown to increase their serum stability at temperatures below LCST and to enhance the thermal sensitivity at higher temperatures.[93,100,103] Kono et al. and Han et al. have shown that both PEG_{550}-$2C_{12}$ and DSPE-PEG_{2000} improve serum stability at body temperature and dramatically increase the percentage of drug release over a narrow temperature range.[93,100,103] Recently, Kono et al. reported the optimization of EPC:CHOL liposomes surface coated with p(EOEOVE-ODVE) polymer for in vivo administration by including 4 mol % of DSPE-PEG_{2000} into the lipid bilayer. These liposomes showed less than 10% DOX leakage at 37 °C as compared to more than 20% from non-PEGylated liposomes.

The same concept applied to cellular internalization studies of polymer-modified liposomes. The cell uptake of this type of TSL was found largely temperature dependent. This effect has been studied by Kono et al. looking at the interaction of MTX-loaded EPC liposomes modified with p-(APr-NIPAM)-$2C_{12}$ and EPC:CHOL:DSPE-PEG_{2000} liposomes modified with p-(EOEOVE-ODVE) thermosensitive polymer with CV1 and HeLa cells, respectively. Polymer-coated liposomes did not affect cell viability at 37 °C; however, cytotoxic activity was dramatically enhanced with temperature increase (almost similar to free drug).[107] HeLa cells treated with polymer-coated liposomes showed limited drug uptake; however, a substantial increase in intracellular drug concentration with nuclear localization was observed after 5 min of heating at 45 °C.[107]

A critical drawback of the early work of NIPAM-based polymers was the large polydispersity index and the difficulty to control the molecular weight of the polymer. Overcoming those limitations in recent designs meant a sharp response to temperature over a narrow temperature range.[102] Examples of such polymers include the p(NIPAM-PAA) prepared by RAFT chemistry[106] and the poly(*N*-vinylethers) synthesized by living cationic polymerization.[102] Liposomes modified with p(NIPAM-PAA)-DMP showed interesting temperature and pH sensitivity due to the presence of ionizable carboxyl groups that lowered the LCST at acidic conditions (e.g., tumor microenvironment) and enhanced drug release.[106]

DOI: 10.1021/acs.chemrev.5b00578
Chem. Rev. 2016, 116, 3883−3918

Table 2. TSL Based on Thermosensitive Biopolymers

liposomal composition	temperature-sensitive biopolymer	LCST (°C)	complexation method	dye/drug	refs
DPPC:DSPC:DSPE-PEG$_{2000}$[a]	coiled-coil leucine zipper peptide	40	self-assembly	DOX	115
PC:DSPE-PEG$_{2000}$	γ-amino acid mutated coiled-coil peptide	40	self-assembly	CF	116
HSPC:CHOL:DSPE-PEG$_{2000}$	DSPE-PEG$_{2000}$-MLAYAYSKGPG-[ELP]$_{20}$-WP	40	covalent linkage to DSPE-PEG$_{2000}$ terminal	DOX	117
DPPC:DSPE-PEG$_{2000}$:CHOL[a]	stearyl-ELP$_3$-NH$_2$	~40 °C at 0.5 mM	covalent linkage to monostearyl chain	DOX	111

[a]These studies represent biopolymer-modified liposome systems that progressed to preclinical investigations.

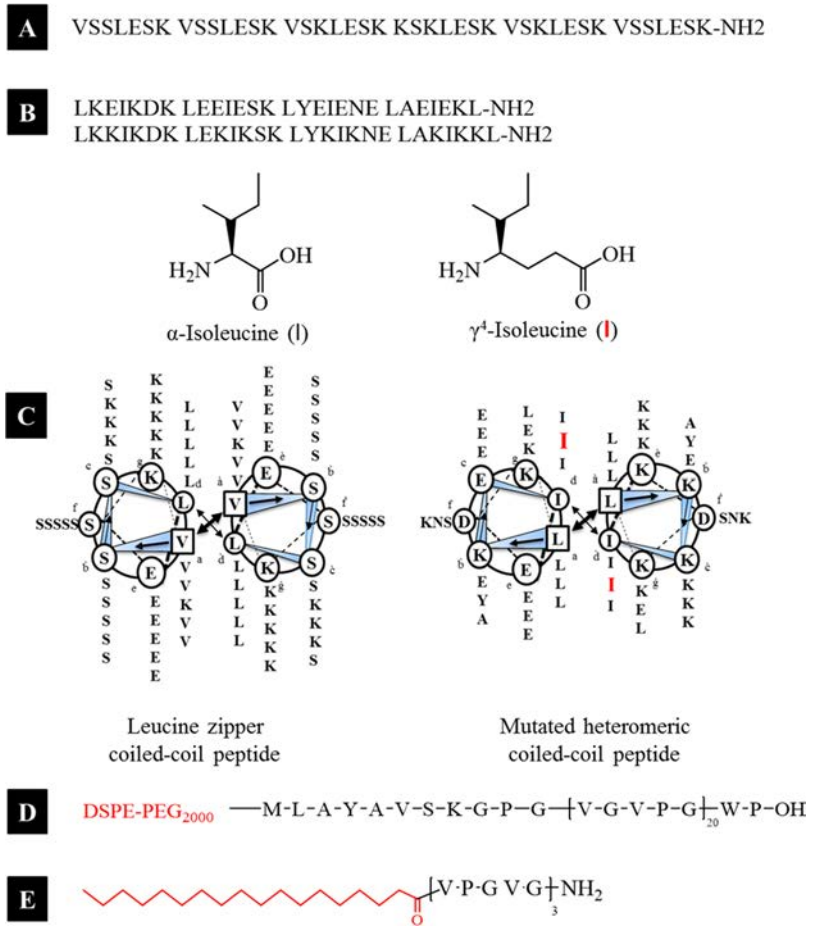

Figure 9. Temperature-sensitive biopolymers used in the design of TSL. Chemical amino acids sequences of different peptides used for the design of TSL are explained: (A) leucine zipper coiled-coil peptide; (B) mutated coiled-coil peptide. Sights of mutations of isoleucine in the hydrophobic positions are represented by (**I**). (C) Wheel diagrams of leucine zipper peptide and mutated coiled-coil peptide. The arrangement of the amino acids illustrated by the wheel diagram, showing the winding of the two α-helices around each other and the formation of the hydrophobic interhelical core. (D,E) ELP$_{20}$ and ELP$_3$ lipid conjugates, respectively.

As an alternative to pNIPAM-based polymers, poly(*N*-vinylethers) have been used recently for the design of TSL. Poly(*N*-vinylethers) act in the same way as pNIPAM; their LCST can be controlled by copolymerization with hydrophobic monomers that serve as anchor moieties to engraft the polymer onto the lipid membrane. Recently, Kono et al. showed that incorporation of p(EOEOVE-ODVE) polymer with a LCST of 40 °C into EPC:CHOL:DSPE-PEG$_{2000}$ liposomes led to less than 10% of DOX leakage at 37 °C and more than 90% of DOX release after 1 min incubation at 45 °C. The interaction of partially dehydrated polymer chains with PEG groups at the surface of liposomes minimized their interaction with the lipid membrane at temperatures below the LCST (40 °C). As LCST was exceeded, a fully dehydrated polymer can result by H-bond formation among the PEG chains. This increases their interaction with the lipid bilayer causing vesicle destabilization and drug release.[107] The enhanced stability at body temperature and ultrafast response to hyperthermic conditions suggested the suitability of this formulation for in vivo applications.[107]

Despite the interesting results of polymer modified liposomes described in vitro, only few preclinical studies were reported to evaluate their in vivo therapeutic activity. Han et al. studied the tumor growth retardation effect of DOX-loaded DPPC:HSPC:CHOL:DSPE-PEG$_{2000}$ liposomes modified with p(NIPAM-AAM) polymer after injection into B16F10 tumor-bearing mice at 6 mg/kg DOX in combination with 10 min local HT at 42 °C. Similarly, Kono et al. evaluated tumor growth retardation using EPC:CHOL:DSPE-PEG$_{2000}$ liposomes modi-

DOI: 10.1021/acs.chemrev.5b00578
Chem. Rev. 2016, 116, 3883−3918

fied with p(EOEOVE-ODVE) after injection into C26 tumor-bearing mice. Therapeutic activity was studied with and without exposure to 10 min local HT at 45 °C 6−12 h after injection.[107] The results of these studies showed promising tumor growth retardation when used in combination with local HT, which agreed with the previous in vitro data. More complex multifunctional liposomes based on this system have been prepared recently, either by surface modification with Gd chelates[108] or by incorporation of iron oxide nanoparticles into the lipid membrane to provide the capability of monitoring liposomes by MR imaging along with their temperature-triggered release properties.[109]

The design of polymer-modified TSL offers more flexibility as compared to other types of TSL. This helps to overcome some of the limitations of the prototypical TSL, such as the types of the lipids available, the size of the drug to be released, and the temperature range required for content release.[89,96,100,102] Nevertheless, more work is warranted before this type of TSL can enter clinical development. The design and synthesis of temperature-sensitive polymers that respond under narrower temperature ranges is necessary to maintain stability under physiological conditions and ensure effective drug release under mild HT. Further in vivo studies are required to compare the pharmacokinetic parameters and toxicological burden of these vesicles by maintaining higher therapeutic efficacy as compared to other TSL types.

2.3.2. TSL Based on Temperature-Responsive Biopolymers. Similar to thermosensitive synthetic polymers, thermosensitive biopolymers have gained more interest recently in the design of TSL. Biopolymers such as poly- and oligo-peptides can be readily produced with a defined sequence and chain length, thus offering better control of transition temperature as compared to synthetic polymers.[110] Biopolymers also overcome some of the problems associated with synthetic polymers such as biodegradability and potential toxicological profile.[111] MacKay and Chilkoti have shown that a highly ordered biopolymer with complex temperature-responsive properties can be produced from oligopeptides with repeated short sequences (<7 amino acids in length). This could provide new molecular tools for engineering hyperthermia-mediated drug delivery systems.[39]

For application in triggered drug delivery, two important properties of temperature-sensitive peptides should be considered: directionality and reversibility. Directionality usually refers to the self-association and dissociation changes of the peptide in response to heating. Reversibility describes whether or not the peptide secondary structure is retained upon cooling.[39] For example, self-associated peptide−drug[112] or peptide−polymer conjugates[113,114] that aggregate in response to HT showed an interesting increase in the amount of drug molecules that could be delivered to tumor tissue. The aggregation of the peptide in response to temperature leads to the formation of self-assembled nanoparticles or micelles and if the peptide is tagged with targeting ligands improvements in target specificity could be achieved by constructing multivalence targeting nanoparticles.[114] In the opposite case, if peptide micelles dissociate by HT, this can facilitate the diffusion of monomeric peptides into the tumor.[39] Examples of different biopolymers used in the design of TSL are summarized in Table 2. The "host" liposomal system, the types of thermosensitive biopolymers used, and their LCST are explained.

Coiled-coil leucine zipper peptides present an interesting example of temperature-responsive biopolymers that have the ability to dissociate above their melting temperature. Coiled-coil peptides composed of two or more α-helices self-assembled to form dimers or higher-order superhelix structures.[118−120] Leucine zipper peptide sequences are characterized by heptad repeats (abcdefg) of 7 amino acids (Figure 9A). At appropriate pH and temperature conditions, the naturally unfolded peptide self-associates, adopting an α-helix conformation that exposes the hydrophobic a and d residues on one side of the helix.[118] Above the melting temperature, dissociation of the coiled-coil structure occurs, leaving disordered peptide monomers.[121] The ability to modulate the peptide transition temperature, its conformational changes in response to heat, and its potential in the field of drug delivery[39,120] make leucine zipper peptides attractive components for the design of temperature-responsive delivery vesicles.[122]

Recently, we have described the previously unreported design of a thermosensitive lipid-peptide hybrid system (Lp-peptide) by self-assembly of the temperature-sensitive coiled-coil leucine zipper peptide within the lipid bilayer of DPPC:DSPC:DSPE-PEG_{2000} (90:10:5) (Figure 10). This system combines the traditional temperature-responsive liposome technology with the dissociative/unfolding properties of a leucine zipper sequence peptide to allow better control, modulation, and timing of drug release under mild hyperthermia while maintaining good drug retention.[115] The Lp-peptide hybrids exhibit a promising enhancement in serum stability at physiological temperatures as compared to LTSL without compromising the thermoresponsiveness of the system at 42 °C. The leucine zipper peptide appears to be in an unfolded state at the higher temperatures required for drug release.

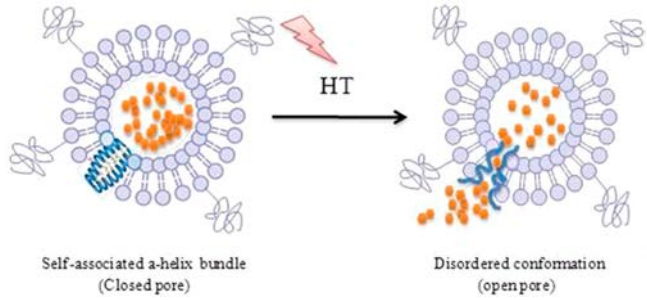

Figure 10. Schematic representation of temperature-triggered release from Lp-peptide hybrids.

In agreement with in vitro data, Lp-peptide hybrids retained more than 50% of encapsulated DOX after intravenous administration. Quantification of ^{14}C-DOX accumulation into B16F10 tumor in combination with HT revealed a DOX level 1 h after injection equivalent to that observed from LTSL tested under the same conditions. Interestingly, the high drug retention capability of Lp-peptide hybrids was clearly reflected in the 3-fold increase in DOX tumor levels 24 h after injection as compared to LTSL formulation.[115] The increase in the early and delayed DOX tumor levels from Lp-peptide hybrids makes this system interesting for both intravascular and interstitial triggered drug release[123] as will be discussed in more detail in section 3.2. Similarly, Jadhav et al. have recently reported the design of self-assembled TSL by mixing PC:DSPE-PEG_{2000} liposomes with mutated coiled-coil temperature-sensitive peptides prior to liposome formation. In this case, α-isoleucine amino acid is replaced by γ-isoleucine at the hydrophobic positions of the heptad repeats (d position) as shown in Figure 9B.

DOI: 10.1021/acs.chemrev.5b00578
Chem. Rev. 2016, 116, 3883−3918

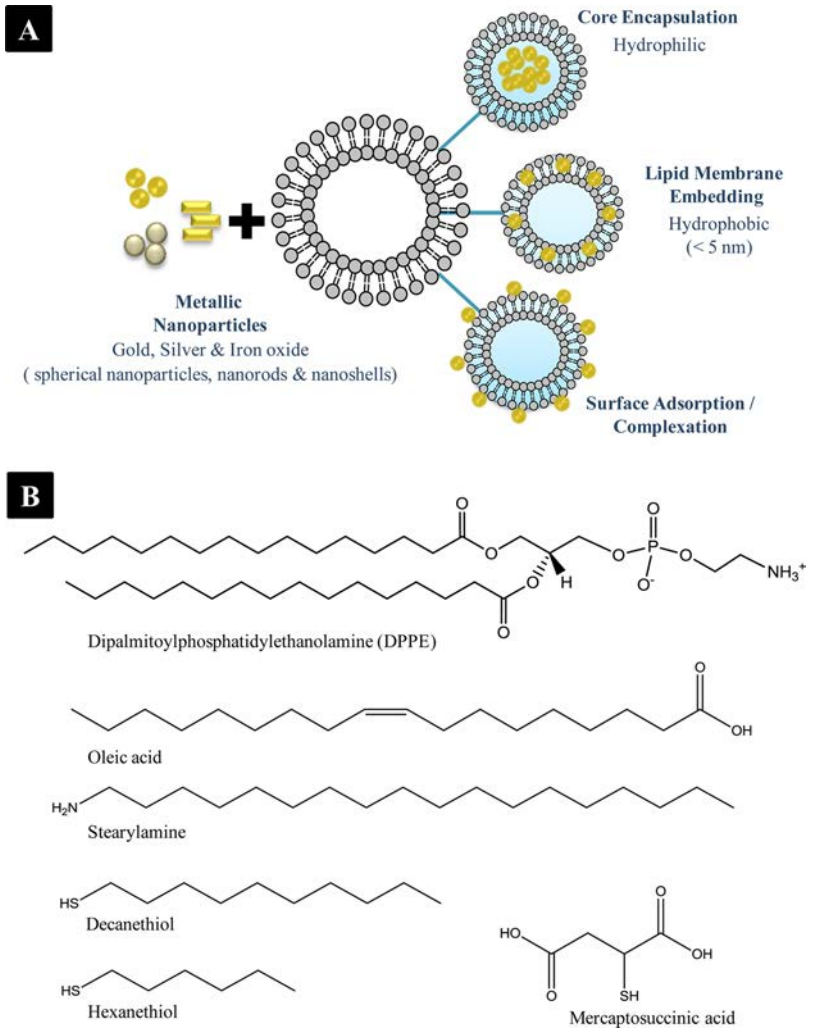

Figure 11. Different strategies used for the design of TSL-NPHs. (A) Three main strategies have been reported for the preparation of TSL having metallic nanoparticles: encapsulation, lipid bilayer embedding, or surface adsorption/complexation. (B) Chemical structures of the coatings used for surface functionalization of metallic nanoparticles.

The selective insertion of γ-isoleucine amino acids led to perturbation of both hydrophobic and ionic forces responsible for the coiled-coil peptide stabilization and resulted in thermal dissociation at approximately 40 °C as compared to 67 °C for the nonmutated heteromeric peptides.[116] As a proof of concept, CF dye was used to test the thermal sensitivity of these liposomes. As expected, thermally induced dye release (at 40 °C) was observed only from liposome peptide hybrids having the mutated coiled-coil peptides as compared to no significant release from nonmutated peptides.[116]

Another example of temperature-responsive biopolymers are the elastin-like polypeptides (ELPs) that have shown promising results in cancer therapy, due to their ability to deposit and switch conformation in heated tissues and tumors. ELP consists of repeated pentapeptide, and its transition temperature can be adjusted according to the length,[124] sequence, concentration,[124] ionic strength,[125,126] and the fusion to other molecules.[127] Below its transition temperature, ELP is present in soluble form that is stabilized by hydrogen bonds formation with the water molecules. Above the transition temperature, intramolecular hydrophobic interactions of ELP resulted in a change in its conformation from a random coil to a β-turn forming gel-like phase.[111,128] Chilkoti's lab has rationally designed several ELPs that respond within the range of mild HT by optimizing their sequence and molecular weight and showed that ELPs retain their thermal properties after chemical conjugation.[128] Using fluorescently labeled ELP, they have also showed that cellular uptake of thermally sensitive ELP increased above the phase transition into three different cell lines as compared to the thermally inactive ELP.[129] This effect was mainly due to increased hydrophobicity of the peptide above the phase transition temperature that enhanced interactions with cell membranes.[129] Recently, DOX-loaded liposomes modified with the thermosensitive ELP have been designed by covalent linkage of the peptide to the terminal end of the DSPE-PEG_{2000} (Figure 9D). These liposomes showed enhanced cellular uptake by tumor cells after heating at the transition temperature of the peptide as a result of the peptide dehydration at the liposomal surface. ELP dehydration after heating at 42 °C was also associated with liposome aggregation (up to 600 nm) as a result of the interaction of ELP molecules at the liposomal surface. Despite contraction of ELP on the liposomal surface, this was not enough to induce drug release. This might be explained by the rigid nature of the liposomes used and the long distance between the peptide and lipid bilayer.[117] This problem was resolved by Kim et al., who described the incorporation of ELP into

DOI: 10.1021/acs.chemrev.5b00578
Chem. Rev. 2016, 116, 3883−3918

temperature-sensitive lipid bilayers using a monostearyl hydrocarbon tail covalently linked to ELP (Figure 9E).[111,130] These liposomes were temperature-sensitive and composed of DPPC:CHOL:DSPE-PEG_{2000}, and therefore less rigid as compared to the previous example. The amount of drug content release in response to hyperthermia was balanced by the phospholipid content, cholesterol, and ELP length and concentration. Incubation of these liposomes in 20% serum at 42 °C released more than 95% of encapsulated DOX in 10 s while maintaining good DOX retention at 37 °C. This might be explained by the short chain length of ELP and the close proximity to the lipid bilayer, so that the conformational changes above the transition temperature could be responsible for the disruption of the dynamic equilibrium within the lipid membrane.[111]

Intravenous injection of these liposomes into squamous cell carcinoma (SCC-7) tumor bearing mice in combination with HIFU immediately after injection showed promising tumor growth regression, particularly in the first 2 days after treatment as a result of intravascular drug release.[111] Similar to the Lp-peptide hybrid system, ELP-TSL also proved to be effective in controlling tumor growth when heated 6 h after intravenous administration to achieve maximum tumor accumulation.[130] Although the field of TSL based on biopolymers is still in its infancy, the examples presented above demonstrated the opportunities of harnessing the interesting thermal properties of biopolymers for successful tuning of drug release at the disease site.[116]

2.4. Metallic Nanoparticle-Based TSL (TSL-Nanoparticle Hybrids)

Liposomes and nanoparticles may be clinically approved as separate entities; however, the field of liposome−nanoparticle hybrids is still relatively new and represents a promising approach for the design of multifunctional delivery systems.[131] Liposome−nanoparticle hybrid engineering involves either encapsulation of nanoparticles inside the aqueous core of liposomes, embedding within the lipid bilayer, or surface adsorption onto the liposome surface and complex formation (Figure 11).[131,132] Such hybrid systems combine the inherent properties of both liposomes and nanoparticles and present potentially innovative multifunctional platforms for therapeutic and imaging applications. In addition, the incorporation of metallic nanoparticles can be used as a heating source when exposed to external stimuli such as alternating electromagnetic field (MF) or light.[133−135]

Nanoparticle-enhanced HT by means of radiofrequency (RF) or photothermal heating has been used to heat local malignant tissues to temperatures between 40 and 45 °C or for thermoablative therapy (>50 °C) to induce cellular necrosis and apoptosis by denaturing of intracellular proteins.[136−138] Furthermore, nanoparticle-induced HT proved to have a synergistic effect when used in combination with chemotherapy.[133,139] HT induced with metallic nanoparticles can address some of the problems encountered with conventional HT techniques such as the difficulty in applying heat to deep or not readily accessible tumors.[131] An example of such approach is the use of iron oxide nanoparticles for the generation of magnetic HT,[137] which has been clinically tested for glioblastoma multiforme[140,141] and prostate cancer.[142,143]

When used in conjunction with liposomes, nanoparticle-induced HT can provide a tool for triggered local drug release and theranostic applications. An example is the folate-targeted magnetic liposomes developed by Pardhan et al. that coencapsulated iron oxide nanoparticles and DOX. These targeted magnetic liposomes depicted a significant increase in cellular uptake equivalent to free DOX and a synergistic cytotoxic response after triggered release with magnetic HT. Besides the biological targeting against folate receptor, this system can be magnetically guided toward the target of choice.[139]

2.4.1. Engineering of TSL-Nanoparticle Hybrids (TSL-NPHs). The design of TSL-NPHs can be divided into three main strategies, by encapsulation into the aqueous core of the liposome, lipid membrane embedding, and surface adsorption/complexation (Figure 11).

Encapsulation of preformed metallic nanoparticles into the core of the liposomes is the simplest and can be prepared by thin film hydration,[139] reverse phase evaporation,[144,145] or interdigitated phase transition.[146] The critical parameters in designing this type of TSL-NPHs are the colloidal stability of the nanoparticle solution and the diameter of the nanoparticles that must be smaller than the diameter of the vesicle aqueous core. The concentration of nanoparticles also restricts the available volume for coencapsulation of other water-soluble molecules.[131]

The incorporation of metallic nanoparticles into the lipid membrane is influenced by the differential osmotic pressure across the lipid membrane and the repulsive and attractive forces between the lipid membrane and the nanoparticles.[131] It also requires the nanoparticles to be hydrophobic with a size that is comparable to or smaller than the thickness of the lipid membrane (5 nm).[147] For larger nanoparticles, lipid molecules can be distorted significantly to accommodate the hydrophobic nanoparticles with sizes larger than their acyl chain length. This is in agreement with the accommodation of large transmembrane proteins within the cell membrane.[148] Nanoparticle adsorption or complexation forms when hydrophilic nanoparticles are coupled to the surface of liposomes by attractive forces or electrostatic interaction. This type of TSL-NPHs is relatively easier to prepare by mixing metallic nanoparticles with preformed liposomes. Nanoparticles incorporated into the lipid membrane or adsorbed onto liposome surfaces may have the advantage of providing direct local heating of the bilayer when exposed to external stimuli.[4,109,149,150]

2.4.2. Applications of TSL-NPHs. The applications of TSL-NPHs are determined by the type of nanoparticles, the "host" lipid bilayer, and the interaction between the nanoparticles and the lipid membrane. In general, TSL-NPHs have the advantage of shielding the nanoparticles, which reduces their interaction with external molecules and increases their biocompatibility.[131] TSL-NPHs increase nanoparticle cellular uptake, which is important for imaging and hyperthermia applications.[151] Besides being a carrier for nanoparticles, TSL-NPHs with thermosensitive properties can overcome the limitations of conventional TSL by offering site-specific drug release utilizing nanoparticle heating to control the onset and duration of drug release.[139,152]

The imaging and thermal characteristics of gold nanoparticles are related to their enhanced surface plasmon resonance properties. The latter allows absorbed light at certain wavelengths to cause oscillation of surface electrons and, subsequently, local heat generation. Heat generation can be controlled by the intensity of the laser light, duration of exposure, and the concentration of gold nanoparticles.[153] Photothermal energy can then transfer into the lipid membrane, leading to phase transition of the bilayer from gel phase to liquid crystalline phase, causing triggered drug release.[149]

DOI: 10.1021/acs.chemrev.5b00578
Chem. Rev. 2016, 116, 3883−3918

Table 3. TSL-NPHs Decorated with Gold NPs

liposomal formulation	NPs type/size	coating	position	dye/drug	function	refs
DPPC	spherical NPs (3−4 nm)	stearyl amine	lipid membrane		concentration-dependent increase in membrane fluidity	156
DPPC:DSPC	spherical NPs (2.5 nm), spherical NPs (2.8 nm), DPPE-nanogold (1.4 nm)	C6-SH, MSA, DPPE	lipid membrane, core, surface adsorbed	calcein	UV light triggered release (250 nm)	157
DPPC	nanoshell (33 nm)	SH-PEG-lipid linker	core/lipid membrane/ surface adsorbed	CF	NIR triggered release (820 nm)	146
DPPC:DPTAP:CHOL	spherical NPs (20 nm)	NR	complex	CF	NIR triggered release (830 nm)	135
DSPC:DPPC	spherical NPs (2.5 nm), spherical NPs (4 nm)	C6-SH, MSA	lipid membrane, core	calcein	UV triggered release (365 nm)	150
DPPC:CHOL:DSPE-PEG_{2000}	DPPE-nanogold (1.4 nm)	DPPE	surface adsorbed		cellular uptake enhancer	151
EPC:CHOL	spherical NPs (5 nm)	di-2-ethylhexyl sulfosuccinate	lipid membrane	berberine	UV light triggered drug release (250 nm)	158
EPC:CHOL	spherical NPs (5 nm)	sodium dioctyl sulfosuccinate	lipid membrane	berberine	UV light triggered drug release (250 nm)	149
DPPC:HSPC:CHOL:DSPE-PEG_{2000}[a]	hollow gold nanospheres (30−50 nm)	OMP	surface adsorbed	DOX	NIR triggered release (808 nm)	159

[a]This study represents TSL-NPHs that progressed to preclinical evaluation.

Table 4. TSL-NPHs Decorated with Silver NPs

liposomal formulation	nanoparticle type/size	coating	position	dye/drug	function	refs
DPPC	spherical NPs (4 nm)	stearylamine	lipid membrane		increase lipid membrane fluidity	160
DPPC	spherical NPs (5.7 nm)	decanethiol	lipid membrane		reduce T_m and increase lipid membrane fluidity	148

Table 5. TSL-NPHs Decorated with Iron Oxide NPs

liposomal formulation	nanoparticle type/size	coating	position	dye/drug	function	refs
DPPC	Fe_3O_4 NPs (5−10 nm)	dextran	core	5-FU	MF-induced drug release	145
DPPC:CHOL[a]	γ-Fe_2O_3 NPs (10 nm)	glutamic acid	core	MTX	magnetic targeting	144
DPPC:CHOL	γ-Fe_2O_3 NPs (45−60 nm)	dextran	core	CF	MF-induced release	161
DPPC	γ-Fe_2O_3 NPs (5 nm)	oleic acid	lipid membrane	CF	MF-induced release	4
DPPC:CHOL:DSPE-PEG(2000)DSPE-PEG(2000)-folate	Fe_3O_4 NPs (10 nm)	SH	core	calcein/ DOX	MF-induced release by HT	139
DPPC:CHOL	Fe_3O_4 NPs (12.5 nm)	NR	core		lipid bilayer temperature measurement with anisotropy	162
DPPC:CHOL[a]	$Mn_{0.5}Zn_{0.5}Fe_2O_4$ NPs (20−30 nm)	NR	core	As_2O_3	MF-induced drug release by HT	163,164
EPC:DSPE-PEG5000-p(EOEOVE-ODVE)	Fe_3O_4 NPs (12 nm)	oleic acid	lipid membrane	pyranine dye	MF-induced release by HT	109
DPPC:DSPC/ DPPC:DSPC:DSPE-PEG 2000:Rhod-PE[a]	γ-Fe_2O_3 NPs (7 nm)	citrate ligands	core		imaging/targeting and HT	165
DPPC:HSPC:CHOL:DSPE-PEG_{2000}	γ-Fe_2O_3 NPs (5 nm)	phosphate salt	core		HIFU-MR imaging	166

[a]These studies represent TSL-NPHs that progressed to preclinical evaluation.

Similarly, the magnetic characteristics of iron oxide nanoparticles (magnetite or maghemite) can be used for both imaging and magnetic heating. Iron oxide nanoparticles are approved as a contrast agent for MRI. Moreover, magnetic drug targeting by application of static magnetic fields and magnetic heat generation by exposure to alternated magnetic fields is now possible. It follows that magnetic hyperthermia is considered as a physiologically accepted noninvasive heating method having good tissue penetration capability.[154,155] For the reasons listed above, interest in design TSL-NPHs has increased. Recent examples of this type of TSL decorated with gold, silver, and iron oxide nanoparticles are listed in Table 3, Table 4, and Table 5, respectively.

Passonen et al. have shown that incorporating 2−4 nm gold nanoparticles into DPPC:DSPC TSL can trigger calcein release after 5−10 min of continuous exposure to UV light at 250 nm. Three different types of TSL-NPHs were compared including nanoparticles encapsulated, membrane embedded, and surface adsorbed. The highest content release was observed from membrane embedded Au-C_6SH NPs and surface adsorbed DPPE-nanogold NPs. The reason behind that was the potential of direct heat transport from the nanoparticles to the liposomal bilayer as compared to encapsulated gold nanoparticles (Au-MSA).[157] However, the penetration depth limitation and the danger of long-term exposure to UV light restrict their clinical applications.[150,157] To overcome this limitation, the design of TSL-NPHs for triggered drug release in the near-infrared region

DOI: 10.1021/acs.chemrev.5b00578
Chem. Rev. 2016, 116, 3883−3918

is required. NIR can penetrate up to 10 cm, allowing noninvasive heating of significant areas of the body.[167]

Alternative to spherical gold nanoparticles, other components such as silica/gold nanoshells (AuNSs)[168] and gold nanorods (AuNRs)[153] can all be equally effective for thermal generation. AuNSs are spherical nanoparticles that are comprised of silica cores covered by thin gold shells developed by Oldenburg et al. through molecular self-assembly and colloidal reduction of gold onto silica nucleation sites.[169] Interestingly, the optical properties of AuNSs can be adjusted by controlling the size of the dielectric silica core and the surrounding solid gold shell.[169] While the maximum absorption of gold nanoparticles usually occurs around 520−575 nm depending on the size,[170] the optical resonance of these nanoshells can be tuned to longer wavelengths beyond the visible region (near-infrared), where blood and tissue scattering is minimized.[171] Optical tunability can be obtained by adjusting the gold:silica ratio with a thinner gold shell leading to a red shift toward longer wavelengths as illustrated in Figure 12.[170]

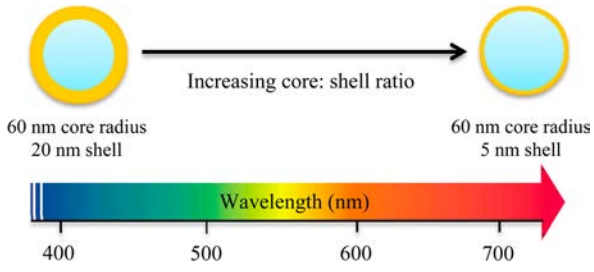

Figure 12. Optical tunability of AuNSs absorbance by changing the core to shell ratio. Adapted with permission from ref 169. Copyright 1998 Elsevier.

AuNSs have shown promising results for photothermal cancer therapy[171] and bioimaging.[172] The photothermal properties of AuNSs result from the ability to absorb light resonant with the nanoshell plasmon energy and then release it in the form of thermal energy. Following the initial electronic excitation of AuNSs by absorption of resonance light, rapid relaxation in the form of electron−electron scattering resulted in fast heating of the metal surface and the surrounding medium at the nanostructure level.[173] This rapid local increase in temperature is behind the photothermal therapeutic effect of AuNSs that has already progressed into clinical trials.[174] The photothermal effect of AuNSs was previously demonstrated in mice by direct injection of PEGylated nanoshells into the tumors followed by exposure of NIR light (820 nm). Following NIR irradiation, a tumor temperature increase within 4−6 min to around 37.4 ± 6.6 °C was associated with irreversible controlled thermal damage.[175] In another subsequent study to determine the therapeutic efficacy of AuNSs, tumor growth and animal survival were monitored up to 90 days following intravenous administration of PEGylated AuNSs of approximately 130 nm.[176] AuNSs were allowed to accumulate into the tumor over 6 h before irradiation with NIR laser light at 808 nm over 3 min. A significant difference in tumor growth was observed with complete regression in the tumor within 10 days after treatment.[176]

Recently, AuNSs have also been used for the design of TSL. Examples of that are DPPC liposomes decorated with hollow gold nanoshells following different association strategies,[146] such as DPPC:DPTAP:CHOL-gold nanoparticles complexes[135] and DPPC:HSPC:CHOL:DSPE-PEG_{2000} hollow gold nanospheres.[159] NIR light absorption by the gold nanoparticles can be converted into heat by surface resonance resulting in the release of encapsulated dye[135] or drug molecules.[159] The percentage of content release is highly dependent on the proximity of the nanoparticles to the lipid bilayer. These results also strongly suggested that the mechanism behind trigger release can be either due to formation of transient pores or due to the mechanical disruption in the lipid membrane.[135,146]

AuNRs represent another interesting example of gold-based materials for photothermal therapy. In this case, surface plasmon resonance is greatly affected by the shape and aspect ratio of the nanorod. Similar to spherical gold nanoparticles, AuNRs showed absorption near 520 nm, but they also have a second dominant surface plasmon band at higher wavelength that correlates with their axial length.[177] Recently, Agarwal et al. showed that codelivery of DOX-loaded TSL and AuNRs can effectively be used to increase tumor temperature after exposure to NIR light with subsequent drug release.[178] This was evidenced as tumor growth regression and longer survival (up to 60 days) observed in mice that received both TSL and AuNRs after exposure to NIR light as compared to other groups that received only one type of treatment.[178] We have also reported the design of liposome-AuNRs hybrids by self-association of AuNRs within the lipid bilayer of nonthermosensitive DOTAP:CHOL liposomes for in vivo imaging purposes. Liposome-AuNRs hybrids showed a high degree of colloidal and optical stability that was maintained after in vivo administration. High resolution deep tissue imaging was achieved after local injection into the brain and tumor.[179] Although this system was not designed for heat trigger release, it highlighted together with the previous study the potential of developing AuNR-based TSL.

Only a few studies have been reported on the development of TSL-NPHs containing silver nanoparticles. These studies were mainly concerned with the effect of nanoparticles on TSL membrane fluidity and T_m.[148,160] On the other hand, many examples of TSL decorated with iron oxide NPs have been previously reported. Most of these studies concentrated on investigating the release of a model dye[139,161] or drugs[139,144,164] from TSL-NPHs incorporating maghemite (γ-Fe_2O_3) or magnetite (Fe_3O_4) nanoparticles in the liposomal core or into their lipid membrane. Parameters controlling the release process were compared including lipid:nanoparticle ratios[4] and the duration and intensity of electromegnetic field (MF) applied.[4] Increasing the number of incorporated nanoparticles decreases spontaneous content leakage without MF, due to their lipid membrane-stabilizing effect, and increases drug release by MF application.[4] The earliest example of thermosensitive liposomes decorated with iron oxide nanoparticles described by Viroonchatapan et al. encapsulated Fe_3O_4 NPs (10 nm) into the core of DPPC:CHOL liposomes. Successful single and multiple release of 5-fluorouracil (5-FU) was achieved after heating with a 500 kHz electromagnetic field.[145] The mechanism of release from iron oxide decorated TSL is a combination of enhanced permeability and partial vesicular rupture.[4] Recently, Katagiri et al. described a new approach for magnetic controlled drug release from polymer-modified TSL incorporating hydrophobic iron oxide nanoparticles in the lipid membrane. The temperature-sensitive component of this system is EOEOVE-ODVE block copolymer anchored into EPC liposomes by the ODVE moiety. The release of fluorescent dye (pyranine) from this hybrid system was dramatically increased by MF irradiation as compared to a negligible release under static conditions. The

DOI: 10.1021/acs.chemrev.5b00578
Chem. Rev. 2016, 116, 3883−3918

Table 6. Different Examples of Actively Targeted TSL

system	TSL composition	targeting ligand	target	ref
Mab anti-H2K	DPPC	palmitoyl anti-H_2K Mab	H_2K antigen on tumor cells	198,205
anti HER2 affisomes	DPPC:Mal-DSPE-PEG_{2000}:DSPE-PEG_{2000}	anti-Her2 affibody	HER2-positive tumor cells	199
folate-targeted magnetic TSL	DPPC:CHOL:DSPE-PEG_{2000}:DSPE-PEG_{2000}-folate	folate	folate receptor	139
anti HER2 TSL	DPPC:MPPC:DPPG:DSPE-PEG_{2000}:DSPE-PEG_{3400}NPHS	trastuzumab Mab	Her-2 overexpressing mammary epithelial cells	201
LLO anti HER2 TSL	DPPC:MPPC:DPPG:DSPE-PEG_{3400}-NPHS	trastuzumab Mab	Her-2 overexpressing mammary epithelial cells	202
anti CD-13 NGR targeted LTSL	DPPC:MSPC:DSPE-PEG_{2000}	cyclic pentapeptide (Lys-Asn-Gly-Arg-Glu)	CD13/aminopeptidase N overexpressed in tumor vasculature and some tumor cells	197
cRGD-ELP-TSL[a]	DSPC:DPPC:CHOL:ELP:DSPE-PEG_{2000}:DSPE-PEG_{2000}-cRGD	cyclic peptide (Arg-Gly-Asp)	$\alpha v\beta 3$ integrin, which is overexpressed on tumor cells and angiogenic vasculature	196
anti-MUC-1 TSL[a]	DPPC:HSPC:CHOL:DSPE-PEG_{2000}	hCTMO1Mab	MUC-1 antigen on tumor cells	193
CREKA-LTSL[a]	DPPC:MSPC:DPPG:DSPE-PEG_{2000}:DSPE-PEG_{2000}-CREKA	tumor-homing peptide (Cys-Arg-Glu-Lys-Ala)	clotted plasma proteins in tumor vessels as well as tumor stroma	203
cRGD-TSL[a]	DPPC:DSPC:DSPE-PEG_{2000}	cyclic pentapeptide (Arg-Cys-D-Phe-Asp-Gly)	integris overexpressed on tumor cells and angiogenic endothelial cells	204

[a]These studies represent targeted TSL that has progressed to preclinical evaluation.

mechanism behind drug release is believed to be due to changes in the thermosensitive polymer conformation by the heat released from excited Fe_3O_4 nanoparticles rather than the disruption or rupture of the hybrid systems.[109]

The therapeutic effect of iron oxide-TSL at the cellular level in combination with magnetic HT revealed a significant enhancement in cytotoxicity and resulted in effective inhibition of cell proliferation.[139,164] Zhu et al. showed increased accumulation of DPPC:CHOL liposomes encapsulating methotrexate (MTX) and γ-Fe_2O_3 NPs in the skeletal muscular tissue in vivo by application of constant magnetic field as compared to the absence of the magnetic field. This observation suggested the potential of iron oxide TSL for magnetic targeting.[144] In another in vivo study by Wang et al., significant VX2 tumor growth retardation in rabbits was achieved from As_2O_3-loaded thermosensitive magneto-liposomes. The liposomes were administered arterially via a trans-catheter in combination with magnetic HT.[164]

In addition to triggered drug release, TSL-NPHs decorated with iron oxide nanoparticles can have a great role in MR imaging. A change in the MR signal of the encapsulated iron oxides around the phase transition of liposomes is expected because the T2 signal of clustered iron oxide nanoparticles is much stronger than that from dispersed nanoparticles. Encapsulation of iron oxide nanoparticles into liposomes decreases the longitudinal relaxivity as compared to free nanoparticles due to restricted water movement across the lipid membrane.[166] Promising in vivo imaging studies of magnetic TSL have been reported by Bealle et al., suggesting their potential in monitoring tumor accumulation after in vivo administration.[165]

The field of TSL decorated with metallic nanoparticles presents a promising area for the development of multifunctional delivery systems. Further studies are warranted to optimize the choice of TSL formulation, drug leakage at physiological temperatures, and the biocompatibility of the TSL-NPHs. Co-encapsulation of therapeutic drugs and nanoparticles needs more optimization as well. Most of the described studies showed the encapsulation of a single component (either a model fluorescent dye or a therapeutic molecule), and only few studies examined the coencapsulation possibility.[139,144,164] Further in vivo evaluation of the performance of those systems is required to optimize their therapeutic potential, in addition to the need for the development of proper clinical techniques for application of MF and NIR light and to control their penetration depth into tissues.

2.5. Targeted TSL

In contrast to passive targeting of liposomes, which depends on the EPR effect, active targeting relies on engineering of the liposome surface with targeting ligands. These ligands can be peptides, antibodies, or antibody fragments that bind specifically to overexpressed receptors at their target site.[180,181] Because PEGylated liposomes are taken up by tumor cells in vitro and in vivo in a more compromised manner,[182] active-targeting can improve target cell recognition and cellular uptake resulting in increased therapeutic potential.[183,184] Despite the great amount of preclinical work performed in the field of actively targeted nanomedicines (including liposomes), their use in the clinical setting is yet to be proven, and only few have progressed into clinical trials. The latter were those designed to improve cellular uptake of certain therapeutics that have, otherwise, no cellular access capability to intracellular targets. An example are cyclodextrin polymeric nanoparticles targeted against transferrin receptor that act by improving siRNA cytoplasmic delivery.[17]

The reason why ligand-targeted nanomedicines have so far failed to show significant effectiveness lies in the number of anatomical and physiological barriers that limit their accumulation into target sites.[17,185] Among the most common barriers in solid tumors are the high cellular density and the elevated interstitial fluid pressure. In addition, several cell layers are present between endothelial cells and tumor cells such as pericytes, smooth muscle cells, and fibroblasts. As a result, the accumulation and penetration of actively targeted delivery systems into solid tumors showed no great difference as compared to passive targeting. However, promising therapeutic activity could be achieved when the targets are easier to reach such as tumor blood vessels,[186] metastatic tumors,[187] blood cancers,[188] and toward targeting ligands that have cellular internalization capacity.[189]

In addition to that, the use of extravasation and penetration enhancers, such as drug molecules including TNF-α, histamine,[190] matrix-degrading enzymes (e.g., hyaluronidase),[191] or nonpharmacological treatments such as radiotherapy,[192] can strongly improve drug delivery from targeted liposomes. In

DOI: 10.1021/acs.chemrev.5b00578
Chem. Rev. 2016, 116, 3883−3918

addition, mild HT may act as a physical alternative to the accumulation of targeted liposomes at the tumor site because HT is able to increase nanoparticle extravasation via several mechanisms such as increasing tumor vascular permeability and blood flow. We and others have proven recently that local heat application can be used to enhance in vivo tumor accumulation of antibody-targeted liposomes.[193]

The other critical issue for active-targeted liposomes is the need for effective content release following their accumulation at target sites.[194] To increase the therapeutic potential of liposomal anticancer drugs, interest in developing new generation of liposomes that combine the advantages of both active-targeting and triggered-release has increased including ligand-targeted TSL. Table 6 summarizes the different examples of actively targeted TSL. Studies with targeted TSL showed that the liposomes reserve their temperature sensitivity after conjugation to the targeting ligands, and this significantly increases the specific uptake and internalization into tumor cells. Furthermore, the potentiation of intracellular content release by exposure to external HT significantly improves cytotoxic activity.[139,193,195]

Targeted TSL can be useful in slowing the transient time in the blood by targeting antigens expressed in the tumor vasculature.[196,197] The cyclic NGR-targeted LTSL against tumor vascular CD13 antigen is such an example.[197] In addition, targeted TSL can also be directed toward tumor-specific or tumor-associated antigens. Once bound to the specific antigen on their target tumor cells, targeted TSL can then release their contents by the application of HT either at the surface of the cells[198] or inside the tumor cells after conjugation to an internalizing ligand.[193,195,199] Moreover, Kullberg et al. have recently reported that cytoplasmic delivery of anti-HER2 TSL can be further improved by attaching them to a pore-forming protein, listeriolysin O.[200−202] To further increase the potential of targeted TSL for intracellular delivery, multifunctional targeted TSLs have been developed by coencapsulation of magnetic nanoparticles and doxorubicin. This approach attains advantages from both biological (active) and physical (passive) targeting by the application of an external magnetic field. In this case, magnetic nanoparticles can also be utilized for the generation of local heat by application of an alternating magnetic field that allowed triggered drug release and further enhanced their uptake by the cells.[139]

Dual targeted capacity can also be obtained by surface functionalization of TSL with target ligands that can bind to receptors on tumor cells as well as the angiogenic endothelial cells.[203,204] Wang et al. have shown recently the surface modification of LTSL liposomes with CREKA (Cys-Arg-Glu-Lys-Ala) penta-peptide that recognize clotted plasma proteins in tumor vessels as well as tumor stroma to trigger drug release from LTSL in the vasculature and stroma of the heated tumor. In vivo optical imaging studies of Cy7-labeled CREKA-LTSL at multiple time points after injection into MCF-7/ADR tumor bearing mice showed higher signals as compared to nontargeted LTSL at all-time points tested.[203] In another study, Dicheva et al. developed cRGD TSL that can efficiently recognize tumor cells and endothelial blood vessels. In vitro cellular uptake studies showed an increase in cellular level by both cancer cells (B16F10 melanoma and B16B16 melanoma) and HUVEC cells; however, in vivo intravital microscopy using B16B16 melanoma tumor model revealed specific accumulation into the tumor vasculature. Application of 1 h HT at 42 °C resulted in dramatic drug release from cRGD TSL bound to tumor vasculature.[204]

Only a few in vivo studies have been reported using targeted TSL, and in these studies HT is mainly applied a few hours after injection (2−5 h) to trigger drug release from targeted TSL after tumor uptake.[203,204] Recently, we have investigated the effects of HT on anti-MUC-1 targeted TSL tumor accumulation and their ensuing therapeutic effect in vivo using different heating protocols. Contrary to previous studies with targeted TSL that were mainly directed toward the tumor vasculature,[203,204] our results showed that both nontargeted TSL and targeted (MUC-1) TSL accumulated to the same extent when injected without application of an initial HT session, similar to what was observed in other studies because of their similar penetration into the tumor.[185] However, significant enhancement in anti-MUC-1 TSL tumor accumulation was achieved when combined with mild HT as compared to nonheated conditions. Maximum tumor accumulation levels were observed when anti-MUC-1 TSL was administered with HT (2−3-fold increase in ^{14}C-DOX tumor levels) as compared to other protocols. The observed intratumoral increase of ^{14}C-DOX from anti-MUC-1 TSL was thought to be a result of enhanced retention of the liposomes. We speculated that active binding and internalization via MUC-1 receptors on MDA-MB-435 tumor cells allowed them to be retained in the tumor for a longer time and prevented them from being washed out of the tumor vasculature and back into systemic circulation. This increase in drug levels within the tumor was reflected in a moderate improvement in tumor growth retardation and survival, proving the potential role of mild HT as a physical enhancer of actively targeted TSL.[193]

2.6. Image-Guided TSL (Paramagnetic TSL)

An important issue in the design of triggered delivery systems is to guarantee the release process at the correct timing, location, and therapeutic dose needed. Ensuring this level of control requires monitoring of both the liposomal tumor accumulation and the drug release process. Progressive development in the field of molecular imaging and nanotechnology inspired the development of delivery systems that combine imaging and therapeutic moieties (theranostics). Several studies have shown the combined delivery of DOX and contrast agent from TSL. In these cases, MR imaging was used to monitor drug release from TSL and to track the liposomal tissue distribution providing noninvasive and dynamic monitoring of drug release under hyperthermic conditions. No nanoparticles were included for this purpose in comparison with TSL-NPHs (Figure 13A).

It is important to note that these techniques monitor the effect of contrast agent on the surrounding water protons rather than the actual drug release process. However, because both the drug and the contrast agent are available in the same compartment and have similar release and distribution profiles, this can be used as an indirect way to estimate the drug release profile.[206] Encapsulation of low molecular weight MR contrast agents into the aqueous compartment of the liposome affects the T_1 relaxation time of accompanied intraliposomal water protons. Water exchange between inside and outside of the liposomal compartments is limited by its exchange rate across the lipid bilayer. Therefore, the interaction of MR contrast agents with the bulk water protons is restricted when encapsulated inside liposomes as compared to free contrast agent, and this can be used as an indirect measure of the water membrane permeability.[207] The release of MR contrast agent from TSL at the T_m of liposomes is associated with a dramatic decrease in the T_1 relaxation time of bulk water protons. This property has been exploited for MR image-guided drug delivery.[208] The increase in

DOI: 10.1021/acs.chemrev.5b00578
Chem. Rev. 2016, 116, 3883−3918

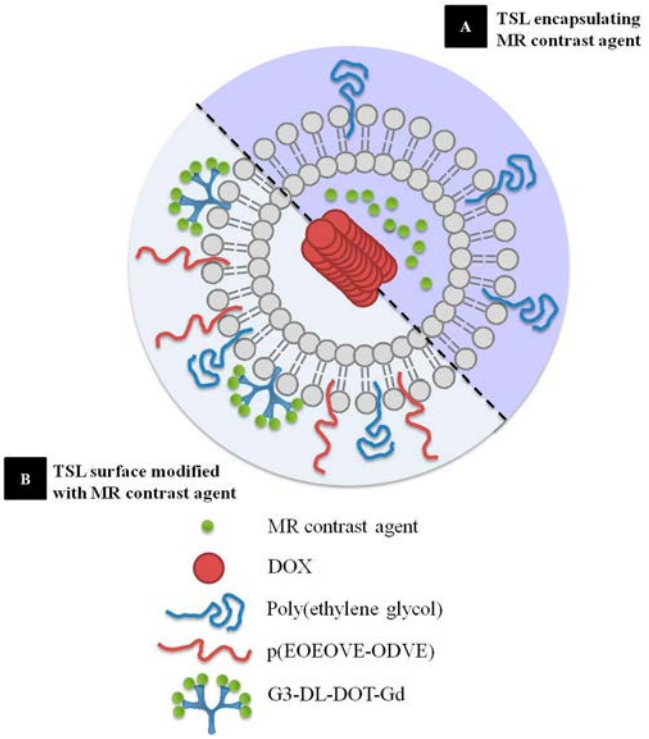

Figure 13. Paramagnetic TSL for image guided drug delivery. Schematic illustration of different types of paramagnetic TSL used for image guided drug delivery in conjugation with mild HT. (A) TSL encapsulating MR contrast agent. (B) Multifunctional polymer-modified TSL surface modified with MR contrast agent.

MR signal after release of encapsulated MR contrast agent and drug from liposomes provides information about spatial and temporal drug release. This concept of MR-based drug quantification is referred to as "dose-painting" or "chemo-dosimetry" described by Viglianti et al. using TSL encapsulating Mn^{2+} and DOX.[208,209]

The release of contrast agents from TSL has been used to image drug release in vivo. Good correlation was reported between MR imaging and thermal ablation,[210] drug delivery,[66,211,212] and therapeutic efficacy.[209,213] The estimated DOX tissue concentration determined from the shortening in T_1 relaxation time demonstrated a linear relationship with actual DOX concentration quantified by HPLC and histological fluorescence analysis. Imaging drug release from liposomes is an important tool to control drug delivery. By using this technology, release from DOX/Mn^{2+}-LTSL liposomes, encapsulating DOX and MR contrast agent (manganese sulfate, $MnSO_4$), administered during HT was detected immediately upon entry into the heated tumor from peripheral circulation. This observation indicated that the release profile from LTSL liposomes was dependent on the tumor vascularization pattern, as well as on tumor temperature at the time of injection.[209] Similar findings have been reported by de Smet et al. where MR images revealed a variation in drug distribution in the tumor that was related to the variation in the vascularization, permeability, and the extent of a necrotic core.[211] The results of those studies demonstrated the suitability of using real-time imaging of drug release and distribution to optimize the choice of the HT protocol and the patient selection process based on estimated therapeutic efficacy (personalized medicine).[214,215]

Although Mn^{2+} has been used to image drug delivery from TSL,[209,212] its toxicity can limit its clinical applications.[216] Gadolinium-based contrast agents are better alternatives because their safety profile makes them more acceptable for clinical applications. Much of the recent work in image-guided TSL involved the use of Gd(HPDO$_3$A) and in particular ProHance, a clinically approved MR contrast agent coencapsulated into TSL with DOX.[66,211,217] Encapsulation of Gd(HPDO$_3$A) inside liposomes was not shown to interfere with DOX loading and formation of DOX crystals inside liposomes.[66]

In another example, Langereis et al. proposed an innovative approach of image-guided drug delivery by using chemical exchange saturation transfer (CEST) and ^{19}F-MR imaging to monitor drug release from TSL. This was accomplished by coencapsulating [Tm(HPDO$_3$A)(H$_2$O)], a thulium-based chemical shift agent, and ammonium hexafluorophosphate (NH_4PF_6) into the interior of a TSL. This allowed the visualization of the intact liposomes (based on the CEST effect) and the monitoring of drug release (based on ^{19}F MR signal restoration as a result of CEST MR signal loss).[218]

Paramagnetic TSL described above involved the encapsulation of an MR contrast agent in the lumen of the liposome. An alternative way to formulate paramagnetic TSL includes the attachment of an MR contrast agent onto the liposomal surface. Kono et al.[108] (Figure 13B) reported a type of polymer-modified TSL that has Gd-dendrons attached to their surface. This was used to probe liposome tumor accumulation but could not monitor drug release because the MR contrast agent was not encapsulated inside the liposomal aqueous compartment.[108] In this case, T_1 shortening of surface-attached metal ions was equivalent that of to the free metal ions.[212] Table 7 summarizes recent studies using MR-guided drug delivery from TSL.

3. PHARMACOLOGICAL POTENTIAL OF TSL

3.1. Hyperthermia as a Treatment Modality for Cancer

HT has been identified for many years as a selective modality for cancer therapy.[220] Thermal ablation is based on direct heating of the tumor to temperatures >50 °C for short durations (4−6 min) using radiofrequency, laser, or microwave applied by a needle-like applicator.[221] The electrical applicator is usually positioned in the center of the tumor, creating a central zone of high temperature surrounded by peripheral areas of sublethal heating.[222] Although great emphasis was given to the use of HT in ablative therapy, therapeutic effectiveness of this treatment modality is usually restricted by the failure to get complete tumor ablation especially at the tumor periphery and close to blood vessels.[223]

Mild HT (e.g., 39−42 °C for 1 h), in the range between the temperature required to ablate the cells and normal body temperature, offers a lot of compelling advantages in cancer therapy.[224] Besides the well-known synergy offered by mild HT when combined with anticancer drugs[225,226] and radiotherapy,[224] mild HT has a significant influence on tumor pathophysiological parameters that favor improved nanoparticle extravasation. HT is a well-established method to augment the accumulation of liposomes[227] and other nanocarriers such as polymeric nanoparticles,[228] monoclonal antibodies,[229] and antibody fragments[230] into solid tumors. This enhancement of tumor accumulation by HT is due to the increase in local blood flow[231] and the improvement in microvascular permeability.[227,232,233] This increase in permeability is mainly due to structural changes in the cytoskeleton of endothelial cells that

DOI: 10.1021/acs.chemrev.5b00578
Chem. Rev. 2016, 116, 3883−3918

Table 7. MR-Guided Drug Delivery from TSL

Liposomal Formulation (mol/mol)	Dox Dose	MR Contrast Agent	Animal / Model	HT Source and Protocol	References
MR-guided TSL co-encapsulate contrast agent inside the liposomal compartment 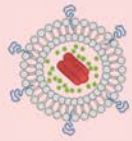					
LTSL	10 mg / kg	Mn^{+2}	Rat / Fibrosarcoma	Catheter (60 min at 44 °C started before injection)	212
LTSL	5mg / kg	Mn^{+2}	Rat / Fibrosarcomas	Catheter (60 min at 42 °C before and / or with HT injection)	209
LTSL	N/A	NH_4PF_6 and Tm(HPDO$_3$A)	Phantom	Water bath	218
LTSL TTSL NTSL	N/A	Gd(HPDO$_3$A)	In vitro	-	66
HaT	5mg / kg	Gd-DTPA	Mice / EMT-6	Water bath (60 at 43 °C min started before injection)	213
LTSL	5mg / kg	Gd(HPDO$_3$A)	Rabbit / VX2	MR-HIFU (4 × 10 min at 41.5 °C)	217
TTSL	5 mg /kg	Gd(HPDO$_3$A)	Rat / 9L gliosarcoma	MR-HIFU (2 × 15 min at 41.5 °C after injection)	211
TTSL	5mg / kg	Gd(HPDO$_3$A)	Rat / Rhabdomyosarcoma	MR-HIFU (2 × 15 min at 41 °C started immediately after injection)	219
MR-guided TSL surface modified with MR contrast agent 					
EYPC:CHOL:p(EOEOVE-ODVE):PEG-PE:G3-DL-DOTA-Gd (42:42:4:2:5-10)	6mg/kg	G3-DL-DOTA-Gd	Mice/ colon carcinoma 26	Radio Frequency / (10 min HT at 44 °C 8 h after injection)	108

increase the pore cutoff size of the tumor.[227,233] Mild HT increases local blood flow by up to 2-fold[234] and decreases tumor interstitial fluid pressure (IFP lowered by 10-fold after 30 min heating at 43 °C),[235] therefore collectively enhancing the overall tumor accumulation. Alongside the improved tumor extravasation, mild localized HT can be used to boost local drug bioavailability when combined with thermosensitive delivery systems.[69,79]

3.2. State-of-the-Art of the Clinical Translation of Temperature-Sensitive Vesicles

As mentioned above in this Review, the ultrafast drug release properties of some TSLs (e.g., LTSL) offered a new paradigm of liposomal drug release as compared to nontemperature-sensitive liposomes that depended mainly on the EPR effect to enhance localization into tumors, but did not improve drug release and bioavailability. Previous studies suggested that the ultrafast drug

DOI: 10.1021/acs.chemrev.5b00578
Chem. Rev. 2016, 116, 3883−3918

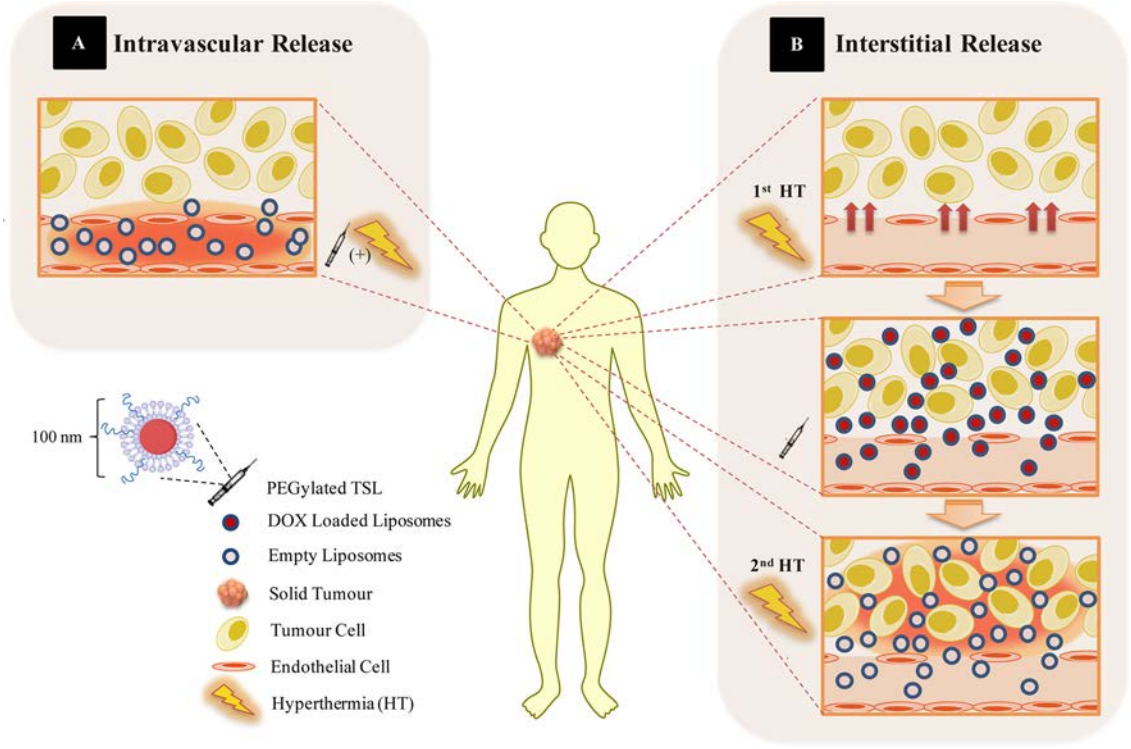

Figure 14. Hyperthemia (HT) protocols that can be used to enhance drug delivery from TSL. The combination of HT and liposomes can be utilized to enhance the drug release from TSL in two different approaches based on the timing between liposome administration and heat application. In the intravascular release approach, TSL are administered during the heating process, resulting in drug release inside blood vessels, when reaching the heated area (drug release is represented by the red gradient seen in the blood vessels). This process is then followed by uptake of the drug by both tumor and endothelial cells. The increased vascular permeability of the blood vessels in response to the first HT treatment increases the level of vesicle accumulation in the tumor. The interstitial release approach takes advantage of the fact that stealth small-sized liposomes have the ability to extravasate through the malformed tumor vasculature as compared to normal blood vessels. After tumor accumulation, a second HT session is applied to trigger drug release interstitially (drug release is represented by the red gradient outside the blood vessels and among tumor cells).

release prolife allows immediate content release when arriving at the heated tumor vasculature.[80,236] This type of drug release is called the "intravascular release" approach (Figure 14).[79] Manzoor et al. have shown that intravascular drug release can also increase free drug penetration into the tumor interstitium in a concentration gradient manner by real time confocal imaging of doxorubicin using skin-fold window chambers.[69] A key parameter for the success of the intravascular release approach using LTSL is the inherent affinity of DOX toward cells of the vascular endothelium leading to cellular uptake. Removal of DOX from the interstitial space by cellular uptake helps maintain the concentration gradient between the high intravascular drug levels and the extravascular concentration that results in enhancement of perivascular penetration.[69]

Such intervascular triggered release may be theoretically also relevant to different drug molecules other than DOX. Presumably, rapid vascular release might not be as beneficial if the specific drug molecules are cleared through blood flow faster than their affinity and adherence to the tumor vascular bed and, subsequently, interstitium. This observation has been reported recently by Allen and colleagues using lysolipid-based thermosensitive liposomes encapsulating cisplatin.[237] The physical properties of cisplatin are significantly different from those of DOX, which may limit tissue accumulation, penetration, and membrane permeability of cisplatin. The tendency of cisplatin to be cleared into the systemic blood circulation is very probable. Despite these fundamental molecular differences, thermoresponsive intravascular release of cisplatin was able to increase drug levels in a cervical (ME-180) tumor model as compared to free drug and proved to contribute to significant improvements in therapeutic efficacy.[237] This example demonstrated once more the critical importance of the bioavailable drug fraction to achieve therapeutic benefits.

The combination of TSL and HT can also be tailored to achieve interstitial drug release after extravasation into the tumor tissue. HT enhances liposome extravasation; therefore, the application of a first HT session prior to TSL injection would be useful to increase tumor vascular permeability. Once vesicles extravasate into the tumor, subsequent HT sessions can be used to trigger interstitial drug release (Figure 14).[32] The duration of the second heating can be adjusted according to the drug release profile of the TSL system. This can vary according to the vesicle properties from ultrafast release within less than 1 min to a slow release over 1 h.[32] The choice and the sequence in which HT and TSL can be administered is critical to achieve the required therapeutic efficacy, because the action of TSL depends on the HT protocol selected as well as the activity of the drug itself.[209]

Most of the previously published preclinical studies of TSL in combination with mild HT have focused on early triggered drug release, where HT was applied directly after injection[56,211,236,238] or shortly after (1−3 h) while the TSL vesicles are still circulating in the bloodstream.[239,240] A limited number of studies were designed to trigger content release from TSL after accumulation into the tumor.[107,109,241] We have shown using dual-radiolabeled TSL and NTSL that the accumulation of both lipid and drug molecules 24 h after administration was directly proportional to

DOI: 10.1021/acs.chemrev.5b00578
Chem. Rev. 2016, 116, 3883−3918

Table 8. HT Protocols Used for Trigger Release from TSL

TSL	Drug	HT Source and Protocol	Experimental design	End Point	Ref.
TTSL	DOX	Water bath (1 h at 42 °C) 1 h after injection 2nd HT 24 h after injection	-Tumor uptake -Drug release	1 h after HT (Data not shown)	240
LTSL TTSL NTSL	DOX	Water bath (1 h at 42 °C) immediately after injection	-Tumor uptake -Growth delay	-immediately after HT -5x tumor volume or up to 60 days	79
LTSL TTSL NTSL	DOX	Water bath (1 h at 42 °C) immediately after injection	-Growth delay	5x tumor volume or up to 60 days	79
PEG-TSL	DOX	RF (20 min at 42 °C) 3 h after injection	-Tumor uptake -Survival	-5 min after HT -Up to 90 days	239
DPPGOG-CF	CF	Water bath (1 h at 42 °C) immediately after injection	-Tumor uptake	up to 6 h after HT	56
LTSL NTSL	DOX	HIFU (15-20 min 42 °C) immediately or 24 h after injection	-Tumor uptake -Growth delay	- immediately after HT -Time to reach 500 mm^3	242
LTSL	DOX & Mn	Catheter (30 min at 42 °C) -injection 15 min after HT -injection 15 min before HT -split dose before & during HT	-Tumor uptake -Growth delay -Survival:	-30-45 min after injection -5x tumor volume -up to 60 days	209
LTSL	DOX	Water bath (1 h at 42 °C) immediately after injection	-Tumor uptake -Growth delay	-immediately after HT -5x tumor volume or up to 60 days	78
Polymer-modified EPC:CHOL:DSPE-PEG	DOX	RF (10 min at 45 °C) 6 h & 12 h after injection	-Growth delay	-up to 8 days	107
Polymer-modified EPC:CHOL:DSPE-PEG-Gd	DOX	RF (10 min at 44 °C) 8 h after injection	-Tumor uptake -Growth delay	-1 h, 3 h & 8 h -up to 8 days	108
TTSL	DOX & Gd	MR-HIFU (2x 15 min) -injection after HT initiation (42 °C)	- Tumor uptake (DOX quantification & MR imaging)	20-30 min after injection	211
LTSL	DOX & Gd	MR-HIFU (4x 10 min at 41 °C) immediately after injection	- Tumor uptake (MR imaging)	-immediately after HT	217
HaT LTSL	DOX	Water bath (1 h at 43 °C) 10 min before injection	- Tumor uptake -Growth delay	-immediately after injection - up to 21 days	86
HaT	DOX & Gd	Water bath (1 h at 43 °C) 10 min before injection	- Tumor uptake (DOX quantification & MR imaging)	-immediately after injection	213

DOI: 10.1021/acs.chemrev.5b00578
Chem. Rev. 2016, 116, 3883−3918

Table 8. continued

HaT-II LTSL	DOX-Cu^{+2}	Water bath (1 h at 43 °C) 10 min before injection	- Tumor uptake -Growth delay	-immediately after injection -up to 21 days	87
LTSL	DOX	Heating coil (30 min at ~41°C) HT plus injection	- Tumor uptake	CLSM imaging every 5 s for 20 min	69
LTSL TTSL NTSL	DOX	Water bath (43.5 °C) immediately after injection	- Tumor uptake	-1 h and 24 h after injection	243
LTSL	DOX	MR-HIFU (3x 10 min at 40-41 °C) within 1 h of LTSL infusion	-Tumor uptake (DOX quantification)	4 h after injection	238
TTSL	DOX & Gd	MR-HIFU (2x 15 min) immediately after injection	-Tumor uptake	-1.5 & 48 h after injection	219
Optimized PEG-TSL-Rho-PE	-	Heating coil (0.5-1 h at 41 °C) 20 min after injection	-Tumor uptake -Blood vessels permeability	-CLSM up to 2 h -4 h, 8 h & 24 h post HT	244
Optimized PEG-TSL-Rho-PE	DOX	Heating coil (1 h at 42 °C) 20 min after injection	-Tumor uptake -Growth delay & survival	-CLSM up to 80 min after injection -up to 26 days	62
fTSL sTSL	DOX	Water bath -1 step HT (after fTSL injection) -2 step HT 1^{st} HT (1 h at 41 °C) before sTSL injection and 2^{nd} HT (1 h at 42 °C) 2 h after injection	-Tumor uptake -Growth delay & survival	-3 h after injection -up to 25 days	241
LTSL NTSL	DOX	RF ablation - 3 min RF 15 min before NTSL injection. - 3 min FR 15 min after LTSL injection	-Tumor uptake -Growth delay & survival	- up to 72 h after injection -up to 90 days	245
HTLC	Cisplatin	Laser induced heating (25 min at 42 °C) HT started 5 min before injection	-Tumor uptake -Growth delay & survival	- 1 h after injection -up to 50 days	237
Lp-Peptide hybrids LTSL TTSL	DOX	Water bath Intravsacular release (1 h at 42 °C immediately after injection) Interstitial release (1 h at 42 °C before injection followed by 0.5 h at 42 °C 24 h later)	-Tumor uptake -Growth delay & survival	-1 h & 24 h after injection -up to 70 days	123

DOI: 10.1021/acs.chemrev.5b00578
Chem. Rev. 2016, 116, 3883−3918

Table 8. continued

Chemical compositions of the different TSL reported in this table are listed below:

HaT: DPPC:Brij 78
LTSL (DPPC:MSPC:DSPE-PEG_{2000})
NTSL (HSPC:CHOL:DSPE-PEG_{2000})
Optimized-PEG-TSL (DPPC:DSPC:DSPE-PEG_{2000})
PEG-TSL (DPPC:DSPC:CHOL:DSPE-PEG)
TTSL (DPPC:HSPC:CHOL:DSPE-PEG_{2000})
Polymer-modified EPC:CHOL:DSPE-PEG (EPC:CHOL:copoly(EOEOVE-block-ODVE):DSPE-PEG_{2000})
Polymer-modified EPC:CHOL:DSPE-PEG-Gd (EPC:CHOL:copoly(EOEOVE-block-ODVE):DSPE-PEG_{5000}-G3-DL-DOTA-Gd)
sTSL (slow TSL composed of DPPC:DSPC:DSPE-PEG_{2000} 55:40:5)
fTSL (fast TSL composed of DPPC:DSPC:DSPE-PEG_{2000} 80:15:5)
HTLC (DPPC:DPPG:MSPC:DSPE-PEG_{2000} 57.7:28.9:9.6:3.8)
Lp-Peptide hybrids: (DPPC:DSPC: DSPE-PEG_{2000}:Leucine zipper peptide 90:10:5:0.5)

the drug retention and blood circulation levels of liposomes. Similarly, de Smet et al. showed that triggering drug release with HIFU can improve drug distribution into the tumor and increase long-term tumor accumulation from long circulating TSL.[219]

In addition, the potential of HT to trigger interstitial drug release has been shown recently by Li et al. by applying a two-step HT treatment protocol to take advantage of enhanced tumor accumulation and to trigger drug release interstitially.[241] This approach theoretically requires specific TSL design characteristics that would be able to retain the encapsulated drug while in the bloodstream, but release at relatively slow rate when the second HT step is applied for maximum therapeutic effectiveness. Li et al. designed two types of traditional TSL: a slow release TSL (sTSL) and a fast release TSL (fTSL) using DPPC/DSPC/DSPE-PEG_{2000} at molar ratios of 80:15:5 and 55:40:5, respectively. They showed that intratumoral doxorubicin accumulation by the two-step hyperthermia protocol from sTSL was equivalent to the levels achieved from the fTSL with intravascular release protocol using a single step HT at 42 °C for 1 h, immediately after injection. However, the two-step HT protocol using the sTSL was not as effective in controlling tumor growth as the intravascular doxorubicin release using the fTSL. This study concluded that creating a high concentration gradient of free drug released intravascularly is more effective, rather than higher liposomal accumulation around the tumor. This was confirmed by showing the NTSL has limited efficacy using the two-step HT protocol that could be due to limited penetration depth and inhomogeneous distribution within the tumor microenvironment.[241] In a very recent study, we further elucidated how crucially important is to fine-tune the drug release properties and pharmacokinetics of TSL with the hyperthermia protocol applied to maximize therapeutic efficacy.[123] Table 8 summarizes the different HT protocols used to trigger drug release from TSL.

The importance of choosing the appropriate heating protocol has been best demonstrated in the case of LTSL (ThermoDox). In preclinical studies, LTSL in combination with mild HT demonstrated significant enhancements in therapeutic effectiveness as compared to free drug.[79,209] This improvement was mainly due to the ultrafast release capacity of LTSL (>80% release in a few seconds) after exposure to mild HT.[67,72] Temperature-induced drug release within the tumor vasculature increased the exposure of tumor endothelial cells to DOX, causing destruction of tumor vessels and improved overall therapeutic efficacy.[80,236]

Despite that, initial analysis of the clinical effectiveness of a Phase III trial using LTSL in combination with radiofrequency ablation (RFA) against liver cancer was less than expected.[246,247] Preclinical studies suggested that the timing between liposome injection and heat application is the most critical factor in the success of this type of TSL. The significant deviation from the optimized preclinical heating protocol parameters was mainly responsible for the efficacy data obtained.[247] A critical limiting factor with ThermoDox is the tendency of these vesicles to leak out DOX once injected into the blood circulation even before HT application.[82] ThermoDox short blood kinetics of encapsulated drug (only 1.3 h) restrict the time frame of the heating protocol.[74,248] Although ThermoDox has a longer blood half-life as compared to free drug, it is still substantially less than that of Doxil. Bearing in mind that the average clinical HT duration is 30−60 min, it is clear that the optimum treatment would be achieved by starting HT prior to drug administration.[48]

The importance of this parameter as a determinant factor of therapeutic efficacy for LTSL systems was revealed previously in preclinical studies by Ponce et al. by studying the effect of timing between HT and injection on the tumor distribution and therapeutic activity of LTSL encapsulating Mn^{2+}. For this type of TSL, higher and faster DOX accumulation into the tumor occurred when injected during HT, as compared to injections before HT, to take advantage of the maximum intravascular LTSL concentration. Preheating the tumor before LTSL injection was essential to achieve rapid drug release in the tumor vasculature. Even though the whole tumor volume was heated, LTSL released most of the drug at the periphery of the tumor. In contrast, LTSL injection before HT allowed liposomes to perfuse into the tumor interstitium before drug release, and therefore central distribution could be achieved.

Phase I clinical trial data of ThermoDox showed that the maximum plasma level of drug was achieved at the end of the 30 min infusion period, suggesting that this is the optimum time for RFA (i.e., HT) application.[248] Yet, in the Phase III clinical trial, tumor heating started at least 15 min after the initiation of infusion and completed no longer than 3 h.[37] Such modifications in the timing of ThermoDox administration and HT treatment between preclinical and clinical studies, together with the short blood circulation half-life, may explain in part the initial clinical outcome. Although the timing and duration of heating may be the critical factors, it is worth pointing out here different hurdles that were experienced during this pioneering and challenging clinical trial. These difficulties have been discussed by Needham[247] in detail, but we would like to highlight: (a) the rapid move from the Phase I (liver safety) trial toward the Phase III (hepatocellular carcinoma efficacy) trial in the absence of a Phase II study to establish treatment protocol standardization; (b) the engagement of around 75 five clinical centers in 11 countries performing the Phase III trial, that meant wide variation in the protocol implementation, at times forced by their local rules and regulations; (c) consistent achievement of the right temperature in the tumor and continuous monitoring; and (d) the size of the tumors enrolled for treatment.

Recently, meta-analysis of the data extracted from that Phase III clinical trial was reported to show that ThermoDox noticeably

DOI: 10.1021/acs.chemrev.5b00578
Chem. Rev. 2016, 116, 3883−3918

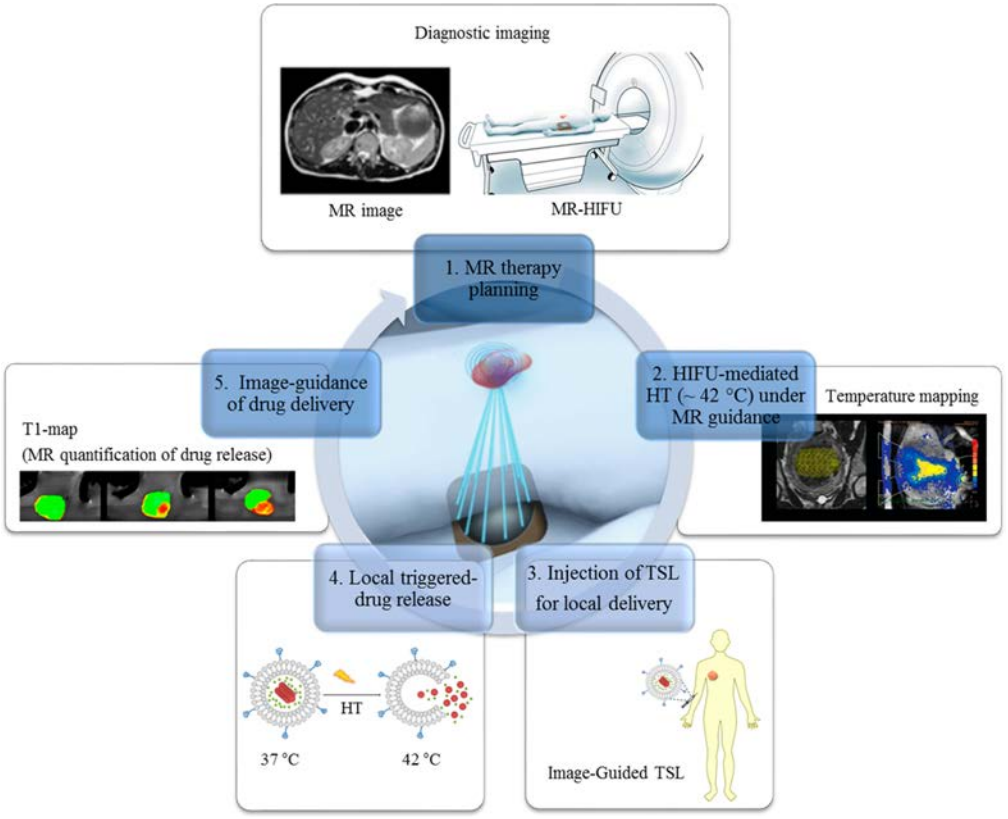

Figure 15. Schematic presentation of drug delivery from TSL using MR-HIFU. Triggered drug release from TSL coencapsulating drug and an MR contrast agent by MR-HIFU can play a pivotal role in individualized and controlled treatment. MR plays a crucial role in therapy planning, temperature control during treatment, and imaging of drug delivery. Temperature and drug release mapping provides continuous feedback to the HIFU system transducer to adjust the sonication time and/or dose until the desired signal is obtained. Adapted with permission from ref 250. Copyright 2012 Elsevier.

improved overall survival by 58% in a large subgroup of patients (41% of the total patients enrolled) who received optimized RFA for at least 45 min. This applied to patients with single HCC lesions (3−5 cm and 5−7 cm) and confirmed that the duration of heating from the RFA procedure was also a key parameter to optimize when combined with TSL to obtain added clinical benefit. Additional findings from the most recent analysis of overall survival in the Chinese cohort of the trial showed 75% improvement for the ThermoDox plus optimized RFA group as compared to the group treated with optimized RFA only, again confirming the challenge of logistical variations between different clinical centers.[249] Taking all of the above into consideration, it is evident that further systematic preclinical and clinical studies are required to offer insight into the design, selection, and optimization of the correct HT protocol that best matches the physicochemical properties, drug release rate, pharmacokinetic parameters, and tumor accumulation of the thermoresponsive vesicles.

3.3. Development of Heating Modalities for Temperature-Triggered Drug Delivery

Although the theory of triggered drug delivery by HT has been described since the late 1970s, several obstacles had to be overcome before this technology could be configured for clinical applications. The most important challenge was to achieve controlled noninvasive focal heating of the tumor site with accurate monitoring of the tumor temperature.[250] The majority of the heating techniques available are limited by several factors including the invasiveness of the techniques, the poor control of the temperature in the tumor, the inability to adapt to changes in tumor architecture and blood perfusion, and the restrictions imposed by the location of the tumor. Several techniques have been applied for heat-triggered release from TSL, including regional superficial heating employing heated water baths,[79,240,251] localized superficial heating with external electromagnetic sources,[82] and implanted electrodes heated by continued flow of hot water.[208,209]

In clinical trials, the heating techniques that have been employed to achieve local tumor heating are percutaneous radiofrequency ablation (RFA)[37] for hepatocellular carcinoma (HCC) and superficial microwave heating for chest wall recurrence of breast cancer.[84] In both heating techniques, tissue temperature was monitored with interstitial probes; therefore, control of spatial temperature changes was limited, which was reflected in the achieved drug release.[221,252] To enhance clinical efficacy, the development of heating and monitoring techniques to achieve noninvasive spatial and temporal control of temperature increases is crucial. One promising technique is the HIFU system guided with MR. Ultrasound has been used clinically to apply HT noninvasively (40−45 °C) to tumor areas that are difficult to reach by other heating methods.[253] MR incorporation of this procedure is crucial to provide soft-tissue imaging and real-time thermometry.[254,255] MR thermometry that is based on proton resonance frequency shift (PRFS) is the most commonly used technique for water-containing tissues. This can provide a precise 3D temperature feedback with precision of approximately 1 °C, and therefore it is the basis behind recent developments in the MR-HIFU system. The constant temperature feedback provided will allow control of the tumor temperature for a

DOI: 10.1021/acs.chemrev.5b00578
Chem. Rev. 2016, 116, 3883−3918

prolonged period of time by dynamic adjustment of the sonication parameters.[256]

MR-HIFU has recently been used for thermoablative applications,[257,258] and it also holds great promise in triggering drug delivery as shown in preclinical studies.[250] Temperature-triggered drug release from TSL using MR-HIFU has been demonstrated in several reports in normal tissues,[259] and in animal tumor models.[211,238,242,260] HT induced by HIFU triggered drug release from TSL and increased the long-term liposomal drug uptake into the tumor during and after HT. As a result, MR-HIFU was shown to provide homogeneous intratumoral drug distribution over a large volume and from a larger distance away from blood vessels.[219]

Improved distribution of DOX into the tumor was observed by the combination of TSL with MR-HIFU. This enabled DOX delivery to the core and the periphery of the tumor compared to the tumor volume distribution seen with LTSL or DOX alone, which was mainly restricted to the periphery of the tumor. This improvement in DOX delivery within the tumor did not increase DOX distribution to other organs.[238] Gasselhuber et al. have shown recently that by using computer simulation studies, the amount of drug delivered to the tumor after heating with HIFU can be predicted and used to estimate cell killing induced by a combination of DOX and hyperthermia.[261]

As a consequence of the emergence of the MR-HIFU bed-side system, a noninvasive option for proper treatment planning and monitoring for many patients with advance solid tumors can be potentially offered.[250] This concept is now under clinical evaluation to provide treatment planning and real time thermometry during heat-triggered drug release from ThermoDox using HIFU for liver cancer[83] and will be followed by Phase II study using ThermoDox plus HIFU in patients with breast cancer.[262] MR can also be useful to monitor temperature-triggered drug release from TSL by the coencapsulation of a paramagnetic contrast agent inside the vesicle aqueous compartment along with the drug molecules, as described previously.[211,213,217] In that way, monitoring of local drug concentration and distribution during and after the heating procedure can be achieved. Figure 15 summarizes the potential of MR-HIFU in heat-triggered drug release from TSL. Theoretically, this could be a very elegant method to monitor drug release in real-time, and image-guided TSLs have proved their potential in preclinical studies. It may also provide a more useful tool toward personalization of treatment by selecting patients that are more likely to benefit from triggered liposomal therapies.[212] However, challenges still need to be resolved, such as the interference of the paramagnetic contrast agents (by ±3−4 °C) with the MR-based thermometry that is used for tumor temperature mapping during the HIFU treatment. Such interference with PRFS MR thermometry may lead to false thermal doses. Development of correction methods for the presence of MR contrast ions is definitely required to translate this promising technology to the clinic.[256] Other important issues to be considered are (a) the dose limitation of the MR contrast agents to avoid any toxicological complications; (b) the increased costs of the treatment; and (c) the availability of the required infrastructure. For more details on the potential and clinical translation of this technology, we would refer to recent reviews by Gruell[250,256] and Lammers.[214,215]

4. CONCLUSIVE REMARKS AND PERSPECTIVE

The use of HT to trigger local drug release is a promising and rapidly evolving area. Local triggered release from TSL by mild HT has proven to be a precise and effective method for cancer treatment in many preclinical studies. As such, it holds a great potential to be translated into an effective treatment modality, especially for advanced local tumors that cannot be cured by conventional anticancer drugs. The evolution of advanced technology for applying and monitoring HT allows remote noninvasive local heating to be delivered with a great degree of control. However, all of this greatly depends on the molecular design of temperature-sensitive vesicular systems.

Remarkable advances in the design and development of TSL have been accomplished over the past few years, and the progress is still ongoing. Different types of TSL have been developed, and most of the work was directed toward developing TSL with ultrafast release properties, such as the lysolipid-containing TSL, designed to release their loaded drug within seconds of reaching the heated tumor. The most well-studied example of these systems is ThermoDox, the LTSL formulation that progressed into Phase II/III clinical trials. The clinical development of this TSL system has been a great lesson for the field, because it revealed the critical issues that need to be recognized and resolved for successful clinical translation and adoption.

The development of new TSL technologies holds great promise and opens the space for further improvements. In this Review, we highlighted all different chemical components used to design TSL, as well as other nonvesicle forming thermosensitive components. Polymer-modified TSL can overcome some of the limitations involving the design of relatively stable TSL, because their temperature sensitivity is mainly dependent on the polymer component itself. Nevertheless, more work is warranted in that area to develop temperature-sensitive polymers that respond to narrow temperature changes, maintain good stability under physiological conditions, and ensure effective drug release under mild HT. The replacement of synthetic polymers with biopolymers is promising due to the high degree of control on the temperature sensitivity. In addition, TSLs decorated with metallic nanoparticles have the advantages of providing localized noninvasive self-heating to the liposomal bilayer at the nanoscale level after exposure to external energy such as MF or NIR light. Further in vivo evaluation of the performance of those systems is required to determine their therapeutic potential. This is in addition to the need for the development of appropriate methods for the clinical application of MF and NIR illumination and control of their penetration depth within tissues.

Another promising, yet challenging, approach in the field of TSL is the design of image-guided drug delivery from TSL by coencapsulation of imaging agents. The real-time information that can be provided from these systems about liposomal accumulation within the tumor area can offer optimization of the coordination between HT application to trigger drug release and tumor temperature achieved. However, the multiparametric design of these systems and the heating technologies applied surely require further optimization to be clinically applicable, in addition to the possibility of interference of MR contrast agent with the MR temperature mapping of the tumor.

On the basis of the lessons learned from the ThermoDox clinical trials, it becomes clear that the treatment of cancer with this technology is far more difficult than simply triggering drug release. Therefore, to make real progress in the field, this oversimplification has to change. The translation of newly developed TSL systems into the clinic will depend greatly on the understanding and sophistication of the chemical components included in their design as well as their coordination with the

DOI: 10.1021/acs.chemrev.5b00578
Chem. Rev. 2016, 116, 3883−3918

logistics of practical clinical practice. To that end, careful, rational, and systematic design of studies and trials along with patient enrolment strategies are important, taking into consideration cancer type, volume, vascularization, and treatment standardization.

In this Review, we attempted to offer a thorough description of all of the different chemical components and the rationale in the design of novel TSL vesicle systems, as well as the critical pharmacological parameters that will affect their clinical translation. We conclude that in parallel with the development of TSL with ultrafast release properties, more efforts should be invested to obtain a balance between thermosensitivity, blood stability, and safety profiles of TSL. The development of such systems offers a great opportunity for clinical translation as the next generation, nanoscale vesicle systems of enhanced functionality following from the successful clinical translation legacy of the early liposome technologies.

AUTHOR INFORMATION

Corresponding Author

*E-mail: kostas.kostarelos@manchester.ac.uk.

Notes

The authors declare no competing financial interest.

Biographies

Dr. Zahraa S. Al-Ahmady is a Research Fellow at the North West Centre of Advanced Drug Delivery (NoWCADD), a collaboration between the Manchester School of Pharmacy, the Nanomedicine Lab (School of Medicine), University of Manchester, and AstraZeneca. Prior to this, she was a postdoctoral research fellow in the NANOSOLUTIONS (EC-FP7-NMP) Consortium studying the structure−safety profile relationships of engineered nanomaterials. She completed her Ph.D. at the UCL School of Pharmacy in 2013 on the development of novel therapeutic and biomedical imaging approaches for cancer therapy, with many fundamental insights into the impact of improved drug bioavailability using external triggers, such as mild hyperthermia combined with devising novel heat-sensitive liposomes.

Professor Kostas Kostarelos obtained his Diploma in Chemical Engineering and Ph.D. from the Department of Chemical Engineering at Imperial College London and carried out his postdoctoral training in various medical institutions in the United States (UCSF, Memorial Sloan-Kettering, New York Presbyterian). He was Assistant Professor of Genetic Medicine & Chemical Engineering in Medicine at Cornell University Weill Medical College when he relocated to the UK as the Deputy Director of Imperial College Genetic Therapies Centre in 2002. In 2003 Professor Kostarelos joined the Centre for Drug Delivery Research at the UCL School of Pharmacy as the Deputy Head of the Centre. He was promoted to a personal Chair of Nanomedicine and Head of the Centre in 2007. The entire Nanomedicine Lab was embedded within the Faculty of Medical and Human Sciences and the National Graphene Institute at the University of Manchester in 2013. Kostas is currently Professor of Nanomedicine at the University of Manchester and Honorary Professor at UCL, Faculty of Life Sciences. He has been invited Fellow of the Royal Society of Medicine, Fellow of the Institute of Nanotechnology, and Fellow of the Royal Society of Arts, all in the United Kingdom. In 2010 he was awarded the Japanese Society for the Promotion of Science (JSPS) Professorial Fellowship with the National Institute of Advanced Industrial Science and Technology (AIST) in Tsukuba, Japan.

DEDICATION

This article is dedicated to the late Dr. Gerben Koning and his important contributions to this field of research.

ABBREVIATIONS

4T07	mouse mammary carcinoma
5-FU	5-fluorouracil
AA	acrylic acid
AAM	acrylamide
APr	*N*-acryloylpyrrolidine
B16F10	murine melanoma
C12	didodecyl
C6-SH	hexanethiol
CHOL	cholesterol
DMP	2-dodecyl-sulfanylthiocarbonylsulfanyl-2-methylpropionic acid
DMPC	1,2-dimyristoyl-*sn*-glycero-3-phosphocholine
DOPE	1,2-dioleoyl-*sn*-glycero-3-phosphoethanolamine
DOX	doxorubicin
DPPC	1,2-dipalmitoyl-*sn*-glycero-3-phosphocholine
DPPE	1,2-dipalmitoyl-*sn*-glycero-3-phosphoethanolamine
DPPG	1,2-dipalmitoyl-*sn*-glycero-3-phosphoglycerol
DPPGOG	1,2-dipalmitoyl-*sn*-glycero-3-phosphoglycero-glycerol
DPTAP	1,2-dipalmitoyl-3-trimethylammonium propane (chloride salt)
$DSPE\text{-}PEG_{2000}$	1,2-distearoyl-*sn*-glycero-3-phosphoethanolamine-*N*-[methoxy(polyethylene glycol)-2000]
DTPA	diethylenetriamine pentaacetic acid
EOEOVE	(2-ethoxy)ethoxyethylvinylether
EPC	L-α-phosphatidylcholine
EPR	enhanced permeability and retention
FaDu	human squamous cell carcinoma
FBS	fetal bovine serum
Fe_3O_4	magnetite
$Gd(HPDO_3A)$	gadolinium-[10-(2-hydroxypropyl)-1.4.7.10-tetraazacyclododecane-1.4.7-triacetic acid]
Glu	glutamic acid
GM1	gangliosides
HaT	DPPC:Brij 96:4
HCC	hepatocellular carcinoma
HCT116	human colon carcinoma
HePC	hexadecylphosphocholine
HIFU	high intensity focused
HPMA	*N*-(2-hydroxypropyl)methacrylamide)
HSPC	hydrogenated soy phosphatidylcholine
HT	hyperthermia
LCST	low critical solution temperature
LTSL	lysolipid-containing temperature-sensitive liposomes; $DPPC:MSPC:DSPE\text{-}PEG_{2000}$ (90:10:4)
mAb	momoclonal antibody
MF	electromegnetic field
min	minute
mol	mole
MR	magnetic resonance
MSA	mercaptosuccinic acid
MTX	methotrexate
NR	not reported

DOI: 10.1021/acs.chemrev.5b00578
Chem. Rev. 2016, 116, 3883−3918

NBD	*N*-(7-nitrobenz-2-oxa-1,3-diazol-4-yl)-1,2-dihexadecanoyl-*sn*-glycero-3-phosphoethanolamine)
NDDAM	*N*,*N*-didodecylacrylamide
NHS	*N*-hydroxysuccinimide
NIPAM	*N*-isopropylacrylamide
NIPAMAM	*N*-isopropylmethacrylamide
NIR	near-infrared
NPs	nanoparticles
NTSL	HSPC:CHOL:DSPE-PEG$_{2000}$ (56.3:38.2:5.5)
ODA	octadecyl acrylate
ODVE	octadecylvinylether
OMP	octadecyl-3-mercaptopionate
p-	poly
PAA	propylacrylamide
PEG	polyethylene glycol
RF	radiofrequency
RFA	radiofrequency ablation
SH	sulfhydryl
T_m	phase transition temperature
TSL	temperature-sensitive liposome
TSL-NPHs	temperature-sensitive liposomes−nanoparticle hybrids
TTSL	traditional temperature-sensitive liposome; DPPC:HSPC:CHOL:DSPE-PEG 2000 (54:27:16:3)
γ-Fe_2O_3	maghemite

REFERENCES

(1) Bangham, A. D.; Horne, R. W. Negative Staining of Phospholipids and Their Structural Modification by Surface-Active Agents as Observed in the Electron Microscope. *J. Mol. Biol.* **1964**, *8*, 660−668.

(2) Bangham, A. D.; Standish, M. M.; Watkins, J. C. Diffusion of Univalent Ions across the Lamellae of Swollen Phospholipids. *J. Mol. Biol.* **1965**, *13*, 238−252.

(3) Li, X.; Hirsh, D.; Cabral-Lilly, D.; Zirkel, A.; Gruner, S.; Janoff, A.; Perkins, W. Doxorubicin Physical State in Solution and inside Liposomes Loaded Via a Ph Gradient. *Biochim. Biophys. Acta, Biomembr.* **1998**, *1415*, 23−40.

(4) Chen, Y.; Bose, A.; Bothun, G. D. Controlled Release from Bilayer-Decorated Magnetoliposomes Via Electromagnetic Heating. *ACS Nano* **2010**, *4*, 3215−3221.

(5) Koudelka, Š.; Turánek, J. Liposomal Paclitaxel Formulations. *J. Controlled Release* **2012**, *163*, 322−334.

(6) Gregoriadis, G.; Swain, C. P.; Wills, E. J.; Tavill, A. S. Drug-Carrier Potential of Liposomes in Cancer Chemotherapy. *Lancet* **1974**, *303*, 1313−1316.

(7) Gregoriadis, G. Drug Entrapment in Liposomes. *FEBS Lett.* **1973**, *36*, 292−296.

(8) Gregoriadis, G.; Neerunjun, D. E. Control of the Rate of Hepatic Uptake and Catabolism of Liposome-Entrapped Proteins Injected into Rats. Possible Therapeutic Applications. *Eur. J. Biochem.* **1974**, *47*, 179−185.

(9) Kamps, J. A.; Morselt, H. W.; Swart, P. J.; Meijer, D. K.; Scherphof, G. L. Massive Targeting of Liposomes, Surface-Modified with Anionized Albumins, to Hepatic Endothelial Cells. *Proc. Natl. Acad. Sci. U. S. A.* **1997**, *94*, 11681−11685.

(10) Peer, D.; Karp, J. M.; Hong, S.; Farokhzad, O. C.; Margalit, R.; Langer, R. Nanocarriers as an Emerging Platform for Cancer Therapy. *Nat. Nanotechnol.* **2007**, *2*, 751−760.

(11) Davis, M. E.; Chen, Z. G.; Shin, D. M. Nanoparticle Therapeutics: An Emerging Treatment Modality for Cancer. *Nat. Rev. Drug Discovery* **2008**, *7*, 771−782.

(12) Solomon, R.; Gabizon, A. A. Clinical Pharmacology of Liposomal Anthracyclines: Focus on Pegylated Liposomal Doxorubicin. *Clin. Lymphoma Myeloma* **2008**, *8*, 21−32.

(13) Dvorak, H. F.; Nagy, J. A.; Dvorak, J. T.; Dvorak, A. M. Identification and Characterization of the Blood Vessels of Solid Tumors That Are Leaky to Circulating Macromolecules. *Am. J. Pathol.* **1988**, *133*, 95−109.

(14) Wu, N. Z.; Da, D.; Rudoll, T. L.; Needham, D.; Whorton, A. R.; Dewhirst, M. W. Increased Microvascular Permeability Contributes to Preferential Accumulation of Stealth Liposomes in Tumor Tissue. *Cancer Res.* **1993**, *53*, 3765−3770.

(15) Matsumura, Y.; Maeda, H. A New Concept for Macromolecular Therapeutics in Cancer Chemotherapy: Mechanism of Tumoritropic Accumulation of Proteins and the Antitumor Agent Smancs. *Cancer Res.* **1986**, *46*, 6387−6392.

(16) Maeda, H. The Enhanced Permeability and Retention (Epr) Effect in Tumor Vasculature: The Key Role of Tumor-Selective Macromolecular Drug Targeting. *Adv. Enzyme Regul.* **2001**, *41*, 189−207.

(17) Lammers, T. Drug Targeting to Tumors: Principles, Pitfalls and (Pre-) Clinical Progress. *J. Controlled Release* **2012**, *161*, 175−187.

(18) Iyer, A. K.; Khaled, G.; Fang, J.; Maeda, H. Exploiting the Enhanced Permeability and Retention Effect for Tumor Targeting. *Drug Discovery Today* **2006**, *11*, 812−818.

(19) Barenholz, Y. Doxil® the First Fda-Approved Nano-Drug: Lessons Learned. *J. Controlled Release* **2012**, *160*, 117−134.

(20) Ewer, M. S.; Martin, F. J.; Henderson, C.; Shapiro, C. L.; Benjamin, R. S.; Gabizon, A. A. Cardiac Safety of Liposomal Anthracyclines. *Semin. Oncol.* **2004**, *31*, 161−181.

(21) Safra, T.; Muggia, F.; Jeffers, S.; Tsao-Wei, D. D.; Groshen, S.; Lyass, O.; Henderson, R.; Berry, G.; Gabizon, A. Pegylated Liposomal Doxorubicin (Doxil): Reduced Clinical Cardiotoxicity in Patients Reaching or Exceeding Cumulative Doses of 500 Mg/M2. *Ann. Oncol.* **2000**, *11*, 1029−1033.

(22) Jain, R. K. Transport of Molecules across Tumor Vasculature. *Cancer Metastasis Rev.* **1987**, *6*, 559−593.

(23) Chrastina, A.; Massey, K. A.; Schnitzer, J. E. Overcoming in Vivo Barriers to Targeted Nanodelivery. *Wiley Interdiscip. Rev.: Nanomed. Nanobiotechnol.* **2011**, *3*, 421−437.

(24) Prabhakar, U.; Blakey, D. C.; Maeda, H.; Jain, R. K.; Sevick-Muraca, E. M.; Zamboni, W.; Farokhzad, O. C.; Barry, S. T.; Gabizon, A.; Grodzinski, P. Challenges and Key Considerations of the Enhanced Permeability and Retention Effect (Epr) for Nanomedicine Drug Delivery in Oncology. *Cancer Res.* **2013**, *73*, 2412−2417.

(25) Laginha, K. M.; Verwoert, S.; Charrois, G. J. R.; Allen, T. M. Determination of Doxorubicin Levels in Whole Tumor and Tumor Nuclei in Murine Breast Cancer Tumors. *Clin. Cancer Res.* **2005**, *11*, 6944−6949.

(26) Seetharamu, N.; Kim, E.; Hochster, H.; Martin, F.; Muggia, F. Phase Ii Study of Liposomal Cisplatin (Spi-77) in Platinum-Sensitive Recurrences of Ovarian Cancer. *Anticancer Res.* **2010**, *30*, 541−545.

(27) White, S. C.; Lorigan, P.; Margison, G. P.; Margison, J. M.; Martin, F.; Thatcher, N.; Anderson, H.; Ranson, M. Phase Ii Study of Spi-77 (Sterically Stabilised Liposomal Cisplatin) in Advanced Non-Small-Cell Lung Cancer. *Br. J. Cancer* **2006**, *95*, 822−828.

(28) Gabizon, A. A.; Shmeeda, H.; Zalipsky, S. Pros and Cons of the Liposome Platform in Cancer Drug Targeting*. *J. Liposome Res.* **2006**, *16*, 175−183.

(29) Storm, G.; Steerenberg, P. A.; Emmen, F.; van Borssum Waalkes, M.; Crommelin, D. J. Release of Doxorubicin from Peritoneal Macrophages Exposed in Vivo to Doxorubicin-Containing Liposomes. *Biochim. Biophys. Acta, Gen. Subj.* **1988**, *965*, 136−145.

(30) Harasym, T. O.; Cullis, P. R.; Bally, M. B. Intratumor Distribution of Doxorubicin Following I.V. Administration of Drug Encapsulated in Egg Phosphatidylcholine/Cholesterol Liposomes. *Cancer Chemother. Pharmacol.* **1997**, *40*, 309−317.

(31) Mayer, L. D.; Dougherty, G.; Harasym, T. O.; Bally, M. B. The Role of Tumor-Associated Macrophages in the Delivery of Liposomal Doxorubicin to Solid Murine Fibrosarcoma Tumors. *J. Pharmacol. Exp. Ther.* **1997**, *280*, 1406−1414.

(32) Koning, G. A.; Eggermont, A. M. M.; Lindner, L. H.; ten Hagen, T. L. M. Hyperthermia and Thermosensitive Liposomes for Improved

DOI: 10.1021/acs.chemrev.5b00578
Chem. Rev. 2016, 116, 3883−3918

Delivery of Chemotherapeutic Drugs to Solid Tumors. *Pharm. Res.* **2010**, *27*, 1750−1754.
(33) Needham, D.; Anyarambhatla, G.; Kong, G.; Dewhirst, M. W. A New Temperature-Sensitive Liposome for Use with Mild Hyperthermia: Characterization and Testing in a Human Tumor Xenograft Model. *Cancer Res.* **2000**, *60*, 1197−1201.
(34) Ponce, A. M.; Wright, A.; Dewhirts, M. W.; Needham, D. Targeted Bioavailability of Drugs by Triggered Release from Liposomes. *Future Lipidol.* **2006**, *1*, 25−34.
(35) Bibi, S.; Lattmann, E.; Mohammed, A. R.; Perrie, Y. Trigger Release Liposome Systems: Local and Remote Controlled Delivery? *J. Microencapsulation* **2012**, *29*, 262−276.
(36) Kaasgaard, T.; Andresen, T. L. Liposomal Cancer Therapy: Exploiting Tumor Characteristics. *Expert Opin. Drug Delivery* **2010**, *7*, 225−243.
(37) ClinicalTrials.gov. Phase 3 Study of Thermodox with Radiofrequency Ablation (Rfa) in Treatment of Hepatocellular Carcinoma (Hcc), Nct00617981, http://clinicaltrials.gov/show/NCT00617981; accessed Mar 16, 2013.
(38) Bikram, M.; West, J. L. Thermo-Responsive Systems for Controlled Drug Delivery. *Expert Opin. Drug Delivery* **2008**, *5*, 1077−1091.
(39) Mackay, J. A.; Chilkoti, A. Temperature Sensitive Peptides: Engineering Hyperthermia-Directed Therapeutics. *Int. J. Hyperthermia* **2008**, *24*, 483−495.
(40) Onaca, O.; Enea, R.; Hughes, D. W.; Meier, W. Stimuli-Responsive Polymersomes as Nanocarriers for Drug and Gene Delivery. *Macromol. Biosci.* **2009**, *9*, 129−139.
(41) Mura, S.; Nicolas, J.; Couvreur, P. Stimuli-Responsive Nanocarriers for Drug Delivery. *Nat. Mater.* **2013**, *12*, 991−1003.
(42) Shao, P.; Wang, B.; Wang, Y.; Li, J.; Zhang, Y. The Application of Thermosensitive Nanocarriers in Controlled Drug Delivery. *J. Nanomater.* **2011**, *2011*, 1−12.
(43) Torchilin, V. P. Multifunctional, Stimuli-Sensitive Nanoparticulate Systems for Drug Delivery. *Nat. Rev. Drug Discovery* **2014**, *13*, 813−827.
(44) Yatvin, M. B.; Weinstein, J. N.; Dennis, W. H.; Blumenthal, R. Design of Liposomes for Enhanced Local Release of Drugs by Hyperthermia. *Science* **1978**, *202*, 1290−1293.
(45) Needham, D.; Park, J.-Y.; Wright, A. M.; Tong, J. Materials Characterization of the Low Temperature Sensitive Liposome (LTSL): Effects of the Lipid Composition (Lysolipid and DSPE-PEG2000) on the Thermal Transition and Release of Doxorubicin. *Faraday Discuss.* **2013**, *161*, 515−534.
(46) Torchilin, V. *Liposomes: A Practical Approach* **2003**, 1−301.
(47) Papahadjopoulos, D.; Jacobson, K.; Nir, S.; Isac, I. Phase Transitions in Phospholipid Vesicles Fluorescence Polarization and Permeability Measurements Concerning the Effect of Temperature and Cholesterol. *Biochim. Biophys. Acta, Biomembr.* **1973**, *311*, 330−348.
(48) Landon, C. D.; Park, J.-Y.; Needham, D.; Dewhirst, M. W. Nanoscale Drug Delivery and Hyperthermia: The Materials Design and Preclinical and Clinical Testing of Low Temperature-Sensitive Liposomes Used in Combination with Mild Hyperthermia in the Treatment of Local Cancer. *Open Nanomed. J.* **2011**, *3*, 38−64.
(49) Maruyama, K.; Unezaki, S.; Takahashi, N.; Iwatsuru, M. Enhanced Delivery of Doxorubicin to Tumor by Long-Circulating Thermosensitive Liposomes and Local Hyperthermia. *Biochim. Biophys. Acta, Biomembr.* **1993**, *1149*, 209−216.
(50) Iga, K.; Hamaguchi, N.; Igari, Y.; Ogawa, Y.; Gotoh, K.; Ootsu, K.; Toguchi, H.; Shimamoto, T. Enhanced Antitumor-Activity in Mice after Administration of Thermosensitive Liposome Encapsulating Cisplatin with Hyperthermia. *J. Pharmacol. Exp. Ther.* **1991**, *257*, 1203−1207.
(51) Yatvin, M. B.; Muhlensiepen, H.; Porschen, W.; Weinstein, J. N.; Feinendegen, L. E. Selective Delivery of Liposome-Associated Cis-Dichlorodiammineplatinum(Ii) by Heat and Its Influence on Tumor Drug Uptake and Growth. *Cancer Res.* **1981**, *41*, 1602−1607.
(52) Bassett, J. B.; Anderson, R. U.; Tacker, J. R. Use of Temperature-Sensitive Liposomes in the Selective Delivery of Methotrexate and Cis-Platinum Analogues to Murine Bladder Tumor. *J. Urol.* **1986**, *135*, 612−615.
(53) Gaber, M. H.; Hong, K. L.; Huang, S. K.; Papahadjopoulos, D. Thermosensitive Sterically Stabilized Liposomes - Formulation and in-Vitro Studies on Mechanism of Doxorubicin Release by Bovine Serum and Human Plasma. *Pharm. Res.* **1995**, *12*, 1407−1416.
(54) Unezaki, S.; Maruyama, K.; Takahashi, N.; Koyama, M.; Yuda, T.; Suginaka, A.; Iwatsuru, M. Enhanced Delivery and Antitumor-Activity of Doxorubicin Using Long-Circulating Thermosensitive Liposomes Containing Amphipathic Polyethylene-Glycol in Combination with Local Hyperthermia. *Pharm. Res.* **1994**, *11*, 1180−1185.
(55) Li, L.; ten Hagen, T. L. M.; Schipper, D.; Wijnberg, T. M.; Van Rhoon, G.; Eggermont, A. M. M.; Lindner, L. H.; Koning, G. A. Triggered Content Release from Optimized Stealth Thermosensitive Liposomes Using Mild Hyperthermia. *J. Controlled Release* **2010**, *143*, 274−279.
(56) Lindner, L. H.; Eichhorn, M. E.; Eibl, H.; Teichert, N.; Schmitt-Sody, M.; Issels, R. D.; Dellian, M. Novel Temperature-Sensitive Liposomes with Prolonged Circulation Time. *Clin. Cancer Res.* **2004**, *10*, 2168−2178.
(57) Hossann, M.; Wiggenhorn, M.; Schwerdt, A.; Wachholz, K.; Teichert, N.; Eibl, H.; Issels, R. D.; Lindner, L. H. In Vitro Stability and Content Release Properties of Phosphatidylglyceroglycerol Containing Thermosensitive Liposomes. *Biochim. Biophys. Acta, Biomembr.* **2007**, *1768*, 2491−2499.
(58) Dicheva, B. M.; ten Hagen, T. L.; Schipper, D.; Seynhaeve, A. L.; van Rhoon, G. C.; Eggermont, A. M.; Koning, G. A. Targeted and Heat-Triggered Doxorubicin Delivery to Tumors by Dual Targeted Cationic Thermosensitive Liposomes. *J. Controlled Release* **2014**, *195*, 37−48.
(59) Dicheva, B. M.; Hagen, T. L.; Li, L.; Schipper, D.; Seynhaeve, A. L.; Rhoon, G. C.; Eggermont, A. M.; Lindner, L. H.; Koning, G. A. Cationic Thermosensitive Liposomes: A Novel Dual Targeted Heat-Triggered Drug Delivery Approach for Endothelial and Tumour Cells. *Nano Lett.* **2013**, *13*, 2324−2331.
(60) Ta, T.; Porter, T. M. Thermosensitive Liposomes for Localized Delivery and Triggered Release of Chemotherapy. *J. Controlled Release* **2013**, *169*, 112−125.
(61) Hosokawa, T.; Sami, M.; Kato, Y.; Hayakawa, E. Alteration in the Temperature-Dependent Content Release Property of Thermosensitive Liposomes in Plasma. *Chem. Pharm. Bull.* **2003**, *51*, 1227−1232.
(62) Li, L.; Ten Hagen, T. L.; Hossann, M.; Suss, R.; van Rhoon, G. C.; Eggermont, A. M.; Haemmerich, D.; Koning, G. A. Mild Hyperthermia Triggered Doxorubicin Release from Optimized Stealth Thermosensitive Liposomes Improves Intratumoral Drug Delivery and Efficacy. *J. Controlled Release* **2013**, *168*, 142−150.
(63) Kong, G.; Dewhirst, M. W. Hyperthermia and Liposomes. *Int. J. Hyperthermia* **1999**, *15*, 345−370.
(64) Hossann, M.; Wang, T. T.; Wiggenhorn, M.; Schmidt, R.; Zengerle, A.; Winter, G.; Eibl, H.; Peller, M.; Reiser, M.; Issels, R. D.; et al. Size of Thermosensitive Liposomes Influences Content Release. *J. Controlled Release* **2010**, *147*, 436−443.
(65) Hossann, M.; Syunyaeva, Z.; Schmidt, R.; Zengerle, A.; Eibl, H.; Issels, R. D.; Lindner, L. H. Proteins and Cholesterol Lipid Vesicles Are Mediators of Drug Release from Thermosensitive Liposomes. *J. Controlled Release* **2012**, *162*, 400−406.
(66) de Smet, M.; Langereis, S.; van den Bosch, S.; Gruell, H. Temperature-Sensitive Liposomes for Doxorubicin Delivery under Mri Guidance. *J. Controlled Release* **2010**, *143*, 120−127.
(67) Anyarambhatla, G. R.; Needham, D. Enhancement of the Phase Transition Permeability of Dppc Liposomes by Incorporation of Mppc: A New Temperature-Sensitive Liposome for Use with Mild Hyperthermia. *J. Liposome Res.* **1999**, *9*, 491−506.
(68) Needham, D.; Dewhirst, M. W. Materials Science and Engineering of the Low Temperature Sensitive Liposome (LTSL): Composition-Structure-Property Relationships That Underlie Its Design and Performance. *Smart Materials for Drug Delivery*; The Royal Society of Chemistry: UK, 2012; Vol. *1*, pp 33−79.
(69) Manzoor, A. A.; Lindner, L. H.; Landon, C. D.; Park, J. Y.; Simnick, A. J.; Dreher, M. R.; Das, S.; Hanna, G.; Park, W.; Chilkoti, A.;

DOI: 10.1021/acs.chemrev.5b00578
Chem. Rev. 2016, 116, 3883−3918

et al. Overcoming Limitations in Nanoparticle Drug Delivery: Triggered, Intravascular Release to Improve Drug Penetration into Tumors. *Cancer Res.* **2012**, *72*, 5566−5575.
(70) Thrall, D. E.; Prescott, D. M.; Samulski, T. V.; Dewhirst, M. W.; Cline, J. M.; Lee, J.; Page, R. L.; Oleson, J. R. Serious Toxicity Associated with Annular Microwave Array Induction of Whole-Body Hyperthermia in Normal Dogs. *Int. J. Hyperthermia* **1992**, *8*, 23−32.
(71) Ben-Yosef, R.; Kapp, D. S. Persistent and/or Late Complications of Combined Radiation Therapy and Hyperthermia. *Int. J. Hyperthermia* **1992**, *8*, 733−745.
(72) Mills, J. K.; Needham, D. Lysolipid Incorporation in Dipalmitoylphosphatidylcholine Bilayer Membranes Enhances the Ion Permeability and Drug Release Rates at the Membrane Phase Transition. *Biochim. Biophys. Acta, Biomembr.* **2005**, *1716*, 77−96.
(73) McIntyre, J. C.; Sleight, R. G. Fluorescence Assay for Phospholipid Membrane Asymmetry. *Biochemistry* **1991**, *30*, 11819−11827.
(74) Banno, B.; Ickenstein, L. M.; Chiu, G. N. C.; Bally, M. B.; Thewalt, J.; Brief, E.; Wasan, E. K. The Functional Roles of Poly(Ethylene Glycol)-Lipid and Lysolipid in the Drug Retention and Release from Lysolipid-Containing Thermosensitive Liposomes in Vitro and in Vivo. *J. Pharm. Sci.* **2010**, *99*, 2295−2308.
(75) Wood, B. J.; Poon, R. T.; Locklin, J. K.; Dreher, M. R.; Ng, K. K.; Eugeni, M.; Seidel, G.; Dromi, S.; Neeman, Z.; Kolf, M.; et al. Phase I Study of Heat-Deployed Liposomal Doxorubicin During Radiofrequency Ablation for Hepatic Malignancies. *J. Vasc Interv Radiol.* **2012**, *23*, 248−255.
(76) Chiu, G.; Abraham, S.; Ickenstein, L.; Ng, R.; Karlsson, G.; Edwards, K.; Wasan, E.; Bally, M. Encapsulation of Doxorubicin into Thermosensitive Liposomes Via Complexation with the Transition Metal Manganese. *J. Controlled Release* **2005**, *104*, 271−288.
(77) Needham, D.; McIntosh, T. J.; Zhelev, D. V. Surface Chemistry of the Sterically Stabilized PEG-Liposome: General Principles. In *Liposomes: Rational Design*; Janoff, A., Dekker, M., Eds.; CRC Press: New York, 1998; pp 13−62.
(78) Yarmolenko, P. S.; Zhao, Y.; Landon, C.; Spasojevic, I.; Yuan, F.; Needham, D.; Viglianti, B. L.; Dewhirst, M. W. Comparative Effects of Thermosensitive Doxorubicin-Containing Liposomes and Hyperthermia in Human and Murine Tumours. *Int. J. Hyperthermia* **2010**, *26*, 485−498.
(79) Kong, G.; Anyarambhatla, G.; Petros, W. P.; Braun, R. D.; Colvin, O. M.; Needham, D.; Dewhirst, M. W. Efficacy of Liposomes and Hyperthermia in a Human Tumor Xenograft Model: Importance of Triggered Drug Release. *Cancer Res.* **2000**, *60*, 6950−6957.
(80) Chen, Q.; Krol, A.; Wright, A.; Needham, D.; Dewhirst, M. W.; Yuan, F. Tumor Microvascular Permeability Is a Key Determinant for Antivascular Effects of Doxorubicin Encapsulated in a Temperature Sensitive Liposome. *Int. J. Hyperthermia* **2008**, *24*, 475−482.
(81) Celsion.com. Inovation in Oncology Celsion Corporation, www.celsion.com; accessed Jan 01, 2013.
(82) Hauck, M. L.; LaRue, S. M.; Petros, W. P.; Poulson, J. M.; Yu, D.; Spasojevic, I.; Pruitt, A. F.; Klein, A.; Case, B.; Thrall, D. E.; et al. Phase I Trial of Doxorubicin-Containing Low Temperature Sensitive Liposomes in Spontaneous Canine Tumors. *Clin. Cancer Res.* **2006**, *12*, 4004−4010.
(83) ClinicalTrials.gov. Targeted Chemotherapy Using Focused Ultrasound for Liver Tumours (Tardox), Nct02181075, https://clinicaltrials.gov/ct2/show/NCT02181075; accessed Sep 28, 2015.
(84) ClinicalTrials.gov. Phase 1/2 Study of Thermodox with Approved Hyperthermia in Treatment of Breast Cancer Recurrence at the Chest Wall, https://clinicaltrials.gov/ct2/show/NCT00826085?term=thermodox&rank=1; accessed Oct 28, 2015.
(85) Tagami, T.; Ernsting, M. J.; Li, S.-D. Optimization of a Novel and Improved Thermosensitive Liposome Formulated with Dppc and a Brij Surfactant Using a Robust in Vitro System. *J. Controlled Release* **2011**, *154*, 290−297.
(86) Tagami, T.; Ernsting, M. J.; Li, S.-D. Efficient Tumor Regression by a Single and Low Dose Treatment with a Novel and Enhanced Formulation of Thermosensitive Liposomal Doxorubicin. *J. Controlled Release* **2011**, *152*, 303−309.
(87) Tagami, T.; May, J. P.; Ernsting, M. J.; Li, S.-D. A Thermosensitive Liposome Prepared with a Cu2+ Gradient Demonstrates Improved Pharmacokinetics, Drug Delivery and Antitumor Efficacy. *J. Controlled Release* **2012**, *161*, 142−149.
(88) Lindner, L. H.; Hossann, M.; Vogeser, M.; Teichert, N.; Wachholz, K.; Eibl, H.; Hiddemann, W.; Issels, R. D. Dual Role of Hexadecylphosphocholine (Miltefosine) in Thermosensitive Liposomes: Active Ingredient and Mediator of Drug Release. *J. Controlled Release* **2008**, *125*, 112−120.
(89) Kono, K. Thermosensitive Polymer-Modified Liposomes. *Adv. Drug Delivery Rev.* **2001**, *53*, 307−319.
(90) Shibayama, M.; Mizutani, S.-y.; Nomura, S. Thermal Properties of Copolymer Gels Containing N-Isopropylacrylamide. *Macromolecules* **1996**, *29*, 2019−2024.
(91) Kono, K.; Henmi, A.; Yamashita, H.; Hayashi, H.; Takagishi, T. Improvement of Temperature-Sensitivity of Poly(N-Isopropylacrylamide)-Modified Liposomes. *J. Controlled Release* **1999**, *59*, 63−75.
(92) Kono, K.; Hayashi, H.; Takagishi, T. Temperature-Sensitive Liposomes: Liposomes Bearing Poly (N-Isopropylacrylamide). *J. Controlled Release* **1994**, *30*, 69−75.
(93) Han, H.; Shin, B.; Choi, H. Doxorubicin-Encapsulated Thermosensitive Liposomes Modified with Poly(N-Isopropylacrylamide-Co-Acrylamide): Drug Release Behavior and Stability in the Presence of Serum. *Eur. J. Pharm. Biopharm.* **2006**, *62*, 110−116.
(94) Kim, J. C.; Bae, S. K.; Kim, J. D. Temperature-Sensitivity of Liposomal Lipid Bilayers Mixed with Poly(N-Isopropylacrylamide-Co-Acrylic Acid). *J. Biochem.* **1997**, *121*, 15−19.
(95) Hayashi, H.; Kono, K.; Takagishi, T. Temperature-Controlled Release Property of Phospholipid Vesicles Bearing a Thermo-Sensitive Polymer. *Biochim. Biophys. Acta, Biomembr.* **1996**, *1280*, 127−134.
(96) Hayashi, H.; Kono, K.; Takagishi, T. Temperature-Dependent Associating Property of Liposomes Modified with a Thermosensitive Polymer. *Bioconjugate Chem.* **1998**, *9*, 382−389.
(97) Kono, K.; Nakai, R.; Morimoto, K.; Takagishi, T. Temperature-Dependent Interaction of Thermo-Sensitive Polymer-Modified Liposomes with Cv1 Cells. *FEBS Lett.* **1999**, *456*, 306−310.
(98) Kono, K.; Nakai, R.; Morimoto, K.; Takagishi, T. Thermosensitive Polymer-Modified Liposomes That Release Contents around Physiological Temperature. *Biochim. Biophys. Acta, Biomembr.* **1999**, *12*, 1−2.
(99) Hayashi, H.; Kono, K.; Takagishi, T. Temperature Sensitization of Liposomes Using Copolymers of N-Isopropylacrylamide. *Bioconjugate Chem.* **1999**, *10*, 412−418.
(100) Kono, K.; Yoshino, K.; Takagishi, T. Effect of Poly(Ethylene Glycol) Grafts on Temperature-Sensitivity of Thermosensitive Polymer-Modified Liposomes. *J. Controlled Release* **2002**, *80*, 321−332.
(101) Yoshino, K.; Kadowaki, A.; Takagishi, T.; Kono, K. Temperature Sensitization of Liposomes by Use of N-Isopropylacrylamide Copolymers with Varying Transition Endotherms. *Bioconjugate Chem.* **2004**, *15*, 1102−1109.
(102) Kono, K.; Murakami, T.; Yoshida, T.; Haba, Y.; Kanaoka, S.; Takagishi, T.; Aoshima, S. Temperature Sensitization of Liposomes by Use of Thermosensitive Block Copolymers Synthesized by Living Cationic Polymerization: Effect of Copolymer Chain Length. *Bioconjugate Chem.* **2005**, *16*, 1367−1374.
(103) Han, H. D.; Choi, M. S.; Hwang, T.; Song, C. K.; Seong, H.; Kim, T. W.; Choi, H. S.; Shin, B. C. Hyperthermia-Induced Antitumor Activity of Thermosensitive Polymer Modified Temperature-Sensitive Liposomes. *J. Pharm. Sci.* **2006**, *95*, 1909−1917.
(104) Paasonen, L.; Romberg, B.; Storm, G.; Yliperttula, M.; Urtti, A.; Hennink, W. E. Temperature-Sensitive Poly(N-(2-Hydroxypropyl)-Methacrylamide Mono/Dilactate)-Coated Liposomes for Triggered Contents Release. *Bioconjugate Chem.* **2007**, *18*, 2131−2136.
(105) van Elk, M.; Deckers, R.; Oerlemans, C.; Shi, Y.; Storm, G.; Vermonden, T.; Hennink, W. E. Triggered Release of Doxorubicin from Temperature-Sensitive Poly(N-(2-Hydroxypropyl)-Methacrylamide Mono/Dilactate) Grafted Liposomes. *Biomacromolecules* **2014**, *15*, 1002−1009.

DOI: 10.1021/acs.chemrev.5b00578
Chem. Rev. 2016, 116, 3883−3918

(106) Ta, T.; Convertine, A. J.; Reyes, C. R.; Stayton, P. S.; Porter, T. M. Thermosensitive Liposomes Modified with Poly(N-Isopropylacrylamide-Co-Propylacrylic Acid) Copolymers for Triggered Release of Doxorubicin. *Biomacromolecules* **2010**, *11*, 1915−1920.
(107) Kono, K.; Ozawa, T.; Yoshida, T.; Ozaki, F.; Ishizaka, Y.; Maruyama, K.; Kojima, C.; Harada, A.; Aoshima, S. Highly Temperature-Sensitive Liposomes Based on a Thermosensitive Block Copolymer for Tumor-Specific Chemotherapy. *Biomaterials* **2010**, *31*, 7096−7105.
(108) Kono, K.; Nakashima, S.; Kokuryo, D.; Aoki, I.; Shimomoto, H.; Aoshima, S.; Maruyama, K.; Yuba, E.; Kojima, C.; Harada, A.; et al. Multi-Functional Liposomes Having Temperature-Triggered Release and Magnetic Resonance Imaging for Tumor-Specific Chemotherapy. *Biomaterials* **2011**, *32*, 1387−1395.
(109) Katagiri, K.; Imai, Y.; Koumoto, K.; Kaiden, T.; Kono, K.; Aoshima, S. Magnetoresponsive on-Demand Release of Hybrid Liposomes Formed from Fe_3O_4 Nanoparticles and Thermosensitive Block Copolymers. *Small* **2011**, *7*, 1683−1689.
(110) Aluri, S.; Janib, S. M.; Mackay, J. A. Environmentally Responsive Peptides as Anticancer Drug Carriers. *Adv. Drug Delivery Rev.* **2009**, *61*, 940−952.
(111) Park, S. M.; Kim, M. S.; Park, S. J.; Park, E. S.; Choi, K. S.; Kim, Y. S.; Kim, H. R. Novel Temperature-Triggered Liposome with High Stability: Formulation, in Vitro Evaluation, and in Vivo Study Combined with High-Intensity Focused Ultrasound (Hifu). *J. Controlled Release* **2013**, *170*, 373−379.
(112) McDaniel, J. R.; Macewan, S. R.; Dewhirst, M.; Chilkoti, A. Doxorubicin-Conjugated Chimeric Polypeptide Nanoparticles That Respond to Mild Hyperthermia. *J. Controlled Release* **2012**, *159*, 362−367.
(113) Meyer, D. E.; Shin, B. C.; Kong, G. A.; Dewhirst, M. W.; Chilkoti, A. Drug Targeting Using Thermally Responsive Polymers and Local Hyperthermia. *J. Controlled Release* **2001**, *74*, 213−224.
(114) Hassouneh, W.; Fischer, K.; MacEwan, S. R.; Branscheid, R.; Fu, C. L.; Liu, R.; Schmidt, M.; Chilkoti, A. Unexpected Multivalent Display of Proteins by Temperature Triggered Self-Assembly of Elastin-Like Polypeptide Block Copolymers. *Biomacromolecules* **2012**, *13*, 1598−1605.
(115) Al-Ahmady, Z. S.; Al-Jamal, W. T.; Bossche, J. V.; Bui, T. T.; Drake, A. F.; Mason, J.; Kostarelos, K. Lipid-Peptide Vesicle Nanoscale Hybrids for Triggered Drug Release by Mild Hyperthermia in Vitro and in Vivo. *ACS Nano* **2012**, *6*, 9335−9346.
(116) Jadhav, S. V.; Singh, S. K.; Reja, R. M.; Gopi, H. N. Gamma-Amino Acid Mutated Alpha-Coiled Coils as Mild Thermal Triggers for Liposome Delivery. *Chem. Commun.* **2013**, *49*, 11065−11067.
(117) Na, K.; Lee, S. A.; Jung, S. H.; Hyun, J.; Shin, B. C. Elastin-Like Polypeptide Modified Liposomes for Enhancing Cellular Uptake into Tumor Cells. *Colloids Surf., B* **2012**, *91*, 130−136.
(118) Petka, W. A.; Harden, J. L.; McGrath, K. P.; Wirtz, D.; Tirrell, D. A. Reversible Hydrogels from Self-Assembling Artificial Proteins. *Science* **1998**, *281*, 389−392.
(119) Shen, W.; Lammertink, R. G. H.; Sakata, J. K.; Kornfield, J. A.; Tirrell, D. A. Assembly of an Artificial Protein Hydrogel through Leucine Zipper Aggregation and Disulfide Bond Formation. *Macromolecules* **2005**, *38*, 3909−3916.
(120) Xu, C. Y.; Breedveld, V.; Kopecek, J. Reversible Hydrogels from Self-Assembling Genetically Engineered Protein Block Copolymers. *Biomacromolecules* **2005**, *6*, 1739−1749.
(121) Thompson, K. S.; Vinson, C. R.; Freire, E. Thermodynamic Characterization of the Structural Stability of the Coiled-Coil Region of the Bzip Transcription Factor Gcn4. *Biochemistry* **1993**, *32*, 5491−5496.
(122) Dicheva, B. M.; Koning, G. A. Targeted Thermosensitive Liposomes: An Attractive Novel Approach for Increased Drug Delivery to Solid Tumors. *Expert Opin. Drug Delivery* **2014**, *11*, 83−100.
(123) Al-Ahmady, Z. S.; Scudamore, C. L.; Kostarelos, K. Triggered Doxorubicin Release in Solid Tumors from Thermosensitive Liposome-Peptide Hybrids: Critical Parameters and Therapeutic Efficacy. *Int. J. Cancer* **2015**, *137*, 731−743.
(124) Meyer, D. E.; Chilkoti, A. Quantification of the Effects of Chain Length and Concentration on the Thermal Behavior of Elastin-Like Polypeptides. *Biomacromolecules* **2004**, *5*, 846−851.
(125) Cho, Y.; Zhang, Y.; Christensen, T.; Sagle, L. B.; Chilkoti, A.; Cremer, P. S. Effects of Hofmeister Anions on the Phase Transition Temperature of Elastin-Like Polypeptides. *J. Phys. Chem. B* **2008**, *112*, 13765−13771.
(126) Nettles, D. L.; Chilkoti, A.; Setton, L. A. Applications of Elastin-Like Polypeptides in Tissue Engineering. *Adv. Drug Delivery Rev.* **2010**, *62*, 1479−1485.
(127) Meyer, D. E.; Chilkoti, A. Purification of Recombinant Proteins by Fusion with Thermally-Responsive Polypeptides. *Nat. Biotechnol.* **1999**, *17*, 1112−1115.
(128) McDaniel, J. R.; Dewhirst, M. W.; Chilkoti, A. Actively Targeting Solid Tumours with Thermoresponsive Drug Delivery Systems That Respond to Mild Hyperthermia. *Int. J. Hyperthermia* **2013**, *29*, 501−510.
(129) Raucher, D.; Chilkoti, A. Enhanced Uptake of a Thermally Responsive Polypeptide by Tumor Cells in Response to Its Hyperthermia-Mediated Phase Transition. *Cancer Res.* **2001**, *61*, 7163−7170.
(130) Park, S. M.; Cha, J. M.; Nam, J.; Kim, M. S.; Park, S. J.; Park, E. S.; Lee, H.; Kim, H. R. Formulation Optimization and in Vivo Proof-of-Concept Study of Thermosensitive Liposomes Balanced by Phospholipid, Elastin-Like Polypeptide, and Cholesterol. *PLoS One* **2014**, *9*, 1−13.
(131) Preiss, M. R.; Bothun, G. D. Stimuli-Responsive Liposome-Nanoparticle Assemblies. *Expert Opin. Drug Delivery* **2011**, *8*, 1025−1040.
(132) Al-Jamal, W. T.; Kostarelos, K. Liposomes: From a Clinically Established Drug Delivery System to a Nanoparticle Platform for Theranostic Nanomedicine. *Acc. Chem. Res.* **2011**, *44*, 1094−1104.
(133) Yoshida, M.; Sato, M.; Yamamoto, Y.; Maehara, T.; Naohara, T.; Aono, H.; Sugishita, H.; Sato, K.; Watanabe, Y. Tumor Local Chemohyperthermia Using Docetaxel-Embedded Magnetoliposomes: Interaction of Chemotherapy and Hyperthermia. *J. Gastroenterol. Hepatol.* **2012**, *27*, 406−411.
(134) Wang, Q.; Liu, J. Nanoparticles Enhanced Hyperthermia. In *Intracellular Delivery: Fundamentals and Applications*; Prokop, A., Ed.; Springer: New York, 2011; Vol. *5*, pp 567−598.
(135) Volodkin, D. V.; Skirtach, A. G.; Mohwald, H. Near-Ir Remote Release from Assemblies of Liposomes and Nanoparticles. *Angew. Chem., Int. Ed.* **2009**, *48*, 1807−1809.
(136) Terentyuk, G. S.; Maslyakova, G. N.; Suleymanova, L. V.; Khlebtsov, N. G.; Khlebtsov, B. N.; Akchurin, G. G.; Maksimova, I. L.; Tuchin, V. V. Laser-Induced Tissue Hyperthermia Mediated by Gold Nanoparticles: Toward Cancer Phototherapy. *J. Biomed. Opt.* **2009**, *14*, 3122371−3122379.
(137) Hilger, I.; Kaiser, W. A. Iron Oxide-Based Nanostructures for MRI and Magnetic Hyperthermia. *Nanomedicine* **2012**, *7*, 1443−1459.
(138) Hildebrandt, B.; Wust, P.; Ahlers, O.; Dieing, A.; Sreenivasa, G.; Kerner, T.; Felix, R.; Riess, H. The Cellular and Molecular Basis of Hyperthermia. *Crit Rev. Oncol Hematol.* **2002**, *43*, 33−56.
(139) Pradhan, P.; Giri, J.; Rieken, F.; Koch, C.; Mykhaylyk, O.; Doblinger, M.; Banerjee, R.; Bahadur, D.; Plank, C. Targeted Temperature Sensitive Magnetic Liposomes for Thermo-Chemotherapy. *J. Controlled Release* **2010**, *142*, 108−121.
(140) Maier-Hauff, K.; Ulrich, F.; Nestler, D.; Niehoff, H.; Wust, P.; Thiesen, B.; Orawa, H.; Budach, V.; Jordan, A. Efficacy and Safety of Intratumoral Thermotherapy Using Magnetic Iron-Oxide Nanoparticles Combined with External Beam Radiotherapy on Patients with Recurrent Glioblastoma Multiforme. *J. Neuro-Oncol.* **2011**, *103*, 317−324.
(141) Maier-Hauff, K.; Rothe, R.; Scholz, R.; Gneveckow, U.; Wust, P.; Thiesen, B.; Feussner, A.; von Deimling, A.; Waldoefner, N.; Felix, R.; et al. Intracranial Thermotherapy Using Magnetic Nanoparticles Combined with External Beam Radiotherapy: Results of a Feasibility Study on Patients with Glioblastoma Multiforme. *J. Neuro-Oncol.* **2007**, *81*, 53−60.

DOI: 10.1021/acs.chemrev.5b00578
Chem. Rev. 2016, 116, 3883−3918

(142) Johannsen, M.; Thiesen, B.; Wust, P.; Jordan, A. Magnetic Nanoparticle Hyperthermia for Prostate Cancer. *Int. J. Hyperthermia* **2010**, *26*, 790−795.
(143) Kobayashi, D.; Kawai, N.; Sato, S.; Naiki, T.; Yamada, K.; Yasui, T.; Tozawa, K.; Kobayashi, T.; Takahashi, S.; Kohri, K. Thermotherapy Using Magnetic Cationic Liposomes Powerfully Suppresses Prostate Cancer Bone Metastasis in a Novel Rat Model. *Prostate* **2013**, *73*, 913−922.
(144) Zhu, L.; Huo, Z. L.; Wang, L. L.; Tong, X.; Xiao, Y.; Ni, K. Y. Targeted Delivery of Methotrexate to Skeletal Muscular Tissue by Thermosensitive Magnetoliposomes. *Int. J. Pharm.* **2009**, *370*, 136−143.
(145) Viroonchatapan, E.; Sato, H.; Ueno, M.; Adachi, I.; Tazawa, K.; Horikoshi, I. Release of 5-Fluorouracil from Thermosensitive Magneto-liposomes Induced by an Electromagnetic Field. *J. Controlled Release* **1997**, *46*, 263−271.
(146) Wu, G. Remotely Triggered Liposome Release by near-Infrared Light Absorption Via Hollow Gold Nanoshells. *J. Am. Chem. Soc.* **2008**, *130*, 8175−8177.
(147) Al-Jamal, W. T.; Al-Jamal, K. T.; Tian, B.; Lacerda, L.; Bornans, P. H.; Frederik, P. M.; Kostarelos, K. Lipid-Quanturn Dot Bilayer Vesicles Enhance Tumor Cell Uptake and Retention in Vitro and in Vivo. *ACS Nano* **2008**, *2*, 408−418.
(148) Bothun, G. D. Hydrophobic Silver Nanoparticles Trapped in Lipid Bilayers: Size Distribution, Bilayer Phase Behavior, and Optical Properties. *J. Nanobiotechnol.* **2008**, *6*, 1−10.
(149) An, X.; Zhan, F.; Zhu, Y. Smart Photothermal-Triggered Bilayer Phase Transition in Aunps-Liposomes to Release Drug. *Langmuir* **2013**, *29*, 1061−1068.
(150) Paasonen, L.; Sipila, T.; Subrizi, A.; Laurinmaki, P.; Butcher, S. J.; Rappolt, M.; Yaghmur, A.; Urtti, A.; Yliperttula, M. Gold-Embedded Photosensitive Liposomes for Drug Delivery: Triggering Mechanism and Intracellular Release. *J. Controlled Release* **2010**, *147*, 136−143.
(151) Chithrani, D. B.; Dunne, M.; Stewart, J.; Allen, C.; Jaffray, D. A. Cellular Uptake and Transport of Gold Nanoparticles Incorporated in a Liposomal Carrier. *Nanomedicine* **2010**, *6*, 161−169.
(152) Tai, L.-A.; Wang, Y.-C.; Yang, C.-S. Heat-Activated Sustaining Nitric Oxide Release from Zwitterionic Diazeniumdiolate Loaded in Thermo-Sensitive Liposomes. *Nitric Oxide* **2010**, *23*, 60−64.
(153) Alkilany, A. M.; Thompson, L. B.; Boulos, S. P.; Sisco, P. N.; Murphy, C. J. Gold Nanorods: Their Potential for Photothermal Therapeutics and Drug Delivery, Tempered by the Complexity of Their Biological Interactions. *Adv. Drug Delivery Rev.* **2012**, *64*, 190−199.
(154) Laurent, S.; Forge, D.; Port, M.; Roch, A.; Robic, C.; Vander Elst, L.; Muller, R. N. Magnetic Iron Oxide Nanoparticles: Synthesis, Stabilization, Vectorization, Physicochemical Characterizations, and Biological Applications. *Chem. Rev.* **2008**, *108*, 2064−2110.
(155) Pankhurst, Q. A. Applications of Magnetic Nanoparticles in Biomedicine. *J. Phys. D: Appl. Phys.* **2003**, *36*, R167−R181.
(156) Park, S. H.; Oh, S. G.; Mun, J. Y.; Han, S. S. Loading of Gold Nanoparticles inside the Dppc Bilayers of Liposome and Their Effects on Membrane Fluidities. *Colloids Surf., B* **2006**, *48*, 112−118.
(157) Paasonen, L.; Laaksonen, T.; Johans, C.; Yliperttula, M.; Kontturi, K.; Urtti, A. Gold Nanoparticles Enable Selective Light-Induced Contents Release from Liposomes. *J. Controlled Release* **2007**, *122*, 86−93.
(158) An, X.; Zhang, F.; Zhu, Y.; Shen, W. Photoinduced Drug Release from Thermosensitive Aunps-Liposome Using a Aunps-Switch. *Chem. Commun.* **2010**, *46*, 7202−7204.
(159) You, J.; Zhang, P.; Hu, F.; Du, Y.; Yuan, H.; Zhu, J.; Wang, Z.; Zhou, J.; Li, C. Near-Infrared Light-Sensitive Liposomes for the Enhanced Photothermal Tumor Treatment by the Combination with Chemotherapy. *Pharm. Res.* **2014**, *31*, 554−565.
(160) Park, S. H.; Oh, S. G.; Mun, J. Y.; Han, S. S. Effects of Silver Nanoparticles on the Fluidity of Bilayer in Phospholipid Liposome. *Colloids Surf., B* **2005**, *44*, 117−122.
(161) Tai, L.-A.; Tsai, P.-J.; Wang, Y.-C.; Wang, Y.-J.; Lo, L.-W.; Yang, C.-S. Thermosensitive Liposomes Entrapping Iron Oxide Nanoparticles for Controllable Drug Release. *Nanotechnology* **2009**, *20*, 1−9.
(162) Bothun, G. D.; Preiss, M. R. Bilayer Heating in Magnetite Nanoparticle-Liposome Dispersions Via Fluorescence Anisotropy. *J. Colloid Interface Sci.* **2011**, *357*, 70−74.
(163) Wang, L.; Wang, Z.; Liu, J.; Zhang, J.; Zhang, D. Preparation of a New Nanosized As2o3/Mn0.5zn0.5fe2o4 Thermosensitive Magneto-liposome and Its Antitumor Effect on Mda_Mb_231 Cells. *J. Nanosci. Nanotechnol.* **2011**, *11*, 10755−10759.
(164) Wang, L.; Zhang, J.; An, Y.; Wang, Z.; Liu, J.; Li, Y.; Zhang, D. A Study on the Thermochemotherapy Effect of Nanosized As2o3/Mzf Thermosensitive Magnetoliposomes on Experimental Hepatoma in Vitro and in Vivo. *Nanotechnology* **2011**, *22*, 0957−4484.
(165) Bealle, G.; Di Corato, R.; Kolosnjaj-Tabi, J.; Dupuis, V.; Clement, O.; Gazeau, F.; Wilhelm, C.; Menager, C. Ultra Magnetic Liposomes for Mr Imaging, Targeting, and Hyperthermia. *Langmuir* **2012**, *28*, 11834−11842.
(166) Lorenzato, C.; Cernicanu, A.; Meyre, M. E.; Germain, M.; Pottier, A.; Levy, L.; de Senneville, B. D.; Bos, C.; Moonen, C.; Smirnov, P. MRI Contrast Variation of Thermosensitive Magnetoliposomes Triggered by Focused Ultrasound: A Tool for Image-Guided Local Drug Delivery. *Contrast Media Mol. Imaging* **2013**, *8*, 185−192.
(167) Weissleder, R. A Clearer Vision for in Vivo Imaging. *Nat. Biotechnol.* **2001**, *19*, 316−317.
(168) Gobin, A. M.; Lee, M. H.; Halas, N. J.; James, W. D.; Drezek, R. A.; West, J. L. Near-Infrared Resonant Nanoshells for Combined Optical Imaging and Photothermal Cancer Therapy. *Nano Lett.* **2007**, *7*, 1929−1934.
(169) Oldenburg, S. J.; Averitt, R. D.; Westcott, S. L.; Halas, N. J. Nanoengineering of Optical Resonances. *Chem. Phys. Lett.* **1998**, *288*, 243−247.
(170) Strong, L. E.; West, J. L. Thermally Responsive Polymer-Nanoparticle Composites for Biomedical Applications. *Wiley Interdiscip. Rev.: Nanomed. Nanobiotechnol.* **2011**, *3*, 307−317.
(171) Lal, S.; Clare, S. E.; Halas, N. J. Nanoshell-Enabled Photothermal Cancer Therapy: Impending Clinical Impact. *Acc. Chem. Res.* **2008**, *41*, 1842−1851.
(172) Bardhan, R.; Lal, S.; Joshi, A.; Halas, N. J. Theranostic Nanoshells: From Probe Design to Imaging and Treatment of Cancer. *Acc. Chem. Res.* **2011**, *44*, 936−946.
(173) Link, S.; El-Sayed, M. A. Optical Properties and Ultrafast Dynamics of Metallic Nanocrystals. *Annu. Rev. Phys. Chem.* **2003**, *54*, 331−366.
(174) University, R. Nanoshell Therapy to Be Tested in Lung Cancer Clinical Trial; accessed Jan 23, 2014.
(175) Hirsch, L. R.; Stafford, R. J.; Bankson, J. A.; Sershen, S. R.; Rivera, B.; Price, R. E.; Hazle, J. D.; Halas, N. J.; West, J. L. Nanoshell-Mediated near-Infrared Thermal Therapy of Tumors under Magnetic Resonance Guidance. *Proc. Natl. Acad. Sci. U. S. A.* **2003**, *100*, 13549−13554.
(176) O'Neal, D. P.; Hirsch, L. R.; Halas, N. J.; Payne, J. D.; West, J. L. Photo-Thermal Tumor Ablation in Mice Using near Infrared-Absorbing Nanoparticles. *Cancer Lett.* **2004**, *209*, 171−176.
(177) Alekseeva, A. V.; Bogatyrev, V. A.; Khlebtsov, B. N.; Mel'nikov, A. G.; Dykman, L. A.; Khlebtsov, N. G. Gold Nanorods: Synthesis and Optical Properties. *Colloid J.* **2006**, *68*, 661−678.
(178) Agarwal, A.; Mackey, M. A.; El-Sayed, M. A.; Bellamkonda, R. V. Remote Triggered Release of Doxorubicin in Tumors by Synergistic Application of Thermosensitive Liposomes and Gold Nanorods. *ACS Nano* **2011**, *5*, 4919−4926.
(179) Lozano, N.; Al-Jamal, W. T.; Taruttis, A.; Beziere, N.; Burton, N. C.; Van den Bossche, J.; Mazza, M.; Herzog, E.; Ntziachristos, V.; Kostarelos, K. Liposome−Gold Nanorod Hybrids for High-Resolution Visualization Deep in Tissues. *J. Am. Chem. Soc.* **2012**, *134*, 13256−13258.
(180) Allen, T. M. Ligand-Targeted Therapeutics in Anticancer Therapy. *Nat. Rev. Cancer* **2002**, *2*, 750−763.
(181) Torchilin, V. Antibody-Modified Liposomes for Cancer Chemotherapy. *Expert Opin. Drug Delivery* **2008**, *5*, 1003−1025.
(182) Gabizon, A.; Tzemach, D.; Gorin, J.; Mak, L.; Amitay, Y.; Shmeeda, H.; Zalipsky, S. Improved Therapeutic Activity of Folate-

DOI: 10.1021/acs.chemrev.5b00578
Chem. Rev. 2016, 116, 3883−3918

Targeted Liposomal Doxorubicin in Folate Receptor-Expressing Tumor Models. *Cancer Chemother. Pharmacol.* **2010**, *66*, 43−52.
(183) Park, J. W.; Kirpotin, D. B.; Hong, K.; Shalaby, R.; Shao, Y.; Nielsen, U. B.; Marks, J. D.; Papahadjopoulos, D.; Benz, C. C. Tumor Targeting Using Anti-Her2 Imunoliposomes. *J. Controlled Release* **2001**, *74*, 95−113.
(184) Mamot, C.; Drummond, D. C.; Noble, C. O.; Kallab, V.; Guo, Z.; Hong, K.; Kirpotin, D. B.; Park, J. W. Epidermal Growth Factor Receptor−Targeted Immunoliposomes Significantly Enhance the Efficacy of Multiple Anticancer Drugs in Vivo. *Cancer Res.* **2005**, *65*, 11631−11638.
(185) Kirpotin, D. B.; Drummond, D. C.; Shao, Y.; Shalaby, M. R.; Hong, K.; Nielsen, U. B.; Marks, J. D.; Benz, C. C.; Park, J. W. Antibody Targeting of Long-Circulating Lipidic Nanoparticles Does Not Increase Tumor Localization but Does Increase Internalization in Animal Models. *Cancer Res.* **2006**, *66*, 6732−6740.
(186) Pastorino, F. Vascular Damage and Anti-Angiogenic Effects of Tumor Vessel-Targeted Liposomal Chemotherapy. *Cancer Res.* **2003**, *63*, 7400−7409.
(187) Moase, E. H.; Qi, W.; Ishida, T.; Gabos, Z.; Longenecker, B. M.; Zimmermann, G. L.; Ding, L.; Krantz, M.; Allen, T. M. Anti-Muc-1 Immunoliposomal Doxorubicin in the Treatment of Murine Models of Metastatic Breast Cancer. *Biochim. Biophys. Acta, Biomembr.* **2001**, *1510*, 43−55.
(188) Cheng, W. W. K.; Allen, T. M. Targeted Delivery of Anti-Cd19 Liposomal Doxorubicin in B-Cell Lymphoma: A Comparison of Whole Monoclonal Antibody, Fab' Fragments and Single Chain Fv. *J. Controlled Release* **2008**, *126*, 50−58.
(189) Sapra, P.; Allen, T. M. Internalizing Antibodies Are Necessary for Improved Therapeutic Efficacy of Antibody-Targeted Liposomal Drugs. *Cancer Res.* **2002**, *62*, 7190−7194.
(190) Seynhaeve, A. L.; Hoving, S.; Schipper, D.; Vermeulen, C. E.; de Wiel-Ambagtsheer, G.; van Tiel, S. T.; Eggermont, A. M.; Ten Hagen, T. L. Tumor Necrosis Factor Alpha Mediates Homogeneous Distribution of Liposomes in Murine Melanoma That Contributes to a Better Tumor Response. *Cancer Res.* **2007**, *67*, 9455−9462.
(191) Eikenes, L. Hyaluronidase Induces a Transcapillary Pressure Gradient and Improves the Distribution and Uptake of Liposomal Doxorubicin (Caelyx) in Human Osteosarcoma Xenografts. *Br. J. Cancer* **2005**, *93*, 81−88.
(192) Davies, L.; Lundstrom, L. M.; Frengen, J.; Eikenes, L.; Bruland, S. O.; Kaalhus, O.; Hjelstuen, M. H.; Brekken, C. Radiation Improves the Distribution and Uptake of Liposomal Doxorubicin (Caelyx) in Human Osteosarcoma Xenografts. *Cancer Res.* **2004**, *64*, 547−553.
(193) Al-Ahmady, Z. S.; Chaloin, O.; Kostarelos, K. Monoclonal Antibody-Targeted, Temperature-Sensitive Liposomes: In Vivo Tumor Chemotherapeutics in Combination with Mild Hyperthermia. *J. Controlled Release* **2014**, *196*, 332−343.
(194) Allen, T. Liposomal Drug Delivery Systems: From Concept to Clinical Applications. *Adv. Drug Delivery Rev.* **2013**, *65*, 36−48.
(195) Smith, B.; Lyakhov, I.; Loomis, K.; Needle, D.; Baxa, U.; Yavlovich, A.; Capala, J.; Blumenthal, R.; Puri, A. Hyperthermia-Triggered Intracellular Delivery of Anticancer Agent to HER2(+) Cells by HER2-Specific Affibody (Zher2-Gs-Cys)-Conjugated Thermosensitive Liposomes (HER2(+) Affisomes). *J. Controlled Release* **2011**, *153*, 187−194.
(196) Kim, M. S.; Lee, D. W.; Park, K.; Park, S. J.; Choi, E. J.; Park, E. S.; Kim, H. R. Temperature-Triggered Tumor-Specific Delivery of Anticancer Agents by Crgd-Conjugated Thermosensitive Liposomes. *Colloids Surf., B* **2014**, *116*, 17−25.
(197) Negussie, A. H.; Miller, J. L.; Reddy, G.; Drake, S. K.; Wood, B. J.; Dreher, M. R. Synthesis and in Vitro Evaluation of Cyclic Ngr Peptide Targeted Thermally Sensitive Liposome. *J. Controlled Release* **2010**, *143*, 265−273.
(198) Sullivan, S. M.; Huang, L. Enhanced Delivery to Target Cells by Heat-Sensitive Immunoliposomes. *Proc. Natl. Acad. Sci. U. S. A.* **1986**, *83*, 6117−6121.
(199) Puri, A.; Kramer-Marek, G.; Campbell-Massa, R.; Yavlovich, A.; Tele, S. C.; Lee, S. B.; Clogston, J. D.; Patri, A. K.; Blumenthal, R.; Capala, J. Her2-Specific Affibody-Conjugated Thermosensitive Liposomes (Affisomes) for Improved Delivery of Anticancer Agents. *J. Liposome Res.* **2008**, *18*, 293−307.
(200) Dupuy, D. E.; DiPetrillo, T.; Gandhi, S.; Ready, N.; Ng, T.; Donat, W.; Mayo-Smith, W. W. Radiofrequency Ablation Followed by Conventional Radiotherapy for Medically Inoperable Stage I Non-Small Cell Lung Cancer. *Chest* **2006**, *129*, 738−745.
(201) Kullberg, M.; Mann, K.; Owens, J. L. A Two-Component Drug Delivery System Using Her-2-Targeting Thermosensitive Liposomes. *J. Drug Targeting* **2009**, *17*, 98−107.
(202) Kullberg, M.; Owens, J. L.; Mann, K.; Listeriolysin, O. Enhances Cytoplasmic Delivery by Her-2 Targeting Liposomes. *J. Drug Targeting* **2010**, *18*, 313−320.
(203) Wang, C.; Wang, X.; Zhong, T.; Zhao, Y.; Zhang, W. Q.; Ren, W.; Huang, D.; Zhang, S.; Guo, Y.; Yao, X.; et al. The Antitumor Activity of Tumor-Homing Peptide-Modified Thermosensitive Liposomes Containing Doxorubicin on Mcf-7/Adr: In Vitro and in Vivo. *Int. J. Nanomed.* **2015**, *10*, 2229−2248.
(204) Dicheva, B. M.; Ten Hagen, T. L.; Seynhaeve, A. L.; Amin, M.; Eggermont, A. M.; Koning, G. A. Enhanced Specificity and Drug Delivery in Tumors by Crgd - Anchoring Thermosensitive Liposomes. *Pharm. Res.* **2015**, *32*, 3862−3876.
(205) Sullivan, S. M.; Huang, L. Preparation and Characterization of Heat-Sensitive Immunoliposomes. *Biochim. Biophys. Acta, Biomembr.* **1985**, *812*, 116−126.
(206) May, J. P.; Li, S. D. Hyperthermia-Induced Drug Targeting. *Expert Opin. Drug Delivery* **2013**, *10*, 511−527.
(207) Bacic, G.; Niesman, M. R.; Bennett, H. F.; Magin, R. L.; Swartz, H. M. Modulation of Water Proton Relaxation Rates by Liposomes Containing Paramagnetic Materials. *Magn. Reson. Med.* **1988**, *6*, 445−458.
(208) Viglianti, B. L.; Ponce, A. M.; Michelich, C. R.; Yu, D.; Abraham, S. A.; Sanders, L.; Yarmolenko, P. S.; Schroeder, T.; MacFall, J. R.; Barboriak, D. P.; et al. Chemodosimetry of in Vivo Tumor Liposomal Drug Concentration Using MRI. *Magn. Reson. Med.* **2006**, *56*, 1011−1018.
(209) Ponce, A. M.; Viglianti, B. L.; Yu, D.; Yarmolenko, P. S.; Michelich, C. R.; Woo, J.; Bally, M. B.; Dewhirst, M. W. Magnetic Resonance Imaging of Temperature-Sensitive Liposome Release: Drug Dose Painting and Antitumor Effects. *J. Natl. Cancer Inst.* **2007**, *99*, 53−63.
(210) Frich, L.; Bjornerud, A.; Fossheim, S.; Tillung, T.; Gladhaug, I. Experimental Application of Thermosensitive Paramagnetic Liposomes for Monitoring Magnetic Resonance Imaging Guided Thermal Ablation. *Magn. Reson. Med.* **2004**, *52*, 1302−1309.
(211) de Smet, M.; Heijman, E.; Langereis, S.; Hijnen, N. M.; Gruell, H. Magnetic Resonance Imaging of High Intensity Focused Ultrasound Mediated Drug Delivery from Temperature-Sensitive Liposomes: An in Vivo Proof-of-Concept Study. *J. Controlled Release* **2011**, *150*, 102−110.
(212) Viglianti, B. L.; Abraham, S. A.; Michelich, C. R.; Yarmolenko, P. S.; MacFall, J. R.; Bally, M. B.; Dewhirst, M. W. In Vivo Monitoring of Tissue Pharmacokinetics of Liposome/Drug Using MRI: Illustration of Targeted Delivery. *Magn. Reson. Med.* **2004**, *51*, 1153−1162.
(213) Tagami, T.; Foltz, W. D.; Ernsting, M. J.; Lee, C. M.; Tannock, I. F.; May, J. P.; Li, S.-D. MRI Monitoring of Intratumoral Drug Delivery and Prediction of the Therapeutic Effect with a Multifunctional Thermosensitive Liposome. *Biomaterials* **2011**, *32*, 6570−6578.
(214) Kunjachan, S.; Ehling, J.; Storm, G.; Kiessling, F.; Lammers, T. Noninvasive Imaging of Nanomedicines and Nanotheranostics: Principles, Progress, and Prospects. *Chem. Rev.* **2015**, *115*, 10907−10937.
(215) Lammers, T.; Aime, S.; Hennink, W. E.; Storm, G.; Kiessling, F. Theranostic Nanomedicine. *Acc. Chem. Res.* **2011**, *44*, 1029−1038.
(216) Silva, A. C.; Lee, J. H.; Aoki, I.; Koretsky, A. P. Manganese-Enhanced Magnetic Resonance Imaging (MEMRI): Methodological and Practical Considerations. *NMR Biomed.* **2004**, *17*, 532−543.
(217) Negussie, A. H.; Yarmolenko, P. S.; Partanen, A.; Ranjan, A.; Jacobs, G.; Woods, D.; Bryant, H.; Thomasson, D.; Dewhirst, M. W.; Wood, B. J.; et al. Formulation and Characterisation of Magnetic

DOI: 10.1021/acs.chemrev.5b00578
Chem. Rev. 2016, 116, 3883−3918

Resonance Imageable Thermally Sensitive Liposomes for Use with Magnetic Resonance-Guided High Intensity Focused Ultrasound. *Int. J. Hyperthermia* **2011**, *27*, 140−155.
(218) Langereis, S.; Keupp, J.; van Velthoven, J. L.; de Roos, I. H.; Burdinski, D.; Pikkemaat, J. A.; Gruell, H. A Temperature-Sensitive Liposomal 1h Cest and 19f Contrast Agent for Mr Image-Guided Drug Delivery. *J. Am. Chem. Soc.* **2009**, *131*, 1380−1381.
(219) de Smet, M.; Hijnen, N. M.; Langereis, S.; Elevelt, A.; Heijman, E.; Dubois, L.; Lambin, P.; Gruell, H. Magnetic Resonance Guided High-Intensity Focused Ultrasound Mediated Hyperthermia Improves the Intratumoral Distribution of Temperature-Sensitive Liposomal Doxorubicin. *Invest. Radiol.* **2013**, *48*, 395−405.
(220) Bettaieb, A.; Wrzal, P. K.; Averill-Bates, D. A. *Hyperthermia: Cancer Treatment and Beyond; In Cancer Treatment - Conventional and Innovative Approaches* **2013**, 257−283.
(221) Ahmed, M.; Brace, C. L.; Lee, F. T., Jr.; Goldberg, S. N. Principles of and Advances in Percutaneous Ablation. *Radiology* **2011**, *258*, 351−369.
(222) Goldberg, S. N.; Gazelle, G. S.; Mueller, P. R. Thermal Ablation Therapy for Focal Malignancy: A Unified Approach to Underlying Principles, Techniques, and Diagnostic Imaging Guidance. *AJR, Am. J. Roentgenol.* **2000**, *174*, 323−331.
(223) Ahmed, M.; Moussa, M.; Goldberg, S. N. Synergy in Cancer Treatment between Liposomal Chemotherapeutics and Thermal Ablation. *Chem. Phys. Lipids* **2012**, *165*, 424−437.
(224) Dewhirst, M. W.; Vujaskovic, Z.; Jones, E.; Thrall, D. Re-Setting the Biologic Rationale for Thermal Therapy. *Int. J. Hyperthermia* **2005**, *21*, 779−790.
(225) Issels, R. Hyperthermia Combined with Chemotherapy a Biological Rationale, Clinical Application, and Treatment Results. *Onkologie* **1999**, *22*, 374−381.
(226) Kowal, C. D. Possible Benefits of Hyperthermia to Chemotherapy. *Cancer Res.* **1979**, *39*, 2285−2289.
(227) Kong, G.; Braun, R. D.; Dewhirst, M. W. Hyperthermia Enables Tumor-Specific Nanoparticle Delivery: Effect of Particle Size. *Cancer Res.* **2000**, *60*, 4440−4445.
(228) Lammers, T.; Peschke, P.; Kuhnlein, R.; Subr, V.; Ulbrich, K.; Debus, J.; Huber, P.; Hennink, W.; Storm, G. Effect of Radiotherapy and Hyperthermia on the Tumor Accumulation of Hpma Copolymer-Based Drug Delivery Systems. *J. Controlled Release* **2007**, *117*, 333−341.
(229) Schuster, J. M.; Zalutsky, M. R.; Noska, M. A.; Dodge, R.; Friedman, H. S.; Bigner, D. D.; Dewhirst, M. W. Hyperthermic Modulation of Radiolabelled Antibody Uptake in a Human Glioma Xenograft and Normal Tissues. *Int. J. Hyperthermia* **1995**, *11*, 59−72.
(230) Cope, D. A.; Dewhirst, M. W.; Friedman, H. S.; Bigner, D. D.; Zalutsky, M. R. Enhanced Delivery of a Monoclonal Antibody F(Ab′)2 Fragment to Subcutaneous Human Glioma Xenografts Using Local Hyperthermia. *Cancer Res.* **1990**, *50*, 1803−1809.
(231) Karino, T.; Koga, S.; Maeta, M. Experimental Studies of the Effects of Local Hyperthermia on Blood Flow, Oxygen Pressure and Ph in Tumors. *Jpn. J. Surg.* **1988**, *18*, 276−283.
(232) Fujiwara, K.; Watanabe, T. Effects of Hyperthermia, Radiotherapy and Thermoradiotherapy on Tumor Microvascular Permeability. *Pathol. Int.* **1990**, *40*, 79−84.
(233) Kong, G.; Braun, R. D.; Dewhirst, M. W. Characterization of the Effect of Hyperthermia on Nanoparticle Extravasation from Tumor Vasculature. *Cancer Res.* **2001**, *61*, 3027−3032.
(234) Song, C. W.; Lokshina, A.; Rhee, J. G.; Patten, M.; Levitt, S. H. Implication of Blood Flow in Hyperthermic Treatment of Tumors. *IEEE Trans. Biomed. Eng.* **1984**, *31*, 9−16.
(235) Leunig, M. Interstitial Fluid Pressure in Solid Tumors Following Hyperthermia: Possible Correlation with Therapeutic Response. *Cancer Res.* **1992**, *52*, 487−490.
(236) Chen, Q.; Tong, S.; Dewhirst, M. W.; Yuan, F. Targeting Tumor Microvessels Using Doxorubicin Encapsulated in a Novel Thermosensitive Liposome. *Mol. Cancer Ther.* **2004**, *3*, 1311−1317.
(237) Dou, Y. N.; Zheng, J.; Foltz, W. D.; Weersink, R.; Chaudary, N.; Jaffray, D. A.; Allen, C. Heat-Activated Thermosensitive Liposomal Cisplatin (Htlc) Results in Effective Growth Delay of Cervical Carcinoma in Mice. *J. Controlled Release* **2014**, *178*, 69−78.
(238) Ranjan, A.; Jacobs, G. C.; Woods, D. L.; Negussie, A. H.; Partanen, A.; Yarmolenko, P. S.; Gacchina, C. E.; Sharma, K. V.; Frenkel, V.; Wood, B. J.; et al. Image-Guided Drug Delivery with Magnetic Resonance Guided High Intensity Focused Ultrasound and Temperature Sensitive Liposomes in a Rabbit Vx2 Tumor Model. *J. Controlled Release* **2012**, *158*, 487−494.
(239) Ishida, O.; Maruyama, K.; Yanagie, H.; Eriguchi, H.; Iwatsuru, M. Targeting Chemotherapy to Solid Tumors with Long-Circulating Thermosensitive Liposomes and Local Hyperthermia. *Jpn. J. Cancer Res.* **2000**, *91*, 118−126.
(240) Gaber, M. H.; Wu, N. Z.; Hong, K.; Huang, S. K.; Dewhirst, M. W.; Papahadjopoulos, D. Thermosensitive Liposomes: Extravasation and Release of Contents in Tumor Microvascular Networks. *Int. J. Radiat. Oncol., Biol., Phys.* **1996**, *36*, 1177−1187.
(241) Li, L.; Ten Hagen, T. L.; Haeri, A.; Soullie, T.; Scholten, C.; Seynhaeve, A. L.; Eggermont, A. M.; Koning, G. A. A Novel Two-Step Mild Hyperthermia for Advanced Liposomal Chemotherapy. *J. Controlled Release* **2014**, *28*, 202−208.
(242) Dromi, S.; Frenkel, V.; Luk, A.; Traughber, B.; Angstadt, M.; Bur, M.; Poff, J.; Xie, J.; Libutti, S. K.; Li, K. C.; et al. Pulsed-High Intensity Focused Ultrasound and Low Temperature-Sensitive Liposomes for Enhanced Targeted Drug Delivery and Antitumor Effect. *Clin. Cancer Res.* **2007**, *13*, 2722−2727.
(243) Al-Jamal, W. T.; Al-Ahmady, Z. S.; Kostarelos, K. Pharmacokinetics & Tissue Distribution of Temperature-Sensitive Liposomal Doxorubicin in Tumor-Bearing Mice Triggered with Mild Hyperthermia. *Biomaterials* **2012**, *33*, 4608−4617.
(244) Li, L.; Ten Hagen, T. L.; Bolkestein, M.; Gasselhuber, A.; Yatvin, J.; van Rhoon, G. C.; Eggermont, A. M.; Haemmerich, D.; Koning, G. A. Improved Intratumoral Nanoparticle Extravasation and Penetration by Mild Hyperthermia. *J. Controlled Release* **2013**, *167*, 130−137.
(245) Andriyanov, A. V.; Koren, E.; Barenholz, Y.; Goldberg, S. N. Therapeutic Efficacy of Combining Pegylated Liposomal Doxorubicin and Radiofrequency (Rf) Ablation: Comparison between Slow-Drug-Releasing, Non-Thermosensitive and Fast-Drug-Releasing, Thermosensitive Nano-Liposomes. *PLoS One* **2014**, *9*, 1−12.
(246) Celsion.com, Celsion Announces Results of Phase Iii Heat Study of Thermodox in Primary Liver Cancer. http://investor.celsion.com/releasedetail.cfm?ReleaseID=737033; accessed Jan 31, 2013.
(247) Needham, D. In *Biomaterials for Cancer Therapeutics*; Park, K., Ed.; Woodhead Publishing, 2013; Chapter 12 - Reverse Engineering of the Low Temperature-Sensitive Liposome (LTSL) for Treating Cancer, pp 270−353e.
(248) Poon, R. T.; Borys, N. Lyso-Thermosensitive Liposomal Doxorubicin: A Novel Approach to Enhance Efficacy of Thermal Ablation of Liver Cancer. *Expert Opin. Pharmacother.* **2009**, *10*, 333−343.
(249) Celsion.com, Celsion Corporation Announces Updated Overall Survival Data from Heat Study of Thermodox in Primary Liver Cancer, http://investor.celsion.com/releasedetail.cfm?ReleaseID=926288; accessed Dec 16, 2015.
(250) Gruell, H.; Langereis, S. Hyperthermia-Triggered Drug Delivery from Temperature-Sensitive Liposomes Using MRI-Guided High Intensity Focused Ultrasound. *J. Controlled Release* **2012**, *161*, 317−327.
(251) Needham, D.; Dewhirst, M. W. The Development and Testing of a New Temperature-Sensitive Drug Delivery System for the Treatment of Solid Tumors. *Adv. Drug Delivery Rev.* **2001**, *53*, 285−305.
(252) Van Der Zee, J.; De Bruijne, M.; Mens, J. W.; Ameziane, A.; Broekmeyer-Reurink, M. P.; Drizdal, T.; Linthorst, M.; Van Rhoon, G. C. Reirradiation Combined with Hyperthermia in Breast Cancer Recurrences: Overview of Experience in Erasmus Mc. *Int. J. Hyperthermia* **2010**, *26*, 638−648.
(253) Hynynen, K. Mrighifu: A Tool for Image-Guided Therapeutics. *J. Magn Reson Imaging.* **2011**, *34*, 482−493.
(254) de Senneville, B. D.; Mougenot, C.; Quesson, B.; Dragonu, I.; Grenier, N.; Moonen, C. T. Mr Thermometry for Monitoring Tumor Ablation. *Eur. J. Radiol.* **2007**, *17*, 2401−2410.

DOI: 10.1021/acs.chemrev.5b00578
Chem. Rev. 2016, 116, 3883−3918

(255) Salomir, R.; Vimeux, F. C.; de Zwart, J. A.; Grenier, N.; Moonen, C. T. Hyperthermia by Mr-Guided Focused Ultrasound: Accurate Temperature Control Based on Fast MRI and a Physical Model of Local Energy Deposition and Heat Conduction. *Magn. Reson. Med.* **2000**, *43*, 342−347.
(256) Hijnen, N.; Langereis, S.; Gruell, H. Magnetic Resonance Guided High-Intensity Focused Ultrasound for Image-Guided Temperature-Induced Drug Delivery. *Adv. Drug Delivery Rev.* **2014**, *72*, 65−81.
(257) Zhou, Y. F. High Intensity Focused Ultrasound in Clinical Tumor Ablation. *World J. Clin Oncol.* **2011**, *2*, 8−27.
(258) Li, P. Z.; Zhu, S. H.; He, W.; Zhu, L. Y.; Liu, S. P.; Liu, Y.; Wang, G. H.; Ye, F. High-Intensity Focused Ultrasound Treatment for Patients with Unresectable Pancreatic Cancer. *Hepatobiliary Pancreatic Dis. Int.* **2012**, *11*, 655−660.
(259) Staruch, R.; Chopra, R.; Hynynen, K. Localised Drug Release Using MRI-Controlled Focused Ultrasound Hyperthermia. *Int. J. Hyperthermia* **2011**, *27*, 156−171.
(260) Staruch, R. M.; Ganguly, M.; Tannock, I. F.; Hynynen, K.; Chopra, R. Enhanced Drug Delivery in Rabbit Vx2 Tumours Using Thermosensitive Liposomes and MRI-Controlled Focused Ultrasound Hyperthermia. *Int. J. Hyperthermia* **2012**, *28*, 776−787.
(261) Gasselhuber, A.; Dreher, M. R.; Partanen, A.; Yarmolenko, P. S.; Woods, D.; Wood, B. J.; Haemmerich, D. Targeted Drug Delivery by High Intensity Focused Ultrasound Mediated Hyperthermia Combined with Temperature-Sensitive Liposomes: Computational Modelling and Preliminary in Vivovalidation. *Int. J. Hyperthermia* **2012**, *28*, 337−348.
(262) Celsion.com. Celsion's Thermodox Plus High Intensity Focused Ultrasound Highlighted at 14th International Symposium on Therapeutic Ultrasound, http://investor.celsion.com/releasedetail.cfm?ReleaseID=839117; accessed Sep 28, 2015.

DOI: 10.1021/acs.chemrev.5b00578
Chem. Rev. 2016, 116, 3883−3918